Dynamic system optimum simultaneous route and departure time choice problems: Intersection-movement-based formulations and comparisons

by

Jiancheng Long
Professor
School of Automotive and Transportation Engineering
Hefei University of Technology
Hefei 230009, China
Tel: +86-551-62901960
E-mail: jianchenglong@hfut.edu.cn

Chao Wang
Master student
School of Automotive and Transportation Engineering
Hefei University of Technology
Hefei 230009, China
E-mail: Chao_Wang@mail.hfut.edu.cn

W.Y. Szeto
Associate Professor
Department of Civil Engineering
The University of Hong Kong
Pokfulam Road, Hong Kong
Tel: +852-28578552
Email: ceszeto@hku.hk

Abstract

In this paper, we propose intersection-movement-based models to formulate dynamic system optimum simultaneous route and departure time choice (DSO-SRDTC) problems over general networks and compare the models with the link-based and path-based counterparts. Each of these three types of models has four variants, which are formed by whether to consider first-in-first-out (FIFO) constraints and non-vehicle holding (NVH) constraints. In all three types of DSO-SRDTC models and their variants, the link transmission model (LTM) is incorporated as their traffic flow model. The DSO-SRDTC problems without FIFO constraints are formulated as linear programming (LP) problems, while the DSO-SRDTC problems with FIFO constraints are formulated as non-convex non-linear programming problems. We find that existing link-based NVH constraints cannot completely eliminate vehicle holding (VH) solutions, and propose both intersection-movement-based and path-based NVH constraints, which can completely eliminate VH solutions. We also prove that the link-based, intersection-movement-based, and path-based models of DSO-SRDTC problems without FIFO constraints are equivalent in terms of obtaining the same optimal total system travel cost (TSTC). However, the three types of models for DSO-SRDTC problems with FIFO constraints can obtain different optimal TSTCs. Based on the solution properties of the DSO-SRDTC problems with FIFO constraints, branch-and-bound algorithms are modified to solve the DSO-SRDTC problems with FIFO constraints for global optima. Numerical examples are set up to demonstrate the properties and performance of the proposed models. To the best of our knowledge, we are the pioneers to provide intersection-movement-based formulations for DSO-SRDTC problems and analyze their mathematical properties.

Keywords: Dynamic traffic assignment; system optimum; link transmission model; intersection movement; vehicle holding problem; first-in-first-out.

1. Introduction

Dynamic traffic assignment (DTA) is long recognized as a key component for network planning and transport policy evaluations as well as for real-time traffic operation and management (Szeto and Lo, 2006). System optimum DTA (SO-DTA) is a special case of DTA based on the dynamic extension of Wardrop's (1952) second principle. SO-DTA aims to predict an optimal time-dependent traffic state with minimum total system travel time (TSTT) spent or total system travel cost (TSTC) borne by all travelers in the network. It can give insights into the optimal performance of a traffic system, and hence can further provide a benchmark for controlling and managing dynamic traffic networks (Ma et al., 2014). SO-DTA has been widely used for road congestion pricing (e.g., Yang and Meng, 1998; Carey and Watling, 2012), signal control (e.g., Lo, 2001; Lin and Wang, 2004; Yu et al., 2018), network design problems (e.g., Waller and Ziliaskopoulos, 2001; Waller et al., 2006), emergency evacuation traffic management (e.g., Liu et al., 2006; Chiu et al., 2007), etc.

According to the travel choice dimension, SO-DTA problems can be classified into three categories: (1) the pure departure time choice problems (e.g., Vickrey, 1969; Liu et al., 2015), (2) the pure route choice problems (e.g., Merchant and Nemhauser, 1978a,b; Ghali and Smith, 1995; Peeta and Mahmassani, 1995; Ziliaskopoulos, 2000; Nie, 2011; Zhu and Ukkusuri, 2013; Zheng et al., 2015; Long et al., 2016; Ngoduy et al., 2016), and (3) the simultaneous route and departure time choice (SRDTC) problems (e.g., Chow, 2009a,b; Doan and Ukkusuri, 2012; Qian et al., 2012; Ma et al., 2014, 2017; Zhu and Ukkusuri, 2017). The first two categories of SO-DTA problems are special cases of the last category of problems. If physical-queue traffic flow models, such as the cell transmission model (CTM) (Daganzo, 1995; Ziliaskopoulos, 2000; Nie, 2011; Zhu and Ukkusuri, 2013), the link transmission model (LTM) (Yperman, 2007; Long et al., 2016; Ngoduy et al., 2016; Long and Szeto, 2017), and double queue models (Osorio et al., 2011, Ma et al., 2014, 2017) are applied, departure time choice must be integrated into DSO models (Ma et al., 2014). This is because any predefined departure profile (i.e., demand profile) may not be realized by the traffic flow model due to possible spillbacks at the origins.

SO-DTA problems can be formulated as either continuous-time models (e.g., Ma et al., 2014, 2017) and discrete-time models (e.g., Merchant and Nemhauser, 1978a,b; Ziliaskopoulos, 2000; Chow, 2009a,b; Nie, 2011; Doan and Ukkusuri, 2012; Qian et al., 2012; Zhu and Ukkusuri, 2013; Zheng et al., 2015; Long et al., 2016). The continuous-time SO-DTA models treat the variables as functions of time and usually formulate the SO-DTA problems as optimal control problems (Ma et al., 2014, 2017). The discrete-time SO-DTA models adopt a set of discretized variables at each time step and usually formulate the SO-DTA problems as finite-dimensional mathematical programs (e.g., Merchant and Nemhauser, 1978a,b; Ziliaskopoulos, 2000; Nie, 2011; Doan and Ukkusuri, 2012; Zhu and Ukkusuri, 2013; Long et al., 2016). An important reason why modeling continuous-time SO-DTA problems is that time is continuous by nature and it is natural to formulate

SO-DTA problems in continuous time (Ma et al., 2014). However, time discretization is always needed to solve continuous-time SO-DTA models, since there are no known methods for solving complex continuous-time models analytically. Therefore, most SO-DTA problems are formulated in discrete-time, or formulated in continuous-time and finally solved in discrete-time.

There are two major approaches to model SO-DTA problems: (1) formulating them as standard user equilibrium DTA (UE-DTA) problems (e.g., Ghali and Smith, 1995; Peeta and Mahmassani, 1995; Shen et al., 2007; Qian et al., 2012), and (2) formulating them as mathematical programming problems (e.g., Merchant and Nemhauser, 1978a,b; Ziliaskopoulos, 2000; Chow, 2009a,b; Nie, 2011; Zheng and Chiu, 2011; Doan and Ukkusuri, 2012; Zhu and Ukkusuri, 2013; Ma et al., 2014; Long et al., 2016; Long and Szeto, 2017). The first approach commonly adopts marginal path travel times\costs to formulate the SO-DTA problems as standard UE-DTA problems, and any solution algorithms developed for UE-DTA problems (e.g., Friesz et al., 1993; Huang and Lam, 2002; Lo and Szeto, 2002; Ban et al., 2008; Carey and Ge, 2012; Long et al., 2013; Han et al., 2013, 2015) can be used to solve the SO-DTA problems. However, the evaluation of marginal path travel times is notoriously difficult in general networks (Qian et al., 2012). The second approach usually formulates the SO-DTA problems as mathematical programming problems. Whether it is easy to solve the resultant models highly depends on the underlying DNL models, such as point queue models (e.g., Huang and Lam, 2002; Ban et al., 2012), exit flow models (e.g., Merchant and Nemhauser, 1978a,b; Carey and Srinivasan, 1993; Wie et al., 2002), link delay model (e.g., Friesz et al., 1993), and kinematic wave models (e.g., Newell, 1993; Daganzo, 1995; Lo and Szeto, 2002; Yperman, 2007; Nie, 2011; Zheng et al., 2015). The SO-DTA models incorporating the exit flow functions are usually formulated as non-convex nonlinear programming problems (e.g., Merchant and Nemhauser, 1978a,b) that are difficult to solve. In contrast, the SO-DTA models incorporating the kinematic wave models can lead to a linear programming (LP) formulation, which makes the formulation computationally efficient and solvable for a reasonable size network (Zhu and Ukkusuri, 2013).

The traffic flow models used in DTA models, including SO-DTA models, should have some desirable properties to capture actual traffic behavior, such as queue spillback (e.g., Daganzo, 1995; Lo and Szeto, 2002; Szeto and Lo, 2004; Ma et al., 2014), first-in-first-out (FIFO) (e.g., Carey, 1992; Astarita, 1996; Wu et al., 1998; Huang and Lam, 2002; Carey et al., 2014; Long and Szeto, 2017), and non-vehicle holding (NVH) (e.g., Ziliaskopoulos, 2000; Nie, 2011; Zheng and Chiu, 2011; Doan and Ukkusuri, 2012; Zhu and Ukkusuri, 2013; Long et al., 2016, 2017). Queue spillback refers to the end of queue spilling backward in the network. This property can be easily captured in SO-DTA models by incorporating a physical-queue traffic flow model. FIFO implies that vehicles that enter a link earlier will leave it sooner (Wu et al. 1998; Lo and Szeto, 2002; Long et al., 2011; Carey et al., 2014). It is well known that the FIFO requirement can yield a non-convex constraint set in DTA models, especially if there are multiple destinations or commodities (Carey, 1992).

Explicitly imposing this category of constraints may increase the complexity of solving the DTA models. Vehicle holding (VH) implies that traffic flows are reluctant to move forward from upstream links to their downstream links even if there are vacant spaces on the downstream links. The VH problem often occurs due to relaxation (i.e., replacing the nonlinear equality constraints with inequality ones) or linearization, and is a well-known problem for SO-DTA models in the literature (e.g., Merchant and Nemhauser, 1978a; Carey and Subrahmanian, 2000; Ziliaskopoulos, 2000; Nie, 2011; Doan and Ukkusuri, 2012; Zhu and Ukkusuri, 2013; Long et al., 2016; Long and Szeto, 2017). VH is not a critical issue when SO-DTA is only used to provide a benchmark for developing network management strategies. However, VH should be considered when some specific schemes (such as pricing or incentives) to control traffic to reach the dynamic system optimal (DSO) state. This is because the DSO state achieved by these schemes is also a dynamic user optimal (DUO) state from the point of view of travelers, and VH represents an unrealistic traffic flow phenomenon for the DUO state and should be completely eliminated.

According to the choice of decision variables used in the formulation, existing SO-DTA models can be broadly classified into two categories: link-based models (e.g., Merchant and Nemhauser, 1978a,b; Ziliaskopoulos, 2000; Nie, 2011; Doan and Ukkusuri, 2012; Zhu and Ukkusuri, 2013; Ma et al., 2014, 2017; Zheng et al., 2015; Long et al., 2016; Long and Szeto, 2017) and path-based models (e.g., Ghali and Smith, 1995; Peeta and Mahmassani, 1995; Chow, 2009a,b; Doan and Ukkusuri, 2012; Qian et al., 2012). Link-based models do not require having the path set information in advance, in which the path set can be large even for a medium-scale highway network. Hence, they can avoid path enumeration and path set generation heuristic in the solution procedure of SO-DTA problems and have the potential to be applied to large-scale highway networks. However, traditional link-based SO-DTA models cannot explicitly model traffic movements at intersections, and their optimal link-based traffic flow patterns do not contain detailed path information. As a result, traditional link-based SO-DTA models cannot capture queue spillback, unlike a few recent link-based SO-DTA models (e.g., Ma et al., 2014, 2017) that have been developed to overcome this issue. In contrast, because path-based models have important information, such as path inflows and the path set, to explicitly model traffic movements at diverges and merges, path-based models can capture queue spillback easily when a physical-queue traffic flow model is encapsulated. Nevertheless, the main disadvantage of path-based models is that they require an explicit enumeration of the path choice set, which can be very time-consuming, even for medium networks.

To retain the advantages of both link-based and path-based DSO models, intersection-movement-based DSO models can be developed, by drawing upon the development of dynamic user equilibrium or dynamic user optimal (DUO) route choice models (e.g., Long et al., 2013; Jiang et al., 2016). In intersection-movement-based DUO route choice models, two adjacent links are used to define an intersection movement. An intersection-movement-based flow pattern implicitly contains the travelers' path information since a path can be deduced by checking the downstream links involved in intersection-movement-based flows from the origin to the destination. As a result, this type of model can retain the advantages of both the link-based and the path-based DTA models: Path enumeration and path generation heuristics can be avoided in

the solution procedure, and queue spillback can be easily captured when a physical-queue traffic flow model is encapsulated. Therefore, intersection-movement-based DUO route choice models are superior to the link-based and path-based DUO route choice models. However, the intersection-movement-based approach has been only extended to formulate stochastic DUO (SDUO) route choice problems (e.g., Long et al., 2015). Whether this approach can be applied to modeling DSO-SRDTC problems and the resultant problems have good mathematical properties is questionable.

In this paper, we formulate and analyze dynamic system optimum SRDTC (DSO-SRDTC) problems using the intersection-movement-based approach. Yperman's (2007) link transmission model (LTM) is incorporated into the resultant DSO-SRDTC models. The LTM relies on Newell's (1993) simplified kinematic wave theory when the fundamental diagram is assumed to be triangular. Because each whole link can be treated as one cell, the computational efficiency of the LTM is much higher than that of classic numerical solution schemes for the Lighthill-Whitham-Richards (LWR) model, whilst retaining the same accuracy (Yperman, 2007). Same as the CTM, the LTM can also lead to an LP formulation for the DSO-SRDTC problem without the considerations of FIFO and NVH, which is referred to as the relaxed DSO-SRDTC (R-DSO-SRDTC) problem. For comparison purposes, we also present link- and path-based R-DSO-SRDTC formulations. We are the pioneers to provide intersection-movement-based formulations for DSO-SRDTC problems and analyze their mathematical properties. To the best of our knowledge, the connections between different SO-DTA formulations have not been discussed in the literature. Compared with link-based DSO-SRDTC models, intersection-movement-based models have travelers' path information, and can easily trace how queues spill backward over links when a physical-queue traffic flow model is encapsulated. This is particularly useful for queue management, e.g., in signal control. Compared with path-based DSO-SRDTC models, intersection-movement-based models do not require path enumeration and path generation heuristics in the solution procedure and can be solved more efficiently. This computation efficiency is essential for real-time applications.

We further provide definitions on NVH-DSO solutions and formulate NVH constraints as a set of mixed-integer linear inequality constraints (e.g., Lo, 2001; Pavlis and Recker, 2009; Han et al., 2014, 2016; Long et al., 2016; Long and Szeto, 2017). We find that existing link-based NVH constraints (e.g., Zheng and Chiu, 2011; Long et al., 2016; Long and Szeto, 2017) cannot completely eliminate VH solutions. Instead, our proposed intersection-movement-based NVH constraints and path-based NVH constraints can completely eliminate VH solutions. By integrating link-based, intersection-movement-based, and path-based NVH constraints into the proposed R-DSO-SRDTC formulations, we obtain NVH-DSO-SRDTC models. Equivalent NVH-DSO-SRDTC models can be obtained by introducing an additional product of a sufficiently small coefficient and the sum of cumulative link outflows into the objective function of the R-DSO-SRDTC formulations. The resultant models do not need to include the NVH constraints and are thus linear. We prove that the proposed models can obtain NVH-DSO solutions when the coefficient of the penalty term is positive

and sufficiently small. Furthermore, we prove that without the FIFO consideration, the intersection-movement-based DSO-SRDTC model gives the same optimal TSTC as the link-based and path-based DSO-SRDTC models, no matter whether NVH is considered or not.

To consider FIFO in DSO models, we use entry time to define link-based, intersection-movement-based, and path-based FIFO conditions and formulate the corresponding FIFO constraints, which contain bi-linear terms and lead to a non-convex feasible solution set. By integrating the FIFO constraints into the corresponding LP formulation of the R-DSO-SRDTC problems, we obtain a non-convex *nonlinear* program for the FIFO-DSO-SRDTC problem. To further consider NVH, we integrate both NVH and FIFO constraints into the corresponding LP formulation of the R-DSO-SRDTC problems to obtain a non-convex *nonlinear mixed-integer* program for the NVH-FIFO-DSO-SRDTC problem, in which the integer variables are introduced due to the NVH constraints. Usually, existing solution algorithms for non-convex mixed-integer nonlinear programs can only be used to obtain a local optimum for the FIFO- and NVH-FIFO-DSO-SRDTC problems. Based on the optimality condition of these two problems, the branch-and-bound algorithm proposed by Long and Szeto (2017) is extended to solve them. The merit of the proposed branch-and-bound algorithm is that it can obtain a global optimum. Finally, numerical examples are developed to illustrate the properties and performance of the proposed models.

The contributions of this paper include the following:

First, to the best of our knowledge, we are the pioneers to provide intersection-movement-based formulations for DSO-SRDTC problems and analyze their mathematical properties. The connections of intersection-movement-based DSO-SRDTC models with the link-based and path-based DSO-SRDTC models are clarified. The proposed intersection-movement-based DSO-SRDTC models lead to new analytical results compared to their link-based counterparts and can be solved more efficiently compared to their path-based counterparts.

Second, we find that existing link-based NVH constraints (Long and Szeto, 2017) cannot completely eliminate VH solutions. We propose intersection-movement-based and path-based NVH constraints, which can completely eliminate VH solutions.

Third, we prove that link-based, intersection-movement-based, and path-based DSO-SRDTC models without FIFO constraints are equivalent in terms of obtaining the same optimal TSTC, and illustrate that the three types of formulations of DSO-SRDTC problems with FIFO constraints can obtain different optimal TSTCs because link-based, intersection-movement-based, and path-based FIFO are not equivalent. Link-based FIFO is weaker than intersection-movement-based FIFO, and the intersection-movement-based FIFO is weaker than path-based FIFO. These properties lead to the resulting TSTC for a link-based DSO-SRDTC problem with FIFO constraints is no more than the intersection-movement-based counterpart, and the intersection-movement-based counterpart is no more than the path-based counterpart.

Fourth, we illustrate that cyclic flows can exist in optimal solutions to DSO-SRDTC problems in a general network with time-varying link capacities. This implies that path-based DSO-SRDTC models may not be able to be used for cyclic networks with time-varying link capacities because there can be too many time-dependent cyclic paths to be enumerated first. In contrast, link-based and intersection-movement-based DSO-SRDTC models can be used in general networks with time-varying link capacities and can be solved more efficiently than path-based counterparts.

The rest of this paper is organized as follows: in the next section, the DSO-SRDTC problems without FIFO constraints are formulated as LP problems. The DSO-SRDTC problems with FIFO constraints are formulated as non-convex nonlinear programs or non-convex nonlinear mixed-integer programs in Section 3. Numerical examples are given in Section 4, and finally, conclusions are provided in Section 5.

2. The DSO-SRDTC problems without FIFO constraints

2.1. Notations

We consider a network $G(N, A)$ with multiple origins and destinations, where N and A are defined as the set of nodes and the set of arcs (links), respectively. R and S denote the set of origin nodes and the set of destination nodes, respectively. It is assumed that $R \bigcap S = \varnothing$, i.e., none of the origins are destinations. If a node is neither an origin nor a destination, it is referred to as a general node. We assume there are three types of links in the network: source links, destination links, and general links. Each source (destination) link connects only to one origin (destination) in the network, and each origin (destination) connects only to one source (destination) link. Both source and destination links are dummy links. All source links have infinite inflow capacity and all destination links have infinite storage capacity. Similar to the concept of destination cells in the cell-based DSO-SRDTC problems (e.g., Ziliaskopoulos, 2000; Zhu and Ukkusuri, 2013), we assume that vehicles finally enter destination links and stay on these links. We discretize the time period T of interest into a finite set of time intervals $K = \{k = 1, 2, \cdots, \underline{K}\}$. Let δ be the interval length such that $\delta \underline{K} = T$. As suggested by Ma et al. (2014), the interval length should be chosen such that the free flow travel time and backward shock-wave travel time (i.e., the travel time required by the backward shock-wave from the exit to the entry of a link) of each link are multiples of the time interval. Without loss of generality, we let $\delta = 1$. The following notations are adopted throughout this paper:

Sets

A_R	set of origin links
A_S	set of destination links
$A(i)$	set of links whose tail node is i
$B(i)$	set of links whose head node is i
P^s	set of routes to destination s

$\Gamma(a)$	set of successor links of link *a* (downstream links directly connected to link *a*)
$\Gamma^{-1}(a)$	set of predecessor links of link *a* (upstream links directly connected to link *a*)
Φ	set of index pairs $\{(a,k): a \in A \setminus A_S, k \in K\}$
Φ_L	set of index pairs $\{(s,a,k): s \in S, a \in A \setminus A_S, k \in K\}$
$\bar{\Phi}_L$	set of index pairs $\{(s,a,k): s \in S, a \in A, k \in K\}$
Φ_I	set of index pairs $\{(s,a,b,k): s \in S, a \in A \setminus A_S, b \in \Gamma(a), k \in K\}$
Φ_P	set of index pairs $\{(s,p,k): a \in A \setminus A_S, k \in K\}$

Parameters

L_a	length of link *a*
v_a	free flow speed of vehicles on link *a*
$\bar{\tau}_a$	free flow travel time of vehicles on link *a*
w_a	backward shock-wave speed of traffic on link *a*
$\bar{\iota}_a$	travel time required by the backward shock-wave from the exit to the entry of link *a*
ρ_{jam}	jam density
$Q_a(k)$	link inflow capacity during interval *k*
$C_a(k)$	link outflow capacity during interval *k*
D_a^s	total demand between the entry of origin link *a* and destination *s*

Variables

$U_a(k)$	cumulative number of vehicles (flow) that enter link *a* by the end of interval *k*
$U_a^s(k)$	cumulative number of vehicles that enter link *a* to destination *s* by the end of interval *k*
$U_{ab}^s(k)$	cumulative number of vehicles that enter link *a* by the end of interval *k* and pass through link $b \in \Gamma(a)$ to destination *s*.
$U_{ap}^s(k)$	cumulative number of vehicles on route $p \in P^s$ entering link *a* by the end of interval *k*
$V_a(k)$	cumulative number of vehicles that leave link *a* by the end of interval *k*
$V_a^s(k)$	cumulative number of vehicles that leave link *a* to destination *s* by the end of interval *k*
$V_{ab}^s(k)$	cumulative number of vehicles that leave link *a* by the end of interval *k* and pass through link $b \in \Gamma(a)$ to destination *s*.
$V_{ap}^s(k)$	cumulative number of vehicles on route $p \in P^s$ leaving link *a* by the end of interval *k*

Vectors

$\mathbf{U}$	$[U_a^s(k), s \in S, a \in A, k \in K]$
$\mathbf{V}$	$[V_a^s(k), s \in S, a \in A \setminus A_S, k \in K]$
$\mathbf{x}$	link-based solution vector $\mathbf{x} = [\mathbf{U}, \mathbf{V}]$
$\bar{\mathbf{U}}$	$[U_{ab}^s(k), s \in S, a \in A \setminus A_S, b \in \Gamma(a), k \in K]$
$\bar{\mathbf{V}}$	$[V_{ab}^s(k), s \in S, a \in A \setminus A_S, b \in \Gamma(a), k \in K]$

$\mathbf{y}$	intersection-movement-based solution vector $\mathbf{y} = [\bar{\mathbf{U}}, \bar{\mathbf{V}}]$
$\tilde{\mathbf{U}}$	$[U_{ap}^s(k), s \in S, p \in P^s, a \in A, k \in K]$
$\tilde{\mathbf{V}}$	$[V_{ap}^s(k), s \in S, p \in P^s, a \in A \setminus A_S, k \in K]$
$\mathbf{z}$	path-based solution vector $\mathbf{z} = [\tilde{\mathbf{U}}, \tilde{\mathbf{V}}]$

Acronyms of the DSO-SRDTC problems

R-DSO-SRDTC	DSO-SRDTC problem without both NVH and FIFO constraints
NVH-DSO-SRDTC	DSO-SRDTC problem with NVH constraints
FIFO-DSO-SRDTC	DSO-SRDTC problem with FIFO constraints
NVH-FIFO-DSO-SRDTC	DSO-SRDTC problem with NVH and FIFO constraints

Following Yperman (2007) and Long et al. (2011), a linear interpolation procedure is applied to calculate cumulative flows at non-integer time instants. For example, the cumulative flows of link *a* at time instant $(k+\mu)\delta$ with $0 < \mu < 1$ can be formulated as follows:

$$\begin{cases} U_a^s(k+\mu) = (1-\mu)U_a^s(k) + \mu U_a^s(k+1), \\ V_a^s(k+\mu) = (1-\mu)V_a^s(k) + \mu V_a^s(k+1). \end{cases} \tag{1}$$

2.2. An overview of the link transmission model

The LTM integrates a triangular shaped fundamental diagram and Newell's (1993) simplified method to determine sending and receiving flows (Yperman, 2007). The sending flow of a link is constrained both by the boundary conditions at the upstream end of the link and the outflow capacity of the link. According to Newell's (1993) simplified theory, if a free-flow traffic state occurs at the downstream link boundary at the end of interval *k*, then this state must have been emitted from the upstream boundary $L_a / \delta v_a$ time units earlier (i.e., a free-flow travel time $\bar{\tau}_a$). The sending flow of link *a* during interval *k* can be mathematically expressed as follows (Yperman, 2007):

$$S_a(k) = \min\{U_a(k - \bar{\tau}_a) - V_a(k-1), C_a(k)\}. \tag{2}$$

The receiving flow of a link is constrained both by the boundary conditions at the downstream end of the link and the inflow capacity of the link. According to Newell's (1993) simplified theory, if a congested traffic state occurs at the upstream boundary at the end of interval *k*, then this state must have been emitted from the downstream boundary $-L_a / \delta w_a$ time units earlier (i.e., backward shock-wave travel time $\bar{\iota}_a$), since a congested traffic state travels with a negative speed w_a. The receiving flow of link *a* during interval *k* can be mathematically expressed as follows (Yperman, 2007):

$$R_a(k) = \min\{V_a(k - \bar{\iota}_a) + L_a \rho_{jam} - U_a(k-1), Q_a(k)\}. \tag{3}$$

For each link, its inflow and outflow during an interval should be restricted by its sending and receiving flows during that interval. Hence, we have

$$U_a(k) - U_a(k-1) \le R_a(k), \forall a \in A, k \in K \quad \text{and} \tag{4}$$

$$V_a(k) - V_a(k-1) \le S_a(k), \forall a \in A \setminus A_S, k \in K. \tag{5}$$

Substituting Eqs. (2) and (3) into inequalities (4) and (5), we can obtain the following system of LTM-based flow constraints:

$$\begin{cases} V_a(k) \le U_a(k-\overline{\tau}_a), \forall a \in A \setminus A_S, k \in K, \\ V_a(k) - V_a(k-1) \le C_a(k), \forall a \in A \setminus A_S, k \in K, \\ U_a(k) \le V_a(k-\overline{l}_a) + L_a \rho_{jam}, \forall a \in A \setminus A_S, k \in K, \\ U_a(k) - U_a(k-1) \le Q_a(k), \forall a \in A, k \in K. \end{cases} \tag{6}$$

2.3. Feasible solution sets

2.3.1. The link-based feasible solution set

By definition, we have

$$U_a(k) = \sum_{s \in S} U_a^s(k), \forall a \in A, k \in K \quad \text{and} \tag{7}$$

$$V_a(k) = \sum_{s \in S} V_a^s(k), \forall a \in A \setminus A_S, k \in K. \tag{8}$$

Substituting Eqs. (7) and (8) into the system of inequalities (6), we have

$$\begin{cases} \sum_{s \in S} V_a^s(k) \le \sum_{s \in S} U_a^s(k-\overline{\tau}_a), \forall a \in A \setminus A_S, k \in K, \\ \sum_{s \in S} \left[V_a^s(k) - V_a^s(k-1) \right] \le C_a(k), \forall a \in A \setminus A_S, k \in K, \\ \sum_{s \in S} U_a^s(k) \le \sum_{s \in S} V_a^s(k-\overline{l}_a) + L_a \rho_{jam}, \forall a \in A \setminus A_S, k \in K, \\ \sum_{s \in S} \left[U_a^s(k) - U_a^s(k-1) \right] \le Q_a(k), \forall a \in A, k \in K. \end{cases} \tag{9}$$

The cumulative link outflow disaggregated by destination should also be constrained by the boundary condition at the upstream end of the link, and hence we have

$$V_a^s(k) \le U_a^s(k-\overline{\tau}_a), \forall s \in S, a \in A \setminus A_S, k \in K. \tag{10}$$

Traffic flows in the LTM should also satisfy the FIFO, flow conservation, and definitional constraints. In this section, we do not consider FIFO constraints, but they will be left to be formulated in the next section. The flow conservation constraints require that the flow that enters any node (except the destination node), together with the demand generated at that node, must all exit from that node. All traffic demands should enter the network and arrive at their destinations during the studied period. Hence, we have

$$U_a^s(\underline{K}) = D_a^s, \forall a \in A_R, s \in S \quad \text{and} \tag{11}$$

$$U_a^s(\underline{K}) = \sum_{b \in A_R} D_b^s, \forall a \in A_S, s \in S. \tag{12}$$

Different from the CTM treating cells as ordinary, merging, and diverging cells, we adopt a general node model to describe traffic transmission from link to link, which does not distinguish ordinary, merging, and diverging links. Because general nodes do not generate traffic demand, we have the following flow conservation constraint:

$$\sum_{a\in B(i)} V_a^s(k) = \sum_{a\in A(i)} U_a^s(k), \forall s \in S, i \in N \setminus \{R,S\}, k \in K . \tag{13}$$

Definitional constraints are used to describe the nonnegative and non-decreasing properties of cumulative link inflows and outflows disaggregated by destination, and given as follows:

$$U_a^s(k) - U_a^s(k-1) \geq 0, \forall s \in S, a \in A, k \in K , \text{ and} \tag{14}$$

$$V_a^s(k) - V_a^s(k-1) \geq 0, \forall s \in S, a \in A \setminus A_S, k \in K . \tag{15}$$

Constraints (14) and (15) imply that the cumulative flows disaggregated by destination are non-decreasing. Initially, the disaggregated cumulative flows equal zero:

$$U_a^s(0) = 0, \forall s \in S, a \in A , \text{ and} \tag{16}$$

$$V_a^s(0) = 0, \forall s \in S, a \in A \setminus A_S . \tag{17}$$

We note that the initial conditions (16) and (17) are inputs to constraints (14) and (15) for $k = 1$, respectively.

Definition 1 (Link-based feasible solution set): Constraints (9)-(15) form a feasible solution set for the link-based DSO-SRDTC problem. The set is formulated as follows:

$$\Omega = \{\mathbf{x} \,|\, \text{constraints (9)-(15) hold}\}. \tag{18}$$

2.3.2. The intersection-movement-based feasible solution set

By definition, we have

$$U_a^s(k) = \sum_{b\in\Gamma(a)} U_{ab}^s(k), \forall s \in S, a \in A \setminus A_S, k \in K , \tag{19}$$

$$U_a^s(k) = \sum_{b\in\Gamma^{-1}(a)} V_{ba}^s(k), \forall s \in S, a \in A_S, k \in K , \text{ and} \tag{20}$$

$$V_a^s(k) = \sum_{b\in\Gamma(a)} V_{ab}^s(k), \forall s \in S, a \in A \setminus A_S, k \in K . \tag{21}$$

Definition 2 (Transfer function from an intersection-movement-based solution vector to a link-based solution vector). A transfer function from an intersection-movement-based solution vector to a link-based solution vector is defined as follows:

$$\mathbf{x} = \boldsymbol{\varphi}_1(\mathbf{y}), \tag{22}$$

where $\boldsymbol{\varphi}_1(\mathbf{y})$ is a point-to-point mapping and defined by Eqs. (19)-(21).

Substituting Eqs. (19)-(21) into constraints (9), (11), and (12), we have

$$\begin{cases} \sum_{s\in S}\sum_{b\in\Gamma(a)} V_{ab}^s(k) \leq \sum_{s\in S}\sum_{b\in\Gamma(a)} U_{ab}^s(k-\bar{\tau}_a), \forall a \in A \setminus A_S, k \in K, \\ \sum_{s\in S}\sum_{b\in\Gamma(a)} \left[V_{ab}^s(k) - V_{ab}^s(k-1)\right] \leq C_a(k), \forall a \in A \setminus A_S, k \in K, \\ \sum_{s\in S}\sum_{b\in\Gamma(a)} U_{ab}^s(k) \leq \sum_{s\in S}\sum_{b\in\Gamma(a)} V_{ab}^s(k-\bar{l}_a) + L_a\rho_{jam}, \forall a \in A \setminus A_S, k \in K, \\ \sum_{s\in S}\sum_{b\in\Gamma(a)} \left[U_{ab}^s(k) - U_{ab}^s(k-1)\right] \leq Q_a(k), \forall a \in A, k \in K, \end{cases} \tag{23}$$

$$\sum_{b\in\Gamma(a)} U_{ab}^{s}(\underline{K}) = D_{a}^{s}, \forall s \in S, a \in A_R, \text{ and} \tag{24}$$

$$\sum_{b\in\Gamma^{-1}(a)} V_{ba}^{s}(\underline{K}) = \sum_{b\in A_R} D_{b}^{s}, \forall s \in S, a \in A_S. \tag{25}$$

The cumulative link outflows disaggregated by intersection movement and destination should also be constrained by the boundary condition at the upstream end of the link, and hence we have

$$V_{ab}^{s}(k) \le U_{ab}^{s}(k-\overline{\tau}_a), \forall s \in S, a \in A \setminus A_S, b \in \Gamma(a), k \in K. \tag{26}$$

The intersection-movement-based flow conservation constraint can be formulated as follows:

$$\sum_{b\in\Gamma^{-1}(a)} V_{ba}^{s}(k) = \sum_{b\in\Gamma(a)} U_{ab}^{s}(k), \forall s \in S, a \in A \setminus A_S, k \in K. \tag{27}$$

The non-negative and non-decreasing properties of cumulative link inflows and outflows disaggregated by intersection movement and destination can be formulated as the following constraints:

$$U_{ab}^{s}(k) - U_{ab}^{s}(k-1) \ge 0, \forall s \in S, a \in A \setminus A_S, b \in \Gamma(a), k \in K \quad \text{and} \tag{28}$$

$$V_{ab}^{s}(k) - V_{ab}^{s}(k-1) \ge 0, \forall s \in S, a \in A \setminus A_S, b \in \Gamma(a), k \in K. \tag{29}$$

The initial conditions for constraints (28) and (29) are given as follows, respectively:

$$U_{ab}^{s}(0) = 0, \forall s \in S, a \in A \setminus A_S, b \in \Gamma(a) \quad \text{and} \tag{30}$$

$$V_{ab}^{s}(0) = 0, \forall s \in S, a \in A \setminus A_S, b \in \Gamma(a). \tag{31}$$

Definition 3 (Intersection-movement-based feasible solution set): Constraints (23)-(29) form a feasible solution set for the intersection-movement-based DSO-SRDTC problem. The set is formulated as follows:

$$\overline{\Omega} = \{\mathbf{y} \mid \text{constraints (23)-(29) hold}\}. \tag{32}$$

Proposition 1: For all $\mathbf{y} \in \overline{\Omega}$, we have $\mathbf{x} = \boldsymbol{\varphi}_1(\mathbf{y}) \in \Omega$.

The proof is given in Appendix A.1.

Proposition 2: For any $\mathbf{x} \in \Omega$, there exists a vector $\mathbf{y} \in \overline{\Omega}$ such that $\mathbf{x}$ and $\mathbf{y}$ satisfy Eqs. (19)-(21), i.e., $\mathbf{x} = \boldsymbol{\varphi}_1(\mathbf{y})$.

The proof is given in Appendix A.2.

Proposition 1 implies that any feasible intersection-movement-based solution vector can be transformed into a unique feasible link-based solution vector. Proposition 2 implies that a link-based solution vector can be obtained from multiple intersection-movement-based solution vectors. The proof of Proposition 2 provides a method to retrieve a feasible intersection-movement-based solution vector from a feasible link-based solution vector.

2.3.3. The path-based feasible solution set

By definition, we have

$$U_a^s(k) = \sum_{p \in P^s} U_{ap}^s(k), \forall s \in S, a \in A, k \in K \,, \tag{33}$$

$$V_a^s(k) = \sum_{p \in P^s} V_{ap}^s(k), \forall s \in S, a \in A \setminus A_S, k \in K \,, \tag{34}$$

$$U_{ab}^s(k) = \sum_{p \in P^s} \varsigma_{abp} U_{ap}^s(k), \forall s \in S, a \in A \setminus A_S, k \in K \text{, and} \tag{35}$$

$$V_{ab}^s(k) = \sum_{p \in P^s} \varsigma_{abp} V_{ap}^s(k), \forall s \in S, a \in A \setminus A_S, k \in K \,, \tag{36}$$

where $\varsigma_{abp} = 1$ if link *b* is the next link after leaving link *a* along route *p*; otherwise, $\varsigma_{abp} = 0$.

Definition 4 (Transfer function from a path-based solution vector to an intersection-movement-based solution vector). A transfer function from a path-based solution vector to an intersection-movement-based solution vector is defined as follows:

$$\mathbf{y} = \boldsymbol{\varphi}_2(\mathbf{z}), \tag{37}$$

where $\boldsymbol{\varphi}_2(\mathbf{y})$ is a point-to-point mapping, and defined by Eqs. (35) and (36).

Substituting Eqs. (33) and (34) into constraints (9), (11), and (12), we have

$$\begin{cases} \sum_{s \in S} \sum_{p \in P^s} V_{ap}^s(k) \le \sum_{s \in S} \sum_{p \in P^s} U_{ap}^s(k - \overline{\tau}_a), \forall a \in A \setminus A_S, k \in K, \\ \sum_{s \in S} \sum_{p \in P^s} \left[V_{ap}^s(k) - V_{ap}^s(k-1) \right] \le C_a(k), \forall a \in A \setminus A_S, k \in K, \\ \sum_{s \in S} \sum_{p \in P^s} U_{ap}^s(k) \le \sum_{s \in S} \sum_{p \in P^s} V_{ap}^s(k - \overline{\iota}_a) + L_a \rho_{jam}, \forall a \in A \setminus A_S, k \in K, \\ \sum_{s \in S} \sum_{p \in P^s} [U_{ap}^s(k) - U_{ap}^s(k-1)] \le Q_a(k), \forall a \in A, k \in K, \end{cases} \tag{38}$$

$$\sum_{s \in S} \sum_{p \in P^s} U_{ap}^s(\underline{K}) = D_a^s, \forall s \in S, a \in A_R \text{, and} \tag{39}$$

$$\sum_{p \in P^s} U_{ap}^s(\underline{K}) = \sum_{b \in A_R} D_b^s, \forall s \in S, a \in A_S \,. \tag{40}$$

The cumulative link outflow disaggregated by path should also be constrained by the boundary condition at the upstream end of the link and hence we have

$$V_{ap}^s(k) \le U_{ap}^s(k - \overline{\tau}_a), \forall s \in S, p \in P^s, a \in A \setminus A_S, k \in K \,. \tag{41}$$

The path-based flow conservation constraint can be formulated as follows:

$$V_{ap}^s(k) = \sum_{b \in \Gamma(a)} \varsigma_{abp} U_{bp}^s(k), \forall s \in S, p \in P^s, a \in A \setminus A_S, k \in K. \tag{42}$$

The non-negative and non-decreasing properties of cumulative link inflows and outflows disaggregated by path can be formulated as the following constraints:

$$U_{ap}^s(k) - U_{ap}^s(k-1) \ge 0, \forall s \in S, p \in P^s, a \in A, k \in K \text{ and} \tag{43}$$

$$V_{ap}^s(k) - V_{ap}^s(k-1) \ge 0, \forall s \in S, p \in P^s, a \in A, k \in K \,. \tag{44}$$

The initial conditions for constraints (43) and (44) are given as follows, respectively:

$$U_{ap}^{s}(0) = 0, \forall s \in S, p \in P^{s}, a \in A \text{ and} \tag{45}$$

$$V_{ap}^{s}(0) = 0, \forall s \in S, p \in P^{s}, a \in A \setminus A_{S}. \tag{46}$$

Definition 5 (Path-based feasible solution set): Constraints (38)-(44) form a feasible solution set for the path-based DSO-SRDTC problem. The set is formulated as follows:

$$\tilde{\Omega} = \{\mathbf{z} \mid \text{constraints (38)-(44) hold}\}. \tag{47}$$

Proposition 3: If $\mathbf{z} \in \tilde{\Omega}$, we have $\mathbf{y} = \boldsymbol{\varphi}_2(\mathbf{z}) \in \bar{\Omega}$ and $\mathbf{x} = \boldsymbol{\varphi}_1(\boldsymbol{\varphi}_2(\mathbf{z})) \in \Omega$.

The proof is given in Appendix A.3.

Proposition 4: For any $\mathbf{y} \in \bar{\Omega}$, there exists a vector $\mathbf{z} \in \tilde{\Omega}$ such that $\mathbf{y} = \boldsymbol{\varphi}_2(\mathbf{z})$.

The proof is given in Appendix A.4.

Proposition 5: For any $\mathbf{x} \in \Omega$, there exists a vector $\mathbf{z} \in \tilde{\Omega}$ such that $\mathbf{x} = \boldsymbol{\varphi}_1(\boldsymbol{\varphi}_2(\mathbf{z}))$.

This proposition follows directly from Propositions 2 and 4.

Proposition 3 implies that any feasible path-based solution vector can be transformed into a unique intersection-movement-based solution vector and a unique feasible link-based solution vector. Proposition 4 implies that an intersection-movement-based solution vector can be obtained from multiple path-based solution vectors. The proof of Proposition 4 provides a method to retrieve a feasible path-based solution vector from a feasible intersection-movement-based solution vector. Proposition 5 implies that a link-based solution vector can be derived from multiple path-based solution vectors.

2.4. Non-vehicle holding constraints

Constraints (2) and (3) in the LTM are relaxed to a set of less-than-or-equal-to constraint (9) in the link-based DSO-SRDTC models that will be introduced later. For an optimal solution to the link-based DSO-SRDTC models, if there exists an index pair $(a,k) \in \Phi$ such that all of the constraints in condition (9) fall into the inequality region, vehicles are held on link *a* without moving forward to their successor link $b \in \Gamma(a)$ during interval *k*, even if there is enough capacity in successor link *b* during interval *k*. Such a solution property is referred to as the link-based VH problem. The definition of the link-based VH problem directly follows the definition introduced by Shen et al. (2007), Zheng and Chiu (2011), and Zhu and Ukkusuri (2013). According to this definition, Long and Szeto (2017) developed link-based NVH constraints by using the big-M method.

In the following subsections, we will separately define an NVH solution vector for link-based, intersection-movement-based, and path-based DSO-SRDTC problems. There are two major reasons for the separate definitions. Firstly, the decision variables of link-based, intersection-movement-based, and path-based DSO-SRDTC problems are different. Secondly, a link-based solution vector does not contain path information, and the link-based NVH solution vector is defined on each link and its downstream links directly

connected to it. However, both intersection-movement-based and path-based solution vectors contain path information, and the intersection-movement-based and path-based NVH solution vectors can be defined on each intersection movement. We will point out that the existing link-based NVH constraints (Long and Szeto, 2017) cannot completely eliminate VH solutions and we will prove that the proposed intersection-movement-based and path-based NVH constraints can completely eliminate VH solutions. Due to different definitions on NVH solution vectors, we will develop different big-M methods to formulate intersection-movement-based and path-based NVH constraints.

Section 2.4 contains four subsections. In Section 2.4.1, we first provide an overview on the existing definitions of link-based NVH and VH solution vectors, which are referred to as weak link-based NVH and strong link-based VH solution vectors, respectively, to distinguish from the proposed definitions of strong link-based NVH and weak VH solution vectors in Section 2.4.4. Note that a strong solution vector is obtained under a tighter or more restricted condition than a weak solution vector. We then introduce existing link-based NVH constraints, which are referred to weak link-based NVH conditions, as they are looser than the proposed link-based NVH conditions. In Section 2.4.2, the existing definitions of weak link-based NVH and strong link-based VH solution vectors are extended to define weak intersection-movement-based NVH and strong intersection-movement-based VH solution vectors, and the intersection-movement-based NVH constraints are formulated. In Section 2.4.3, the existing definitions of weak link-based NVH and strong link-based VH solution vectors are extended to define weak path-based NVH and strong path-based VH solution vectors, and the path-based NVH constraints are formulated. In Section 2.4.4, we first propose definitions of strong link-based NVH, weak link-based VH, strong intersection-movement-based NVH, weak intersection-movement-based VH, strong path-based NVH, and weak path-based VH solution vectors. We then illustrate that there are differences between the classical and proposed NVH definitions and the differences in the definitions between the terms “strong NVH”, “weak NVH”, “strong VH”, and “weak VH”. We finally formulate the strong intersection-movement-based and path-based NVH conditions. Again, “strong” herein means “tight” or “restricted”.

2.4.1. An overview of existing link-based non-vehicle holding constraints

According to the definition of the link-based VH problem, weak link-based NVH and strong link-based VH solution vectors can be stated as follows (Long and Szeto, 2017):

Definition 6 (Weak link-based NVH and strong link-based VH solution vectors). Let $\mathbf{x} \in \Omega$ be a feasible solution vector. $\mathbf{x}$ is defined as a weak link-based NVH solution vector if it satisfies the condition that, for all $a \in A \setminus A_S$ and $k \in K$, at least one of the following less-than-or-equal-to inequalities becomes binding (i.e., the equality holds in at least one of the following inequalities):

$$\begin{cases} \sum_{s\in S} V_a^s(k) \le \sum_{s\in S} U_a^s(k-\overline{\tau}_a), \\ \sum_{s\in S} \left[V_a^s(k) - V_a^s(k-1) \right] \le C_a(k), \\ \sum_{s\in S} U_b^s(k) \le \sum_{s\in S} V_b^s(k-\overline{l}_b) + L_b \rho_{jam}, \forall b \in \Gamma(a), \\ \sum_{s\in S} \left[U_b^s(k) - U_b^s(k-1) \right] \le Q_b(k), \forall b \in \Gamma(a). \end{cases} \tag{48}$$

Otherwise, $\mathbf{x}$ is defined as a strong link-based VH solution vector.

Definition 6 implies that an upstream link can have vehicles not discharged due to congestion of one or some downstream links, but not necessarily all downstream links directly connected to the upstream link. In other words, this definition allows the existence of vehicles on upstream links that do not move forward to their own downstream link even if there is no congestion on their own downstream link.

For any link a (except destination links) with $|\Gamma(a)|$ successor links, the first two inequalities in the system (48) restrict the sending flow of link a, and the last two inequalities in the system (48) restrict the receiving flows of all successor links of link a. Hence, the number of constraints in the system (48) with respect to interval k is $2+2|\Gamma(a)|$. The weak link-based NVH conditions require that the equality holds in at least one of the $2+2|\Gamma(a)|$ constraints. The weak link-based NVH conditions can be formulated within the mixed integer programming (MIP) framework using the well-known "Big M" method, which introduces a large positive coefficient, M, to the constraints, as follows (Pavlis and Recker, 2009; Long and Szeto, 2017):

$$-\left[\theta_a^0(k) + \sum_{i=1}^{m_a} \theta_a^i(k) \right] M \le V_a^s(k) - U_a^s(k-\overline{\tau}_a), \tag{49a}$$

$$-\left[1 - \theta_a^0(k) + \sum_{i=1}^{m_a} \theta_a^i(k) \right] M \le \sum_{s\in S} \left[V_a^s(k) - V_a^s(k-1) \right] - C_a(k), \tag{49b}$$

$$-\left[\sum_{i=1}^{m_a} \sigma_i^j + \theta_a^0(k) - \sum_{i=1}^{m_a} (2\sigma_i^j - 1)\theta_a^i(k) \right] M \le \sum_{s\in S} U_{b_j}^s(k) - \sum_{s\in S} V_{b_j}^s(k-\overline{l}_{b_j}) - L_{b_j}\rho_{jam}, \forall j \in J_a, \tag{49c}$$

$$-\left[1 + \sum_{i=1}^{m_a} \sigma_i^j - \theta_a^0(k) - \sum_{i=1}^{m_a} (2\sigma_i^j - 1)\theta_a^i(k) \right] M \le \sum_{s\in S} \left[U_{b_j}^s(k) - U_{b_j}^s(k-1) \right] - Q_{b_j}(k), \forall j \in J_a \quad , \tag{49d}$$

$$\sum_{i=0}^{m_a} 2^i \theta_a^i(k) \le 1 + 2|\Gamma(a)|, \text{ and} \tag{49g}$$

$$\theta_a^i(k) \in \{0,1\}, \forall i = 0,1,\cdots,m_a, \tag{49h}$$

where $J_a = \{1,2,\cdots,|\Gamma(a)|\}$ is an index set for successor links of link a. b_j is the j-th link in $\Gamma(a)$. $m_a = \arg\min_m \left\{ 2^{m+1} \ge 2+2|\Gamma(a)| \right\}$. σ_i^j equals 0 or 1 such that $\sum_{i=1}^{m_a} 2^{i-1}\sigma_i^j = j$, which implies that the value of σ_i^j is unique and can be predetermined. Introducing σ_i^j in the NVH constraints aims to reduce the number of binary variables $\theta_a^i(k)$ used. For each interval k, there are m_a+1 binary variables in the system (49), which can form 2^{m_a+1} combinations. There are $2+2|\Gamma(a)|$ LTM-based flow constraints in

the system (48). Constraint (49g) implies that we only use $2+2|\Gamma(a)|$ combinations of the binary variables.

2.4.2. Intersection-movement-based non-vehicle holding constraints

The definitions of weak link-based NVH and strong link-based VH solution vectors can be modified to define weak intersection-movement-based NVH and strong intersection-movement-based VH solution vectors as follows:

Definition 7 (Weak intersection-movement-based NVH and strong intersection-movement-based VH solution vectors). Let $\mathbf{y} \in \bar{\Omega}$ be a feasible solution vector. $\mathbf{y}$ is defined as a weak intersection-movement-based NVH solution vector if it satisfies the condition that, for all $a \in A \setminus A_S$ and $k \in K$, at least one of the following less-than-or-equal-to inequalities becomes binding:

$$\begin{cases} \sum_{s\in S}\sum_{b\in\Gamma(a)} V_{ab}^{s}(k) \le \sum_{s\in S}\sum_{b\in\Gamma(a)} U_{ab}^{s}(k-\bar{\tau}_a), \\ \sum_{s\in S}\sum_{b\in\Gamma(a)} \left[V_{ab}^{s}(k)-V_{ab}^{s}(k-1)\right] \le C_a(k), \\ \sum_{s\in S}\sum_{c\in\Gamma(b)} U_{bc}^{s}(k) \le \sum_{s\in S}\sum_{c\in\Gamma(b)} V_{bc}^{s}(k-\bar{t}_b) + L_b\rho_{jam}, \forall b\in\Gamma(a), \\ \sum_{s\in S}\sum_{c\in\Gamma(b)} \left[U_{bc}^{s}(k)-U_{bc}^{s}(k-1)\right] \le Q_b(k), \forall b\in\Gamma(a). \end{cases} \tag{50}$$

Otherwise, $\mathbf{y}$ is defined as a strong intersection-movement-based VH solution vector.

Proposition 6: If $\mathbf{y} \in \bar{\Omega}$ is a weak intersection-movement-based NVH solution vector, then $\mathbf{x} = \boldsymbol{\varphi}_1(\mathbf{y})$ is a weak link-based NVH solution vector.

The proof is given in Appendix A.5.

Similar to the link-based NVH constraint (49), the intersection-movement-based NVH conditions for any link $a \in A \setminus A_S$ and interval $k \in K$ can be formulated within the MIP framework as follows:

$$-\left[\theta_a^0(k)+\sum_{i=1}^{m_a}\theta_a^i(k)\right]M \le \sum_{b\in\Gamma(a)}\left[V_{ab}^{s}(k)-U_{ab}^{s}(k-\bar{\tau}_a)\right], \tag{51a}$$

$$-\left[1-\theta_a^0(k)+\sum_{i=1}^{m_a}\theta_a^i(k)\right]M \le \sum_{s\in S}\sum_{b\in\Gamma(a)}\left[V_{ab}^{s}(k)-V_{ab}^{s}(k-1)\right]-C_a(k), \tag{51b}$$

$$-\left[\sum_{i=1}^{m_a}\sigma_i^j+\theta_a^0(k)-\sum_{i=1}^{m_a}(2\sigma_i^j-1)\theta_a^i(k)\right]M \le \sum_{s\in S}\sum_{c\in\Gamma(b_j)}\left[U_{b_jc}^{s}(k)-V_{b_jc}^{s}(k-\bar{t}_{b_j})\right]-L_{b_j}\rho_{jam}, \forall j\in J_a, \tag{51c}$$

$$-\left[1+\sum_{i=1}^{m_a}\sigma_i^j-\theta_a^0(k)-\sum_{i=1}^{m_a}(2\sigma_i^j-1)\theta_a^i(k)\right]M \le \sum_{s\in S}\sum_{c\in\Gamma(b_j)}\left[U_{b_jc}^{s}(k)-U_{b_jc}^{s}(k-1)\right]-Q_{b_j}(k), \forall j\in J_a, \tag{51d}$$

$$\sum_{i=0}^{m_a}2^i\theta_a^i(k) \le 1+2|\Gamma(a)|, \text{ and} \tag{51g}$$

$$\theta_a^i(k)\in\{0,1\}, \forall i=0,1,\cdots,m_a. \tag{51h}$$

2.4.3. Path-based non-vehicle holding constraints

The definitions of weak link-based and weak intersection-movement-based NVH solution vectors and strong link-based and strong intersection-movement-based VH solution vectors can be modified to define weak path-based NVH and strong path-based VH solution vectors as follows:

Definition 8 (Weak path-based NVH and strong path-based VH solution vectors). Let $\mathbf{z} \in \tilde{\Omega}$ be a feasible solution vector. $\mathbf{z}$ is defined as a weak path-based NVH solution vector if it satisfies the condition that, for all $a \in A \setminus A_S$ and $k \in K$, at least one of the following less-than-or-equal-to inequalities becomes binding:

$$\begin{cases} \sum_{s\in S}\sum_{p\in P^s} V_{ap}^s(k) \le \sum_{s\in S}\sum_{p\in P^s} U_{ap}^s(k-\bar{\tau}_a) \\ \sum_{s\in S}\sum_{p\in P^s} \left[V_{ap}^s(k) - V_{ap}^s(k-1)\right] \le C_a(k), \\ \sum_{s\in S}\sum_{p\in P^s} U_{bp}^s(k) \le \sum_{s\in S}\sum_{p\in P^s} V_{bp}^s(k-\bar{t}_b) + L_b\rho_{jam}, \forall b \in \Gamma(a), \\ \sum_{s\in S}\sum_{p\in P^s} \left[U_{bp}^s(k) - U_{bp}^s(k-1)\right] \le Q_b(k), \forall b \in \Gamma(a). \end{cases} \tag{52}$$

Otherwise, $\mathbf{z}$ is defined as a strong path-based VH solution vector.

Proposition 7: If $\mathbf{z} \in \tilde{\Omega}$ is a weak path-based NVH solution vector, then $\mathbf{y} = \boldsymbol{\varphi}_2(\mathbf{z})$ is a weak intersection-movement-based NVH solution vector, and $\mathbf{x} = \boldsymbol{\varphi}_1(\boldsymbol{\varphi}_2(\mathbf{z}))$ is a weak link-based NVH solution vector.

The proof is given in Appendix A.6.

Similar to the link-based NVH constraint (49) and the intersection-movement-based NVH constraint (51), the weak path-based NVH conditions can be formulated within the MIP framework as follows:

$$-\left[\theta_a^0(k) + \sum_{i=1}^{m_a}\theta_a^i(k)\right]M \le \sum_{p\in P^s}\left[V_{ap}^s(k) - U_{ap}^s(k-\bar{\tau}_a)\right], \tag{53a}$$

$$-\left[1 - \theta_a^0(k) + \sum_{i=1}^{m_a}\theta_a^i(k)\right]M \le \sum_{s\in S}\sum_{p\in P^s}\left[V_{ap}^s(k) - V_{ap}^s(k-1)\right] - C_a(k), \tag{53b}$$

$$-\left[\sum_{i=1}^{m_a}\sigma_i^j + \theta_a^0(k) - \sum_{i=1}^{m_a}(2\sigma_i^j - 1)\theta_a^i(k)\right]M \le \sum_{s\in S}\sum_{p\in P^s}\left[U_{b_j p}^s(k) - V_{b_j p}^s(k-\bar{t}_{b_j})\right] - L_{b_j}\rho_{jam}, \forall j \in J_a, \tag{53c}$$

$$-\left[1 + \sum_{i=1}^{m_a}\sigma_i^j - \theta_a^0(k) - \sum_{i=1}^{m_a}(2\sigma_i^j - 1)\theta_a^i(k)\right]M \le \sum_{s\in S}\sum_{p\in P^s}\left[U_{b_j p}^s(k) - U_{b_j p}^s(k-1)\right] - Q_{b_j}(k), \forall j \in J_a, \tag{53d}$$

$$\sum_{i=0}^{m_a} 2^i\theta_a^i(k) \le 1 + 2|\Gamma(a)|, \text{ and} \tag{53g}$$

$$\theta_a^i(k) \in \{0,1\}, \forall i = 0,1,\cdots,m_a. \tag{53h}$$

2.4.4. The proposed definitions of strong NVH solution vectors

According to the definition of VH, we propose the definition of a strong link-based NVH solution vector

as follows: a solution vector of the link-based DSO-SRDTC problem is defined as a strong link-based NVH solution vector if no more vehicles can move forward from an upstream link to their own downstream link. This differs from the weak link-based NVH solution vector in the literature mentioned earlier. Because the FIFO requirement is not considered in this section, FIFO violations can exist in a strong link-based NVH solution vector. Similarly, FIFO violations can exist in a weak link-based NVH solution vector. Mathematically, strong link-based NVH and weak link-based VH solution vectors can be defined as follows:

Definition 9 (Strong link-based NVH and weak link-based VH solution vectors). Let $\mathbf{x} \in \Omega$ be a link-based feasible solution vector. $\mathbf{x}$ is defined as a weak link-based VH solution vector if there exists a link-based feasible solution vector $\tilde{\mathbf{x}} \in \Omega$ such that $\tilde{\mathbf{x}} \neq \mathbf{x}$ and $\tilde{\mathbf{x}} \geq \mathbf{x}$. Otherwise, $\mathbf{x}$ is defined as a strong link-based NVH solution vector.

Because $\mathbf{x} \in \Omega$, $\tilde{\mathbf{x}} \in \Omega$, and $\tilde{\mathbf{x}} \geq \mathbf{x}$, the flow conservation constraint implies that $\mathbf{x}$ and $\tilde{\mathbf{x}}$ have the same cumulative link flow by the end of the last time interval $\underline{K}$, i.e., we have $U_a^s(\underline{K}) = \tilde{U}_a^s(\underline{K}), \forall s \in S, a \in A$, and $V_a^s(\underline{K}) = \tilde{V}_a^s(\underline{K}), \forall s \in S, a \in A \setminus A_S$. This implies that the total inflow and outflow of the whole studied period of each link are the same for both solution vectors. Moreover, the condition $\tilde{\mathbf{x}} \geq \mathbf{x}$ can ensure that the cumulative flows of all routes in solution vector $\tilde{\mathbf{x}}$ are not less than those in solution vector $\mathbf{x}$, and the routes of all vehicles in solution vector $\tilde{\mathbf{x}}$ are the same as those in solution vector $\mathbf{x}$. In addition, $\tilde{\mathbf{x}} \neq \mathbf{x}$, $\tilde{\mathbf{x}} \geq \mathbf{x}$, and the flow conservation constraint (13) imply that there exists an index pair $\{s, a, k\} \in \Phi_L$ such that $V_a^s(k) < \tilde{V}_a^s(k)$, which indicates that some more vehicles can move forward from upstream links to their downstream links. Note that because the FIFO requirement is not considered in Definition 9, FIFO violations can exist in a strong link-based NVH solution vector. This implies that vehicles on an upstream link can overpass the vehicles on the same upstream link with different downstream links (including those congested downstream links) and can be discharged to their own downstream links. Hence, it is possible that under Definition 9, an upstream link has vehicles discharged to their own downstream link when other downstream links are congested.

Proposition 8: Any strong link-based VH solution vector $\mathbf{x} \in \Omega$ defined by Definition 6 satisfies the weak link-based VH condition defined by Definition 9, and any strong link-based NVH solution vector $\mathbf{x}' \in \Omega$ defined by Definition 9 satisfies the weak link-based NVH condition defined by Definition 6.

The proof is given in Appendix A.7.

Let Ω_{11} be the set of weak link-based NVH solution vectors defined by Definition 6, and Ω_{12} be the set of strong link-based VH solution vectors defined by Definition 6. Based on Definition 6, we have $\Omega_{11} \bigcap \Omega_{12} = \varnothing$ and $\Omega_{11} \bigcup \Omega_{12} = \Omega$. Let Ω_{21} be the set of strong link-based NVH solution vectors defined by Definition 9, and Ω_{22} be the set of weak link-based VH solution vectors defined by Definition 9. Based on Definition 9, we have $\Omega_{21} \bigcap \Omega_{22} = \varnothing$ and $\Omega_{21} \bigcup \Omega_{22} = \Omega$. Based on Proposition 8, we have $\Omega_{21} \subseteq \Omega_{11}$ and $\Omega_{12} \subseteq \Omega_{22}$. This is consistent with the definition that a strong solution vector is obtained

under a tighter or more restricted condition than a weak solution vector. As will be shown by Example 1 in Section 4, a weak link-based VH solution vector defined by Definition 9 may not satisfy the strong link-based VH condition defined by Definition 6, and a weak link-based NVH solution vector defined by Definition 6 may not satisfy the strong link-based NVH condition defined by Definition 9.

Similar to the definition of strong link-based NVH solution vectors, strong intersection-movement-based and strong path-based NVH solution vectors can be defined as follows:

Definition 10 (Strong intersection-movement-based NVH and weak intersection-movement-based VH solution vectors). Let $\mathbf{y} \in \overline{\Omega}$ be an intersection-movement-based feasible solution vector. $\mathbf{y}$ is defined as a weak intersection-movement-based VH solution vector if there exists an intersection-movement-based feasible solution vector $\tilde{\mathbf{y}} \in \overline{\Omega}$ such that $\tilde{\mathbf{y}} \neq \mathbf{y}$ and $\tilde{\mathbf{y}} \geq \mathbf{y}$. Otherwise, $\mathbf{y}$ is defined as a strong intersection-movement-based NVH solution vector.

Definition 11 (Strong path-based NVH and weak path-based VH solution vectors). Let $\mathbf{z} \in \tilde{\Omega}$ be a path-based feasible solution vector. $\mathbf{z}$ is defined as a weak path-based VH solution vector if there exists a path-based feasible solution vector $\tilde{\mathbf{z}} \in \tilde{\Omega}$ such that $\tilde{\mathbf{z}} \neq \mathbf{z}$ and $\tilde{\mathbf{z}} \geq \mathbf{z}$. Otherwise, $\mathbf{z}$ is defined as a strong path-based NVH solution vector.

Similar to Proposition 8, we can prove that any strong intersection-movement-based NVH solution vector defined by Definition 10 satisfies the weak intersection-movement-based NVH condition defined by Definition 7, and any strong path-based NVH solution vector defined by Definition 11 satisfies the weak path-based NVH condition defined by Definition 8. The proofs basically follow the proof of Proposition 8 with changes in notations and are omitted.

Because intersection-movement-based solution vectors contain path information, a strong intersection-movement-based NVH solution vector can be *equivalently* defined on each intersection movement and we have the following proposition:

Proposition 9: Let $\mathbf{y} \in \overline{\Omega}$ be a feasible solution vector. $\mathbf{y}$ is a strong intersection-movement-based NVH solution vector if and only if $\mathbf{y}$ satisfies the condition that, for all $a \in A \setminus A_S$, $b \in \Gamma(a)$, and $k \in K$, at least one of the following less-than-or-equal-to inequalities becomes binding:

$$\begin{cases} \sum_{s\in S}\sum_{b'\in\Gamma(a)}\left[V^s_{ab'}(k)-V^s_{ab'}(k-1)\right] \leq C_a(k), \\ \sum_{s\in S}\sum_{c\in\Gamma(b)} U^s_{bc}(k) \leq \sum_{s\in S}\sum_{c\in\Gamma(b)} V^s_{bc}(k-\overline{t}_b) + L_b\rho_{jam}, \\ \sum_{s\in S}\sum_{c\in\Gamma(b)}\left[U^s_{bc}(k)-U^s_{bc}(k-1)\right] \leq Q_b(k), \\ \sum_{s\in S} V^s_{ab}(k) \leq \sum_{s\in S} U^s_{ab}(k-\overline{\tau}_a). \end{cases} \tag{54}$$

The proof is given in Appendix A.8.

Due to different definitions of intersection-movement-based NVH solution vectors (see Definition 7 and

Proposition 9), we develop different big-M methods to formulate the strong intersection-movement-based NVH conditions. Using the "Big M" method, the strong intersection-movement-based NVH conditions can be formulated within the MIP framework, as follows:

$$\sum_{s\in S}\sum_{b\in\Gamma(a)}\left[V_{ab}^{s}(k)-V_{ab}^{s}(k-1)\right]+[1-\omega_a^1(k)]M\geq C_a(k),\forall a\in A\setminus A_S,k\in K, \tag{55a}$$

$$\sum_{s\in S}\sum_{b\in\Gamma(a)}U_{ab}^{s}(k)+[1-\omega_a^2(k)]M\geq\sum_{s\in S}\sum_{b\in\Gamma(a)}V_{ab}^{s}(k-\overline{t}_a)+L_a\rho_{jam},\forall a\in A\setminus A_S,k\in K, \tag{55b}$$

$$\sum_{s\in S}\sum_{b\in\Gamma(a)}\left[U_{ab}^{s}(k)-U_{ab}^{s}(k-1)\right]+[1-\omega_a^3(k)]M\geq Q_a(k),\forall a\in A,k\in K, \tag{55c}$$

$$\sum_{s\in S}V_{ab}^{s}(k)+[1-\omega_{ab}(k)]M\geq\sum_{s\in S}U_{ab}^{s}(k-\overline{\tau}_a),\forall a\in A\setminus A_S,b\in\Gamma(a),k\in K, \tag{55d}$$

$$\omega_a^1(k)+\omega_b^2(k)+\omega_b^3(k)+\omega_{ab}(k)\geq 1,\forall a\in A\setminus A_S,b\in\Gamma(a),k\in K, \tag{55e}$$

$$\omega_a^i(k)\in\{0,1\},\forall a\in A,k\in K,i\in\{1,2,3\}\text{, and} \tag{55f}$$

$$\omega_{ab}(k)\in\{0,1\},\forall a\in A\setminus A_S,b\in\Gamma(a),k\in K. \tag{55g}$$

Constraint (55e)-(55g) implies that for all $a\in A\setminus A_S$, $b\in\Gamma(a)$, and $k\in K$, at least one of the less-than-or-equal-to inequalities in (54) becomes binding.

Because path-based solution vectors contain path information, a strong path-based NVH solution vector can be equivalently defined by each intersection movement, and we have the following proposition:

Proposition 10: Let $\mathbf{z}\in\tilde{\Omega}$ be a feasible solution vector. $\mathbf{z}$ is a strong path-based NVH solution vector if and only if $\mathbf{z}$ satisfies the condition that, for all $a\in A\setminus A_S$, $b\in\Gamma(a)$, and $k\in K$, at least one of the following less-than-or-equal-to inequalities becomes binding:

$$\begin{cases}\sum_{s\in S}\sum_{p\in P^s}\left[V_{ap}^{s}(k)-V_{ap}^{s}(k-1)\right]\leq C_a(k),\\ \sum_{s\in S}\sum_{p\in P^s}U_{bp}^{s}(k)\leq\sum_{s\in S}\sum_{p\in P^s}V_{bp}^{s}(k-\overline{t}_b)+L_b\rho_{jam},\\ \sum_{s\in S}\sum_{p\in P^s}[U_{bp}^{s}(k)-U_{bp}^{s}(k-1)]\leq Q_b(k),\\ \sum_{s\in S}\sum_{p\in P^s}\varsigma_{abp}V_{ap}^{s}(k)\leq\sum_{s\in S}\sum_{p\in P^s}\varsigma_{abp}U_{ap}^{s}(k-\overline{\tau}_a).\end{cases} \tag{56}$$

The proof is similar to that of Proposition 9.

Proposition 11: If $\mathbf{z}\in\tilde{\Omega}$ is a strong path-based NVH solution vector, then $\mathbf{y}=\boldsymbol{\varphi}_2(\mathbf{z})$ is a strong intersection-movement-based NVH solution vector.

The proof is given in Appendix A.9.

Similar to the strong intersection-movement-based NVH conditions, the strong path-based NVH conditions can be formulated as follows:

$$\sum_{s\in S}\sum_{p\in P^s}\left[V_{ap}^{s}(k)-V_{ap}^{s}(k-1)\right]+[1-\omega_a^1(k)]M\geq C_a(k),\forall a\in A\setminus A_S,k\in K, \tag{57a}$$

$$\sum_{s\in S}\sum_{p\in P^s}U_{ap}^{s}(k)+[1-\omega_a^2(k)]M\geq\sum_{s\in S}\sum_{p\in P^s}V_{ap}^{s}(k-\overline{t}_a)+L_a\rho_{jam},\forall a\in A\setminus A_S,k\in K, \tag{57b}$$

$$\sum_{s\in S}\sum_{p\in P^s}[U^s_{ap}(k)-U^s_{ap}(k-1)]+[1-\omega^3_a(k)]M \geq Q_a(k), \forall a\in A, k\in K, \quad (57c)$$

$$\sum_{s\in S}\sum_{p\in P^s}\varsigma_{abp}V^s_{ap}(k)+[1-\omega_{ab}(k)]M \geq \sum_{s\in S}\sum_{p\in P^s}\varsigma_{abp}U^s_{ap}(k-\bar{\tau}_a), \forall a\in A\setminus A_S, b\in\Gamma(a), k\in K, \quad (57d)$$

$$\omega^1_a(k)+\omega^2_b(k)+\omega^3_b(k)+\omega_{ab}(k)\geq 1, \forall a\in A\setminus A_S, b\in\Gamma(a), k\in K, \quad (57e)$$

$$\omega^i_a(k)\in\{0,1\}, \forall a\in A, k\in K, i\in\{1,2,3\}, \text{ and} \quad (57f)$$

$$\omega_{ab}(k)\in\{0,1\}, \forall a\in A\setminus A_S, b\in\Gamma(a), k\in K. \quad (57g)$$

Constraint (57e) implies that, for all $a\in A\setminus A_S$, $b\in\Gamma(a)$ and $k\in K$, at least one of the less-than-or-equal-to inequalities in (56) becomes binding.

We have the following two propositions:

Proposition 12: If $\mathbf{y}\in\bar{\Omega}$ and a vector $\boldsymbol{\omega}=[\omega^i_a(k),\omega_{ab}(k)]$ satisfying the intersection-movement-based NVH constraint (55), then $\mathbf{y}$ is a strong intersection-movement-based NVH solution vector.

The proof is given in Appendix A.10.

Proposition 13: If $\mathbf{z}\in\tilde{\Omega}$ and a vector $\boldsymbol{\omega}=[\omega^i_a(k),\omega_{ab}(k)]$ satisfying the path-based NVH constraint (57), then $\mathbf{z}$ is a strong path-based NVH solution vector.

The proof is similar to that of Proposition 12.

Propositions 12 and 13 imply that the intersection-movement-based NVH constraint (55) and the path-based NVH constraint (57) can completely eliminate weak VH solutions.

2.5. The DSO-SRDTC models without FIFO constraints

2.5.1. Total system travel cost

In this paper, the generalized travel cost for travelers consists of three components: (1) the monetary value of the trip travel time, (2) the penalty cost of schedule delay early, and (3) the penalty cost of schedule delay late. It is assumed that travelers have a desired arrival time period, which is expressed as the arrival time window $[\underline{k}^*_s,\bar{k}^*_s]$, where $\underline{k}^*_s$ and $\bar{k}^*_s$ represent the earliest and latest official work start time window for travelers to destination *s*, respectively.

The TSTC for the whole network can be formulated as follows:

$$\begin{aligned}\eta &= \alpha\sum_{a\in A\setminus A_S}\sum_{k\in K}[U_a(k)-V_a(k)]+\beta\sum_{a\in A_S}\sum_{k<\underline{k}^*_s}[U_a(k)-U_a(k-1)](\underline{k}^*_s-k)\\ &+\gamma\sum_{a\in A_S}\sum_{k>\bar{k}^*_s}[U_a(k)-U_a(k-1)](k-\bar{k}^*_s), \quad (58)\\ &= \alpha\sum_{a\in A\setminus A_S}\sum_{k\in K}[U_a(k)-V_a(k)]+\beta\sum_{a\in A_S}\sum_{k<\underline{k}^*_s}U_a(k)+\gamma\sum_{a\in A_S}\left[(\underline{K}+1-\bar{k}^*_s)U_a(\underline{K})-\sum_{k\geq\bar{k}^*_s}U_a(k)\right],\end{aligned}$$

where α is the unit cost of travel time, and β and γ are the unit costs of schedule delay early and late, respectively. According to empirical results (Small, 1982), we have $0<\beta<\alpha<\gamma$. The three terms on the right-hand side of the first equation of Eq. (58) are the total monetary value of the trip travel time, the total

penalty cost of schedule delay early, and the total penalty cost of schedule delay late, respectively.

Substituting Eqs. (7), (8), and (12) into Eq. (58) and rearranging the resultant equation, we have the TSTC in terms of a link-based solution vector as follows:

$$\eta(\mathbf{x}) = \sum_{s\in S}\left\{\sum_{a\in A\setminus A_S}\sum_{k\in K}\alpha[U_a^s(k)-V_a^s(k)]+\sum_{a\in A_S}\left[\sum_{k<\underline{k}_s^*}\beta U_a^s(k)-\sum_{k\geq\bar{k}_s^*}\gamma U_a^s(k)\right]\right\}+\eta_0, \tag{59}$$

where $\eta_0 = \sum_{s\in S}\sum_{a\in A_S}\sum_{b\in A_R}(\underline{K}+1-\bar{k}_s^*)\gamma D_b^s$. Because all parameters in this equation are predetermined, η_0 is a constant.

Substituting Eqs. (19)-(21) into Eq. (59), we have the TSTC in terms of an intersection-movement-based solution vector as follows:

$$\bar{\eta}(\mathbf{y}) = \sum_{s\in S}\left\{\sum_{a\in A\setminus A_S}\sum_{k\in K}\sum_{b\in\Gamma(a)}\alpha[U_{ab}^s(k)-V_{ab}^s(k)]+\sum_{a\in A_S}\sum_{b\in\Gamma^{-1}(a)}\left[\sum_{k<\underline{k}_s^*}\beta V_{ba}^s(k)-\sum_{k\geq\bar{k}_s^*}\gamma V_{ba}^s(k)\right]\right\}+\eta_0. \tag{60}$$

Substituting Eqs. (33) and (34) into Eq. (59), we have the TSTC in terms of a path-based solution vector as follows:

$$\tilde{\eta}(\tilde{\mathbf{x}}) = \sum_{s\in S}\sum_{p\in P^s}\left\{\sum_{a\in A\setminus A_S}\sum_{k\in K}\alpha[U_{ap}^s(k)-V_{ap}^s(k)]+\sum_{a\in A_S}\left[\sum_{k<\underline{k}_s^*}\beta U_{ap}^s(k)-\sum_{k\geq\bar{k}_s^*}\gamma U_{ap}^s(k)\right]\right\}+\eta_0. \tag{61}$$

Proposition 14: For all $\mathbf{y}\in\bar{\Omega}$, we have $\bar{\eta}(\mathbf{y}) = \eta(\boldsymbol{\varphi}_1(\mathbf{y}))$.

The proof is given in Appendix A.11.

Proposition 15: For all $\mathbf{z}\in\tilde{\Omega}$, we have $\tilde{\eta}(\mathbf{z}) = \bar{\eta}(\boldsymbol{\varphi}_2(\mathbf{z})) = \eta(\boldsymbol{\varphi}_1(\boldsymbol{\varphi}_2(\mathbf{z})))$.

The proof is given in Appendix A.12.

2.5.2. Linear programming formulation for the R-DSO-SRDTC problems

Expressing the TSTC in terms of a link-based solution vector, we can formulate the link-based R-DSO-SRDTC problem, which considers neither FIFO constraints nor NVH constraints, as the following LP problem:

$$\min_{\mathbf{x}\in\Omega}\eta = \eta(\mathbf{x}). \tag{62}$$

Similarly, we can formulate the intersection-movement-based and path-based R-DSO-SRDTC problems without the considerations of FIFO constraints and NVH constraints as the following LP problems, respectively:

$$\min_{\mathbf{y}\in\bar{\Omega}}\bar{\eta} = \bar{\eta}(\mathbf{y}) \quad \text{and} \tag{63}$$

$$\min_{\mathbf{z}\in\tilde{\Omega}}\tilde{\eta} = \tilde{\eta}(\mathbf{z}). \tag{64}$$

2.5.3. Formulations for the NVH-DSO-SRDTC problems

Integrating the link-based NVH constraint (49) into LP problem (62), we can formulate the link-based

NVH-DSO-SRDTC problem as the following mixed-integer LP (MILP) problem:

$$\min_{\mathbf{x}\in\Omega,\boldsymbol{\theta}} \eta = \eta(\mathbf{x}) \tag{65}$$

Subject to: Constraint (49) for all $a \in A \setminus A_S, k \in K$,

where the vector $\boldsymbol{\theta} = [\theta_a^i(k)]$.

Integrating the intersection-movement-based NVH constraint (55) into LP problem (63), we can formulate the intersection-movement-based NVH-DSO-SRDTC problem as the following MILP:

$$\min_{\mathbf{y}\in\bar{\Omega},\boldsymbol{\omega}} \bar{\eta} = \bar{\eta}(\mathbf{y}) \tag{66}$$

Subject to: Constraint (55).

Integrating the path-based NVH constraint (57) into LP problem (64), we can formulate the path-based NVH-DSO-SRDTC problem as the following MILP:

$$\min_{\mathbf{z}\in\tilde{\Omega},\boldsymbol{\omega}} \tilde{\eta} = \tilde{\eta}(\mathbf{z}) \tag{67}$$

Subject to: Constraint (57).

The following LP problem is proposed to completely address the VH problem in the link-based DSO-SRDTC problems:

Proposition 16. Any optimal solution to the following LP problem is a strong link-based NVH solution vector:

$$\max_{\mathbf{x}\in\Omega} \xi(\mathbf{x}) = \sum_{s\in S}\sum_{k\in K}\sum_{a\in A\setminus A_R} V_a^s(k), \tag{68}$$

Subject to: $\eta(\mathbf{x}) = \eta^*$, (69)

where η^* is the value of the objective function for an optimal solution to LP problem (62), i.e., the minimum TSTC of the link-based R-DSO-SRDTC problem (62).

The proof is given in Appendix A.13.

Proposition 16 implies that LP problem (68)-(69) can completely eliminate VH solutions. According to Propositions 8 and 16, optimal solutions to LP problem (68)-(69) satisfy the weak link-based NVH condition defined by Definition 6. Because MILP problem (65) integrates the weak link-based NVH condition, optimal solutions to the MILP problem (65) satisfy the weak link-based NVH condition. Hence, we have the following proposition:

Proposition 17. Let $\mathbf{x}^*$ be an optimal solution to LP problem (68)-(69). Then, there exists a vector $\boldsymbol{\theta}^*$ such that $[\mathbf{x}^*, \boldsymbol{\theta}^*]$ is an optimal solution to MILP problem (65).

The proof is given in Appendix A.14.

Before solving LP problem (68)-(69), we should solve LP problem (62) to obtain the minimum TSTC η^*. This implies that two LP problems should be solved sequentially to obtain an optimal solution to LP problem (68)-(69). To enhance computational efficiency for solving the link-based NVH-DSO-SRDTC problem, the

following LP problem can be used to address the VH problem:

Proposition 18. For a given $\phi > 0$, let $\mathbf{x}^*$ be an optimal solution to the following LP problem:

$$\min_{\mathbf{x}\in\Omega} \varpi = \eta(\mathbf{x}) - \phi \sum_{a\in A\setminus A_S} \sum_{k\in K} \sum_{s\in S} V_a^s(k). \tag{70}$$

If $\mathbf{x}^*$ is also an optimal solution to LP problem (62), then $\mathbf{x}^*$ is also an optimal solution to LP problem (68)-(69) and all optimal solutions to the following LP problem are also optimal to LP problem (68)-(69):

$$\min_{\mathbf{x}\in\Omega} \varpi = \eta(\mathbf{x}) - \hat{\phi} \sum_{a\in A\setminus A_S} \sum_{k\in K} \sum_{s\in S} V_a^s(k), \tag{71}$$

where $0 < \hat{\phi} < \phi$.

The proof is similar to that of Proposition 1 in Long and Szeto (2017).

The results presented in Proposition 18 indicate that we can select a small enough positive parameter ϕ and solve only one LP problem to obtain a link-based NVH system optimum solution vector. Similarly, the MILPs (66) and (67) for the intersection-movement-based and path-based NVH-DSO-SRDTC problems can, respectively, be reformulated as follows:

$$\min_{\mathbf{y}\in\bar{\Omega}} \bar{\varpi} = \bar{\eta}(\mathbf{y}) - \phi \sum_{k\in K} \sum_{s\in S} \sum_{a\in A\setminus A_S} \sum_{b\in\Gamma(a)} V_{ab}^s(k) \quad \text{and} \tag{72}$$

$$\min_{\mathbf{z}\in\tilde{\Omega}} \tilde{\varpi} = \tilde{\eta}(\mathbf{z}) - \phi \sum_{a\in A\setminus A_S} \sum_{k\in K} \sum_{p\in P} V_{ap}(k), \tag{73}$$

where ϕ is a sufficiently small positive coefficient. The proofs basically follow the proof of Proposition 18 with changes in notations and are omitted.

Theorem 1. Let η^*, $\bar{\eta}^*$, and $\tilde{\eta}^*$ be the optimal TSTCs of the link-based, intersection-movement-based, and path-based R-DSO-SRDTC problems, respectively. Let η_N^*, $\bar{\eta}_N^*$, and $\tilde{\eta}_N^*$ be the optimal TSTCs of the link-based, intersection-movement-based, and path-based NVH-DSO-SRDTC problems, respectively. We have $\eta^* = \bar{\eta}^* = \tilde{\eta}^* = \eta_N^* = \bar{\eta}_N^* = \tilde{\eta}_N^*$.

The proof is given in Appendix A.15.

Theorem 1 implies that the three formulations of the DSO-SRDTC problem without FIFO constraints are equivalent in terms of obtaining the same optimal TSTC. This is consistent with Shen et al. (2007) that an optimal solution to single-destination SO-DTA problems that maintain the NVH property always exists. In other words, SO-DTA problems without NVH constraints can have multiple optimal solutions and at least one of them is an NVH-SO flow pattern. Therefore, if SO-DTA is only used to provide a benchmark for developing network management strategies, any one of the three formulations of the DSO-SRDTC problem without FIFO constraints can be applied.

3. The DSO-SRDTC problems with FIFO constraints

3.1. FIFO conditions and FIFO solution vectors

3.1.1. An overview of link-based FIFO conditions and FIFO solution vectors

Cumulative link inflows and outflows can be related to link travel times as follows (Long et al., 2011;

Carey et al., 2014):

$$U_a(\ell) = V_a(\ell + \tau_a(\ell)), \forall a \in A, \ell \in [0,T], s \in S \,. \tag{74}$$

Using the link travel times of vehicles that travel to each destination, the weak link-based FIFO condition and a FIFO solution vector can be defined as follows (Long and Szeto, 2017):

Definition 12 (Link-based FIFO condition): Traffic flow on link *a* satisfies the link-based FIFO condition if and only if

$$\ell' > \ell'' \Rightarrow \ell' + \tau_a^{s_1}(\ell') \geq \ell'' + \tau_a^{s_2}(\ell''), \forall s_1 \in S, s_2 \in S, \ell' \in [0,T], \ell'' \in [0,T] \,. \tag{75}$$

where $\tau_a^{s_1}(\ell')$ ($\tau_a^{s_2}(\ell'')$) is the link travel time of the vehicles entering link *a* to destination s_1 (s_2) at time instant ℓ' (ℓ'').

Definition 13 (Link-based FIFO solution vector): A solution vector $\mathbf{x} \in \Omega$ is a FIFO solution vector if a vector of link travel times $\boldsymbol{\tau} = [\tau_a^s(\ell)]$ exists such that $\boldsymbol{\tau}$ satisfies the link FIFO condition (75) for all $a \in A \setminus A_S$ and the following condition is satisfied:

$$U_a^s(\ell) = V_a^s(\ell + \tau_a^s(\ell)), \forall s \in S, a \in A \setminus A_S, \ell \in [0,T] \,. \tag{76}$$

The following two propositions can be used to identify FIFO violations (Long and Szeto, 2017):

Proposition 19: For a given link-based solution vector $\mathbf{x} \in \Omega$ and an index pair $(a,k) \in \Phi$, if at least one destination s exists such that $U_a^s(\underline{\ell}_{a,k}^*) < V_a^s(k)$, where $\underline{\ell}_{a,k}^*$ is a critical time instant (i.e., the earliest entry time of vehicles that leave link *a* at the end of interval *k*, which may not be an integer) and

$$\underline{\ell}_{a,k}^* = \arg\max_{\tilde{\ell} \leq k - \vec{t}_a} \{U_a^s(\tilde{\ell}) \leq V_a^s(k), \forall s \in S\} \,, \tag{77}$$

then $\mathbf{x}$ involves FIFO violations.

Proposition 20: For a given solution vector $\mathbf{x} \in \Omega$ and an index pair $(a,k) \in \Phi$, if at least one destination s exists such that $U_a^s(\overline{\ell}_{a,k}^*) > V_a^s(k)$, where $\overline{\ell}_{a,k}^*$ is a critical time instant (i.e., the latest entry time of vehicles that leave link *a* at the end of interval *k*, which may not be an integer) and

$$\overline{\ell}_{a,k}^* = \arg\min_{\tilde{\ell} \geq 0} \{U_a^s(\tilde{\ell}) \geq V_a^s(k), \forall s \in S\} \,, \tag{78}$$

then $\mathbf{x}$ involves FIFO violations.

Definition 14 (Link entry time): $e_a^s(k)$ is defined as the time instant at which vehicles enter link *a* to destination *s* and leave the link at the end of interval *k*.

According to Definition 14, we have $k = e_a^s(k) + \tau_a^s(e_a^s(k))$, and can equivalently reformulate Eq. (76) as follows:

$$U_a^s(e_a^s(k)) = V_a^s(k), \forall s \in S, a \in A \setminus A_S, k \in K \,. \tag{79}$$

Proposition 21: For any given link-based FIFO solution vector $\mathbf{x} \in \Omega$, there must exist a vector of entry times $\mathbf{e} = [e_a(k)]$ such that

$$V_a^s(k) = U_a^s(e_a(k)), \forall s \in S, a \in A \setminus A_S, k \in K . \quad (80)$$

Both Propositions 19 and 20 can be used to prove this proposition. See Long and Szeto (2017) for the detailed proof. According to Proposition 21, a link-based FIFO solution vector can also be redefined as follows (Long and Szeto, 2017):

Definition 15 (Alternative link-based FIFO solution vector): A solution vector $\mathbf{x} \in \Omega$ is a link-based FIFO solution vector if a vector of entry times $\mathbf{e} = [e_a(k)]$ exists such that condition (80) is satisfied.

3.1.2. Definitions of intersection-movement-based and path-based FIFO solution vectors

Similar to the alternative definition of a link-based FIFO solution vector, intersection-movement-based and path-based FIFO solution vectors can be defined as follows:

Definition 16 (Intersection-movement-based FIFO solution vector): A solution vector $\mathbf{y} \in \bar{\Omega}$ is an intersection-movement-based FIFO solution vector if a vector of entry times $\mathbf{e} = [e_a(k)]$ exists such that

$$V_{ab}^s(k) = U_{ab}^s(e_a(k)), \forall s \in S, a \in A \setminus A_S, b \in \Gamma(a), k \in K . \quad (81)$$

Definition 17 (Path-based FIFO solution vector): A solution vector $\mathbf{z} \in \tilde{\Omega}$ is a path-based FIFO solution vector if a vector of entry times $\mathbf{e} = [e_a(k)]$ exists such that

$$V_{ap}^s(k) = U_{ap}^s(e_a(k)), \forall s \in S, p \in P^s, a \in A \setminus A_S, k \in K . \quad (82)$$

Proposition 22: If $\mathbf{y} \in \bar{\Omega}$ is an intersection-movement-based FIFO solution vector, then $\mathbf{x} = \boldsymbol{\varphi}_1(\mathbf{y})$ is a link-based FIFO solution vector.

The proof is given in Appendix A.16.

Proposition 23: If $\mathbf{z} \in \tilde{\Omega}$ is a path-based FIFO solution vector, then $\mathbf{y} = \boldsymbol{\varphi}_2(\mathbf{z})$ is an intersection-movement-based FIFO solution vector, and $\mathbf{x} = \boldsymbol{\varphi}_1(\boldsymbol{\varphi}_2(\mathbf{z}))$ is a link-based FIFO solution vector.

The proof is given in Appendix A.17.

Propositions 22 and 23, respectively, indicate that intersection-movement-based FIFO implies link-based FIFO, and path-based FIFO implies intersection-movement-based FIFO and link-based FIFO. Equivalently, link-based FIFO is weaker than intersection-movement-based FIFO and path-based FIFO, and intersection-movement-based FIFO is weaker than path-based FIFO.

Similar to Propositions 19 and 20 for FIFO violation identification in a link-based solution vector, the following two propositions can be used to identify FIFO violations in an intersection-movement-based solution vector:

Proposition 24: For a given solution vector $\mathbf{y} \in \bar{\Omega}$ and an index pair $(a,k) \in \Phi$, if at least one destination s and downstream link b exist such that $U_{ab}^s(\underline{\ell}_{a,k}^*) < V_{ab}^s(k)$, where

$$\underline{\ell}_{a,k}^* = \arg\max_{\tilde{\ell} \le k - \vec{t}_a} \{U_{ab}^s(\tilde{\ell}) \le V_{ab}^s(k), \forall s \in S, b \in \Gamma(a)\} , \quad (83)$$

then $\mathbf{y}$ involves FIFO violations.

Proposition 25: For a given solution vector $\mathbf{y} \in \overline{\Omega}$ and an index pair $(a,k) \in \Phi$, if at least one destination s and downstream link b exist such that $U_{ab}^s(\overline{\ell}_{a,k}^*) > V_{ab}^s(k)$, where

$$\overline{\ell}_{a,k}^* = \arg\min_{\ell \geq 0} \{U_{ab}^s(\tilde{\ell}) \geq V_{ab}^s(k), \forall s \in S, b \in \Gamma(a)\}, \tag{84}$$

then $\mathbf{y}$ involves FIFO violations.

Propositions 24 and 25 are straightforward extensions from Propositions 19 and 20 and hence the proofs are omitted. Similarly, Propositions 19 and 20 can be easily extended to the path-based counterparts:

Proposition 26: For a given solution vector $\mathbf{z} \in \tilde{\Omega}$ and an index pair $(a,k) \in \Phi$, if at least one destination s and one path $p \in P^s$ exists such that $U_{ap}^s(\underline{\ell}_{a,k}^*) < V_{ap}^s(k)$, where

$$\underline{\ell}_{a,k}^* = \arg\max_{\tilde{\ell} \leq k - \overline{\tau}_a} \{U_{ap}^s(\tilde{\ell}) \leq V_{ap}^s(k), \forall s \in S, p \in P^s\}, \tag{85}$$

then $\mathbf{z}$ involves FIFO violations.

Proposition 27: For a given solution vector $\mathbf{z} \in \tilde{\Omega}$ and an index pair $(a,k) \in \Phi$, if at least one destination s and one path $p \in P^s$ exists such that $U_{ap}^s(\overline{\ell}_{a,k}^*) > V_{ap}^s(k)$, where

$$\overline{\ell}_{a,k}^* = \arg\min_{\ell \geq 0} \{U_{ap}^s(\tilde{\ell}) \geq V_{ap}^s(k), \forall s \in S, p \in P^s\}, \tag{86}$$

then $\mathbf{z}$ involves FIFO violations.

3.2. FIFO constraints

Before solving the DSO-SRDTC problem with FIFO constraints, we do not know the exact value of the entry time $e_a(k)$ in condition (80). Hence, we cannot directly use the linear interpolation procedure (1) to reformulate condition but can use a linear combination of two cumulative flows at adjacent time intervals instead. Therefore, according to Definition 15, condition (80) can be reformulated as follows (Long and Szeto, 2017):

$$V_a^s(k) = \sum_{l \leq k - \overline{\tau}_a} \lambda_{a,k,l} U_a^s(l), \forall s \in S, a \in A \setminus A_S, k \in K, \tag{87}$$

where $\lambda_{a,k,l}$ is the linear combination/interpolation coefficient and satisfies

$$\sum_{l \leq k - \overline{\tau}_a} \lambda_{a,k,l} = 1, \forall a \in A, k \in K, \tag{88a}$$

$$\lambda_{a,k,l} \lambda_{a,k,l'} = 0, \forall a \in A, k \in K, l \leq k - \overline{\tau}_a, l' \leq l - 2, \text{ and} \tag{88b}$$

$$\lambda_{a,k,l} \geq 0, \forall a \in A, k \in K, l \leq k - \overline{\tau}_a, \tag{88c}$$

where (88a) is a definitional constraint that requires the sum of linear combination coefficients equal one, (88b) ensures that at most two adjacent intervals are required to represent the linear combination due to linear interpolation, and (88c) ensures that the linear combination coefficients are non-negative.

According to Long and Szeto (2017), we have the following proposition:

Proposition 28: If a vector $\boldsymbol{\lambda} = [\lambda_{a,k,l}]$ exists such that a feasible flow pattern $\mathbf{x} \in \Omega$ satisfies constraints

(87) and (88), then the vector $\mathbf{p} = [p_a(k)] = \left[\sum_{l \le k-\bar{\tau}_a} l\lambda_{a,k,l}\right]$ satisfies the FIFO condition (80) and $\mathbf{x}$ is a FIFO flow pattern.

Proposition 28 implies that the FIFO constraints (87) and (88) can ensure a feasible flow pattern $\mathbf{x} \in \Omega$ to be a FIFO flow pattern.

Similar to link-based FIFO constraints, the intersection-movement-based FIFO constraints can be formulated as follows:

$$V_{ab}^s(k) = \sum_{l \le k-\bar{\tau}_a} \lambda_{a,k,l} U_{ab}^s(l), \forall s \in S, a \in A \setminus A_S, b \in \Gamma(a), k \in K, \tag{89}$$

where $\lambda_{a,k,l}$ satisfies constraint (88).

Similar to link-based and intersection-movement-based FIFO constraints, the path-based FIFO constraints can be formulated as follows:

$$V_{ap}^s(k) = \sum_{l \le k-\bar{\tau}_a} \lambda_{a,k,l} U_{ap}^s(l), \forall s \in S, a \in A \setminus A_S, p \in P^s, k \in K, \tag{90}$$

where $\lambda_{a,k,l}$ satisfies constraint (88).

The result presented in Proposition 28 can be directly extended to intersection-movement-based and path-based FIFO constraints and is omitted here.

3.3. The FIFO-DSO-SRDTC models

Integrating FIFO constraints (87) and (88) into LP problem (62), we can obtain the following link-based FIFO-DSO-SRDTC model:

$$\min_{\mathbf{x} \in \Omega, \boldsymbol{\lambda}} \eta = \eta(\mathbf{x}). \tag{91}$$

Subject to: Constraints (87) and (88),

where the vector $\boldsymbol{\lambda} = [\lambda_{a,k,l}]$.

Integrating FIFO constraints (88) and (89) into LP problem (63), we can obtain the following intersection-movement-based FIFO-DSO-SRDTC model:

$$\min_{\mathbf{y} \in \bar{\Omega}, \boldsymbol{\lambda}} \bar{\eta} = \bar{\eta}(\mathbf{y}). \tag{92}$$

Subject to: Constraints (88) and (89).

Integrating FIFO constraints (88) and (90) into LP problem (64), we can obtain the following path-based FIFO-DSO-SRDTC model:

$$\min_{\mathbf{z} \in \tilde{\Omega}, \boldsymbol{\lambda}} \tilde{\eta} = \tilde{\eta}(\mathbf{z}). \tag{93}$$

Subject to: Constraints (88) and (90).

Similar to Theorem 1 in Long and Szeto (2017), we have the following theorems:

Theorem 2: Let $[\mathbf{x}^*, \boldsymbol{\lambda}^*]$ be an optimal solution to the link-based FIFO-DSO-SRDTC problem (91), and $\mathbf{e}^* = [e_a^*(k)] = \left[\sum_{l \le k-\bar{\tau}_a} l\lambda_{a,k,l}^*\right]$. Then, $\mathbf{x}^*$ is also an optimal solution to the following LP:

$$\min_{\mathbf{x}\in\Omega} \eta = \eta(\mathbf{x})$$

Subject to:

$$V_a^s(k) = U_a^s(e_a^*(k)), \forall s \in S, a \in A \setminus A_S, k \in K . \quad (94)$$

Theorem 3: Let $[\mathbf{y}^*, \boldsymbol{\lambda}^*]$ be an optimal solution to the intersection-movement-based FIFO-DSO-SRDTC problem (92), and $\mathbf{e}^* = [e_a^*(k)] = \left[\sum_{l\le k-\bar{\tau}_a} l\lambda_{a,k,l}^*\right]$. Then, $\mathbf{y}^*$ is also an optimal solution to the following LP:

$$\min_{\mathbf{y}\in\bar{\Omega}} \bar{\eta} = \bar{\eta}(\mathbf{y})$$

Subject to:

$$V_{ab}^s(k) = U_{ab}^s(e_a^*(k)), \forall s \in S, a \in A \setminus A_S, b \in \Gamma(a), k \in K . \quad (95)$$

Theorem 4: Let $[\mathbf{z}^*, \boldsymbol{\lambda}^*]$ be an optimal solution to the path-based FIFO-DSO-SRDTC problem (93), and $\mathbf{e}^* = [e_a^*(k)] = \left[\sum_{l\le k-\bar{\tau}_a} l\lambda_{a,k,l}^*\right]$. Then, $\mathbf{z}^*$ is also an optimal solution to the following LP:

$$\min_{\mathbf{z}\in\tilde{\Omega}} \tilde{\eta} = \tilde{\eta}(\mathbf{z})$$

Subject to:

$$V_{ap}^s(k) = U_{ap}^s(e_a^*(k)), \forall s \in S, a \in A \setminus A_S, p \in P^s, k \in K . \quad (96)$$

Theorems 2-4 link FIFO-DSO solutions to different forms of LP problems, and provide optimal solution properties of the proposed DSO-SRDTC problems. These important properties can be used to develop new or modifying existing solution methods for solving FIFO-DSO solutions. Because there are bilinear terms in FIFO constraints, the FIFO-DSO-SRDTC problems are non-convex optimization problems and are very hard to solve. According to Theorems 2-4, if the vector $[e_a^*(k)]$ is known beforehand, we can solve an LP problem to get the optimal solution to the FIFO-DSO-SRDTC problems. This implies that we can solve the FIFO-DSO-SRDTC problems by finding the optimal vector $[e_a^*(k)]$. Because FIFO-DSO solutions are not known beforehand, we adopt branch-and-bound algorithms (see Long and Szeto, 2017 for details) and solve a sequence of LPs to find the optimal vector $[e_a^*(k)]$ for the FIFO-DSO-SRDTC problems.

Theorem 5: Let η^*, $\bar{\eta}^*$, and $\tilde{\eta}^*$ be the optimal TSTCs of the link-based, intersection-movement-based, and path-based FIFO-DSO-SRDTC problems, respectively. Then, $\eta^* \le \bar{\eta}^* \le \tilde{\eta}^*$.

The proof is given in Appendix A.18.

The proof of Theorem 5 shows that an optimal intersection-movement-based FIFO-DSO-SRDTC solution vector can be directly transferred to a feasible link-based FIFO-DSO-SRDTC solution vector with the same TSTC. This implies that the TSTC of the optimal link-based FIFO-DSO-SRDTC solution vector is not more than the TSTC of the optimal intersection-movement-based FIFO-DSO-SRDTC solution vector. In contrast, an optimal link-based FIFO-DSO-SRDTC solution vector cannot always be transferred to a feasible intersection-movement-based FIFO-DSO-SRDTC solution vector with the same TSTC. This implies that we

can have $\eta^* < \bar{\eta}^*$ (see Example 5 in Section 4). Similar results can be observed between intersection-movement-based and path-based FIFO-DSO-SRDTC problems, and we can have $\bar{\eta}^* < \tilde{\eta}^*$. Therefore, link-based, intersection-movement-based, and path-based FIFO are not equivalent, and the three formulations of DSO-SRDTC problems with FIFO constraints can obtain different optimal TSTCs.

3.4. The NVH-FIFO-DSO-SRDTC models

In a multi-destination network, if the FIFO requirement is considered, an NVH solution vector can allow the existence of vehicles on an entering link of a diverge junction that do not move forward to their own successor link even if there is no congestion on their own successor link. Due to the FIFO requirement, it is possible that in an NVH solution, an upstream link has vehicles not discharged due to congestion of one or some downstream links, but not necessarily all downstream links directly connected to the upstream link. Weak link-based, intersection-movement-based, and path-based NVH solution vectors, respectively, defined by Definitions 6, 7, and 8 can capture this phenomenon. Hence, the corresponding constraints (49), (51), and (53) are used to represent the NVH constraints in the link-based, intersection-movement-based, and path-based NVH-FIFO-DSO-SRDTC problems, respectively.

VH in the DSO-SRDTC problems without FIFO constraints can be eliminated by a penalty approach. However, the penalty approach cannot be directly applied to for the NVH-FIFO formulation. Example 5 in Section 4 shows that the TSTC of a FIFO-DSO solution vector and that of an NVH-FIFO-DSO solution vector can be different, and the TSTC of a FIFO-DSO solution vector is smaller than that of an NVH-FIFO-DSO solution vector. When we introduce the penalty term into the FIFO-DSO-SRDTC model, we will obtain a FIFO-DSO solution vector if the coefficient approaches zero. In this case, to achieve a minimum objective value, the NVH property cannot be ensured. In this subsection, intersection-movement-based constraints (51) and path-based NVH constraints (53) are included in the FIFO-DSO-SRDTC model to eliminate VH. Because the FIFO-DSO-SRDTC model with NVH constraints obtains weak NVH-FIFO-DSO solution vectors, the penalty term is introduced into the objective of the FIFO-DSO-SRDTC models. The penalty term is used to eliminate the redundant holding flows.

Integrating the NVH constraint (49) and FIFO constraints (87) and (88) into LP problem (70), we can obtain the following link-based NVH-FIFO-DSO-SRDTC model:

$$\min_{\mathbf{x}\in\Omega,\boldsymbol{\lambda},\mathbf{0}} \varpi = \eta(\mathbf{x}) - \phi \sum_{a\in A\setminus A_S} \sum_{k\in K} \sum_{s\in S} V_a^s(k) \tag{97}$$

Subject to: Constraints (87) and (88), and constraint (49) for all $a \in A \setminus A_S, k \in K$.

Integrating the NVH constraint (51) and FIFO constraints (88) and (89) into LP problem (72), we can obtain the following intersection-movement-based NVH-FIFO-DSO-SRDTC model:

$$\min_{\mathbf{y}\in\bar{\Omega},\boldsymbol{\lambda},\boldsymbol{\omega}} \bar{\varpi} = \bar{\eta}(\mathbf{y}) - \phi \sum_{k\in K} \sum_{s\in S} \sum_{a\in A\setminus A_S} \sum_{b\in\Gamma(a)} V_{ab}^s(k) \tag{98}$$

Subject to: Constraints (88) and (89), and constraint (51) for all $a \in A \setminus A_S, k \in K$.

Integrating the NVH constraint (53) and FIFO constraints (88) and (90) into LP problem (73), we can obtain the following path-based NVH-FIFO-DSO-SRDTC model:

$$\min_{\mathbf{z}\in\tilde{\Omega},\boldsymbol{\lambda},\boldsymbol{\omega}} \tilde{\varpi} = \tilde{\eta}(\mathbf{z}) - \phi \sum_{a\in A\setminus A_S} \sum_{k\in K} \sum_{p\in P} V_{ap}(k) \tag{99}$$

Subject to: Constraints (88) and (89), and constraint (53) for all $a \in A \setminus A_S, k \in K$.

Similar to Theorem 2 in Long and Szeto (2017), we have the following theorems:

Theorem 6: Let $[\mathbf{x}^*, \boldsymbol{\lambda}^*, \boldsymbol{\theta}^*]$ be an optimal solution to the link-based NVH-FIFO-DSO-SRDTC problem (97), and $\mathbf{e}^* = [e_a^*(k)] = \left[\sum_{l\le k-\bar{l}_a} l\lambda_{a,k,l}^*\right]$. Then, $[\mathbf{x}^*, \boldsymbol{\theta}^*]$ is also an optimal solution to the following mixed-integer linear programming (MILP) problem:

$$\min_{\mathbf{x}\in\Omega,\boldsymbol{\theta}} \eta = \eta(\mathbf{x})$$

Subject to: Constraints (94) and constraint (49) for all $a \in A \setminus A_S, k \in K$.

Theorem 7: Let $[\mathbf{y}^*, \boldsymbol{\lambda}^*, \boldsymbol{\omega}^*]$ be an optimal solution to the intersection-movement-based NVH-FIFO-DSO-SRDTC problem (98), and $\mathbf{e}^* = [e_a^*(k)] = \left[\sum_{l\le k-\bar{l}_a} l\lambda_{a,k,l}^*\right]$. Then, $[\mathbf{y}^*, \boldsymbol{\lambda}^*, \boldsymbol{\omega}^*]$ is also an optimal solution to the following MILP problem:

$$\min_{\mathbf{y}\in\bar{\Omega},\boldsymbol{\omega}} \bar{\eta} = \bar{\eta}(\mathbf{y})$$

Subject to: Constraint (95) and constraint (51) for all $a \in A \setminus A_S, k \in K$.

Theorem 8: Let $[\mathbf{z}^*, \boldsymbol{\lambda}^*, \boldsymbol{\omega}^*]$ be an optimal solution to the path-based NVH-FIFO-DSO-SRDTC problem (99), and $\mathbf{e}^* = [e_a^*(k)] = \left[\sum_{l\le k-\bar{l}_a} l\lambda_{a,k,l}^*\right]$. Then, $[\mathbf{z}^*, \boldsymbol{\lambda}^*, \boldsymbol{\omega}^*]$ is also an optimal solution to the following MILP problem:

$$\min_{\mathbf{z}\in\tilde{\Omega},\boldsymbol{\omega}} \tilde{\eta} = \tilde{\eta}(\mathbf{z})$$

Subject to: Constraint (96) and constraint (53) for all $a \in A \setminus A_S, k \in K$.

Theorems 6-8 link NVH-FIFO-DSO solutions to different forms of MILP problems, and provide optimal solution conditions for the proposed NVH-FIFO-DSO-SRDTC problems. According to Theorems 6-8, if the vector $[e_a^*(k)]$ is known beforehand, we can solve a MILP problem to get the optimal solution to the NVH-FIFO-DSO-SRDTC problems. This implies that we can solve the NVH-FIFO-DSO-SRDTC problems by finding the optimal vector $[e_a^*(k)]$. In this paper, we adopt branch-and-bound algorithms (see Long and Szeto, 2017 for details) and solve a sequence of MILPs to find the optimal vector $[e_a^*(k)]$ for the NVH-FIFO-DSO-SRDTC problems.

Theorem 9: Let η^*, $\bar{\eta}^*$, and $\tilde{\eta}^*$ be the optimal TSTCs of the link-based, intersection-movement-based and path-based NVH-FIFO-DSO-SRDTC problems, respectively. Then, $\eta^* \le \bar{\eta}^* \le \tilde{\eta}^*$.

The proof is given in Appendix A.19.

Theorem 10: Let η_1^*, η_2^*, η_3^*, and η_4^* be the optimal TSTCs of the link-based R-SO-, the NVH-SO-, the

FIFO-SO-, and the NVH-FIFO-DSO-SRDTC problems, respectively. We have $\eta_1^* = \eta_2^* \le \eta_3^* \le \eta_4^*$.

The proof is given in Appendix A.20.

Similar results of Theorem 10 can be proved for the intersection-movement-based and path-based DSO-SRDTC problems, which are omitted here.

3.5. Branch-and-bound algorithms for DSO-SRDTC models with FIFO constraints

The DSO-SRDTC problems without FIFO constraints are formulated as linear programs and can be effectively solved by commercial solvers, such as CPLEX, Gurobi, for reasonable size networks. However, the DSO-SRDTC problems with FIFO constraints have a non-convex set of feasible solutions, and traditional optimization methods may not be effective to solve them even for small networks. Long and Szeto (2017) developed branch-and-bound algorithms to solve link-based DSO-SRDTC models with FIFO constraints, which can be directly extended to solve the intersection-movement-based and path-based DSO-SRDTC problems. Different from traditional branch-and-bound algorithms, the branch-and-bound algorithms for DSO-SRDTC problems do not directly branch decision variables. Based on the properties of the DSO-SRDTC models (see Theorems 2-4 and 6-8), the branch-and-bound algorithms aim to search for the proper ranges of entry times $e_a^*(k)$ by using the set of pairs of link and interval indices of the solution vector with FIFO violations identified by the conditions stated in Propositions 19 and 20 for link-based models, Propositions 24 and 25 for intersection-movement-based models, and Propositions 26 and 27 for path-based models. In the branch-and-bound algorithms, the DSO-SRDTC problems without FIFO constraints are sub-problems to solve the DSO-SRDTC problems with FIFO constraints. We only need to solve LP or MILP sub-problems to evaluate the branches, generate new branches based on the two critical entry times obtained from the FIFO violation identification procedure, update both the lower and upper bounds of the TSTC, and fathom the unnecessary branches.

4. Numerical examples

This section presents six numerical experiments to illustrate the properties and performance of the proposed DSO-SRDTC models. All experiments were run on a computer with an Intel (R) Core(TM) i5-2400 3.10GHz CPU and an 8 GB RAM. All LP problems and MLIP problems were solved by commercial software Gurobi (version 6.5). The parameter for LP problems in Section 2.5.3 was $\phi = 0.0001$. The parameters in branch-and-bound algorithms are the same as those in Long and Szeto (2017). The unit costs of travel time and schedule delay early and late were set as follows: α = 1.2 HKD/min, β =0.6 HKD/min, and γ = 2.4 HKD/min. The initial state for all networks was empty. Unless specified otherwise, the input parameter values of the LTM for each link were the same and are given as follows:

- Jam density: 133 veh/km.
- Free-flow speed: 54 km/h (i.e., 15 m/s), and backward shock-wave speed: -18 km/h (i.e., -5 m/s).

- Flow capacity: 1800 veh/h/lane (i.e., 0.5 veh/s/lane).
- The length of each time interval δ: 10 s.

Example 1. Comparing NVH solution vectors in a diverge network.

This example adopts the test network as shown in Fig. 1. This network has four nodes, three links, and two OD pairs (i.e., OD pairs (r, s_1) and (r, s_2)). The inflow capacities are 10 veh/interval for link 2 and 5 veh/interval for link 3. The outflow capacity of link 1 is 15 veh/interval. The free flow travel times are one interval for all links. The OD demands between OD pairs (r, s_1) and (r, s_2) are 10 vehicles and 3 vehicles, respectively. For the ease of presentation, we only consider a feasible solution that all traffic demands entered the network in the first interval.

Table 1 provides a weak link-based NVH solution vector (denoted by $\mathbf{x}_1$) and an intersection-movement-based solution vector (denoted by $\mathbf{y}_1$ and $\mathbf{x}_1=\boldsymbol{\varphi}_1(\mathbf{y}_1)$) retrieved from the link-based solution vector. According to Definition 7, $\mathbf{y}_1$ is a weak intersection-movement-based NVH solution vector. Table 2 provides a strong intersection-movement-based NVH solution vector (denoted by $\mathbf{y}_2$) and the corresponding link-based solution vector (denoted by $\mathbf{x}_2$ and $\mathbf{x}_2=\boldsymbol{\varphi}_1(\mathbf{y}_2)$). It is easy to check that $\mathbf{x}_2 \neq \mathbf{x}_1$, $\mathbf{x}_2 \geq \mathbf{x}_1$, $\mathbf{y}_2 \neq \mathbf{y}_1$, and $\mathbf{y}_2 \geq \mathbf{y}_1$. According to Definition 9, $\mathbf{x}_1$ is a weak link-based VH solution vector and does not satisfy the strong link-based NVH condition. This implies that the existing definition of a link-based NVH solution vector (i.e., Definition 6) can involve holding flows. According to Definition 7, $\mathbf{y}_2$ is a weak intersection-movement-based NVH solution vector. According to Definition 6, $\mathbf{x}_2=\boldsymbol{\varphi}_1(\mathbf{y}_2)$ is a weak link-based NVH solution vector. Hence, the result presented in Table 2 is consistent with Proposition 6 that a weak intersection-movement-based NVH solution vector can transform into a weak link-based NVH solution vector.

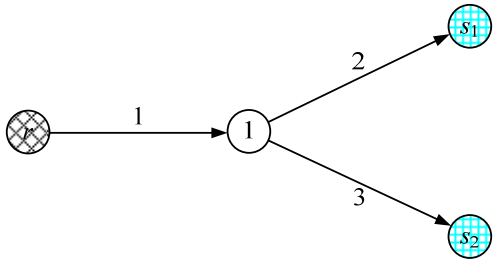

Fig. 1. The test network for Example 1.

Table 1. A weak link-based NVH solution vector in Example 1.

Interval	$U_1^{s_1}(k)$	$U_1^{s_2}(k)$	$V_1^{s_1}(k)$	$V_1^{s_2}(k)$	$U_2^{s_1}(k)$	$U_3^{s_2}(k)$	$U_{12}^{s_1}(k)$	$U_{13}^{s_2}(k)$	$V_{12}^{s_1}(k)$	$V_{13}^{s_2}(k)$
0	0	0	0	0	0	0	0	0	0	0
1	10	3	0	0	0	0	10	3	0	0
2	10	3	10	*0*	10	*0*	10	3	10	*0*
3	10	3	10	*3*	10	3	10	3	10	3

Table 2. A strong intersection-movement-based NVH solution vector in Example 1.

Interval	$U_{12}^{s_1}(k)$	$U_{13}^{s_2}(k)$	$V_{12}^{s_1}(k)$	$V_{13}^{s_2}(k)$	$U_1^{s_1}(k)$	$U_1^{s_2}(k)$	$V_1^{s_1}(k)$	$V_1^{s_2}(k)$	$U_2^{s_1}(k)$	$U_3^{s_2}(k)$
0	0	0	0	0	0	0	0	0	0	0
1	10	3	0	0	10	3	0	0	0	0
2	10	3	10	*3*	10	3	10	*3*	10	*3*
3	10	3	10	3	10	3	10	*3*	10	3

Example 2. Comparing NVH solution vectors with and without the consideration of the FIFO requirement in a diverge network.

In this example, we adopted the test network as shown in Fig. 1. The inflow capacity, outflow capacity, and the free flow travel time of each link are the same as those in Example 1. The OD demands between OD pairs (r, s_1) and (r, s_2) are 6 vehicles and 15 vehicles, respectively. For the ease of presentation, we only consider a feasible solution that the traffic demand of OD pair (r, s_1) entered the network in the second interval, and the traffic demand of OD pair (r, s_2) entered the network in the first interval.

Table 3 provides a strong link-based NVH solution vector without the consideration of FIFO requirement. We can observe from the table that $U_1^{s_1}(\underline{\ell}_{1,k}^{*}) < V_1^{s_1}(k)$ is satisfied for $k = 3$. This implies that the vehicles moving to destination s_1 overpass those moving to destination s_2 during interval 3, and the vehicles on Link 1 moving to destination s_1 are discharged to the downstream Link 2 when the downstream Link 3 is congested. Therefore, a FIFO violation can exist in a strong link-based NVH solution vector defined by Definition 9. If the FIFO requirement is considered, as shown in Table 4, we can obtain a weak link-based NVH solution vector that satisfies the FIFO condition. In this solution vector, although there is no congestion on Link 2 during interval 3, vehicles moving to destination s_1 are held on Link 1 due to congestion on the downstream Link 3. This implies that in a multi-destination network, if the FIFO requirement is considered, a weak NVH solution vector can allow the existence of vehicles on an entering link of a diverge junction that do not move forward to their own successor link even if there is no congestion on their own successor link. In other words, it is possible that in a weak NVH solution that satisfies the FIFO condition, an upstream link has vehicles not discharged due to congestion of one or some downstream links, but not necessarily all downstream links of the junction.

Example 3. Comparing link-based and intersection-movement-based FIFO solution vectors in a four-node network.

This example adopts the test network as shown in Fig. 2. This network has four nodes, four links, and one OD pair (r, s). The inflow capacities are 10 veh/interval for Link 2, 15 veh/interval for Link 3, and 25 veh/interval for Link 4. The outflow capacities are 25 veh/interval for Link 1, 10 veh/interval for Link 2, and 15 veh/interval for Link 3. The free flow travel times are one interval for all links. The demand between OD pair (r, s) is 30 vehicles. For the ease of presentation, we only consider a feasible solution that all traffic demands entered the network in the first interval.

Table 3. A strong link-based NVH solution vector without the consideration of FIFO in Example 2.

Interval	$U_1^{s_1}(k)$	$U_1^{s_2}(k)$	$V_1^{s_1}(k)$	$V_1^{s_2}(k)$	$U_2^{s_1}(k)$	$U_3^{s_2}(k)$	$\underline{\ell}_{1,k}^*$	$U_1^{s_1}(\underline{\ell}_{1,k}^*)$	$U_1^{s_2}(\underline{\ell}_{1,k}^*)$
0	0	0	0	0	0	0	0	0	0
1	0	15	0	0	0	0	0	0	0
2	6	15	0	5	0	5	1/3	0	5
3	6	15	6	10	6	10	2/3	0	10
4	6	15	6	15	6	15	3	6	15

Table 4. A weak link-based NVH solution vector with the consideration of FIFO in Example 2.

Interval	$U_1^{s_1}(k)$	$U_1^{s_2}(k)$	$V_1^{s_1}(k)$	$V_1^{s_2}(k)$	$U_2^{s_1}(k)$	$U_3^{s_2}(k)$	$\underline{\ell}_{1,k}^*$	$U_1^{s_1}(\underline{\ell}_{1,k}^*)$	$U_1^{s_2}(\underline{\ell}_{1,k}^*)$
0	0	0	0	0	0	0	0	0	0
1	0	15	0	0	0	0	0	0	0
2	6	15	0	5	0	5	1/3	0	5
3	6	15	0	10	0	10	2/3	0	10
4	6	15	6	15	6	15	3	6	15

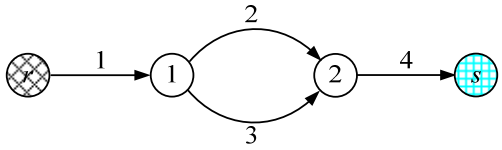

Fig. 2. The test network for Example 3.

Because the test network in Fig. 4 is a single-destination network, according to the definition of link-based FIFO conditions, all feasible link-based solution vectors satisfy link-based FIFO. However, we find that the intersection-movement-based FIFO conditions may not be satisfied in this single-destination network. For example, the feasible intersection-movement-based solution vector presented in Table 5 is not an intersection-movement-based FIFO solution vector. We can observe from Table 5 that $U_{13}^s(\underline{\ell}_{1,k}^*) < V_{13}^s(k)$ and $U_{12}^s(\overline{\ell}_{1,k}^*) > V_{12}^s(k)$ are satisfied for k=2. This implies that the vehicles from Link 1 to Link 3 overpass the vehicles from Link 1 to Link 2 during interval 2, i.e., this solution vector involves FIFO violations. This result is consistent with Propositions 24 and 25.

Table 5. The cumulative inflows and outflows disaggregated by intersection movement and destination on Link 1 in Example 3.

Time interval	$U_{12}^s(k)$	$V_{12}^s(k)$	$U_{13}^s(k)$	$V_{13}^s(k)$	$\underline{\ell}_{1,k}^*$	$U_{12}^s(\underline{\ell}_{1,k}^*)$	$U_{13}^s(\underline{\ell}_{1,k}^*)$	$\overline{\ell}_{1,k}^*$	$U_{12}^s(\overline{\ell}_{1,k}^*)$	$U_{13}^s(\overline{\ell}_{1,k}^*)$
0	0	0	0	0	0	0	0	0	0	0
1	15	0	15	0	0	0	0	0	0	0
2	15	**10**	**15**	15	0.67	10	**10**	1	**15**	15
3	15	15	15	15	1	15	15	1	15	15

Example 4. Comparing intersection-movement-based and path-based FIFO solution vectors in a five-node network.

This example adopts the test network as shown in Fig. 3. This network has five nodes, five links, and one OD pair (i.e., OD pair (*r*, *s*)). OD pair (*r*, *s*) is connected by two paths (i.e., path p_1: 1-2-3-5 and path p_2:

1-2-4-5). The inflow capacities are 15 veh/interval for Link 2, 10 veh/interval for Link 3, 5 veh/interval for Link 4, and 25 veh/interval for Link 5. The outflow capacities are 20 veh/interval for Link 1, 15 veh/interval for Link 2, 10 veh/interval for Link 3, and 5 veh/interval for Link 4. The free flow travel times are one interval for all links. The demand between OD (*r*, *s*) is 20 vehicles. For the ease of presentation, we only consider a feasible solution that all traffic demands entered the network in the first interval.

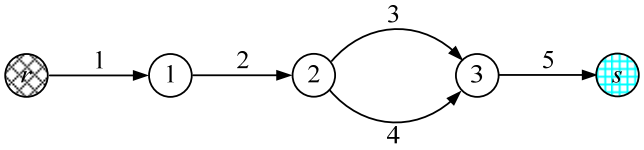

Fig. 3. The test network for Example 4.

The test network in Fig. 3 is a single-destination network and there is a single intersection movement for Link 1. Therefore, according to the definition of link-based and intersection-movement-based FIFO conditions, all feasible link-based solution vectors satisfy link-based FIFO and all feasible intersection-movement-based solution vectors satisfy intersection-movement-based FIFO on Link 1. However, we find that the path-based FIFO conditions may not be satisfied on Link 1. For example, the feasible path-based solution vector presented in Table 6 involves a FIFO violation on Link 1. We can observe from Table 6 that $U^s_{1p_1}(\underline{\ell}^*_{1,k}) < V^s_{1p_1}(k)$ and $U^s_{1p_2}(\overline{\ell}^*_{1,k}) > V^s_{1p_2}(k)$ are satisfied for k = 2. This implies that the vehicles on Path 1 overpass the vehicles on Path 2 when they are both on Link 1 during interval 2. This result is consistent with Propositions 26 and 27.

Table 6. The cumulative inflows and outflows disaggregated by path and destination on Link 1 in Example 4.

Time interval	$U^s_{1p_1}(k)$	$V^s_{1p_1}(k)$	$U^s_{1p_2}(k)$	$V^s_{1p_2}(k)$	$\underline{\ell}^*_{1,k}$	$U^s_{1p_1}(\underline{\ell}^*_{1,k})$	$U^s_{1p_2}(\underline{\ell}^*_{1,k})$	$\overline{\ell}^*_{1,k}$	$U^s_{1p_1}(\overline{\ell}^*_{1,k})$	$U^s_{1p_2}(\overline{\ell}^*_{1,k})$
0	0	0	0	0	0	0	0	0	0	0
1	10	0	10	0	0	0	0	0	0	0
2	10	**10**	10	**5**	0.5	**5**	5	1	10	**10**
3	10	10	10	10	1	10	10	1	10	10

Example 5. Comparing the optimal TSTCs of various models in a nine-node network.

In this example, a network in Fig. 4 is adopted to illustrate the optimal solutions of various models. The test network has nine nodes, nine links, one origin (*r*), two destinations (s_1 and s_2), and two OD pairs (r, s_1) and (r, s_2). The setting of link parameters for the network is provided in Table 7. The OD demands are 30 vehicles for both OD pairs. The parameters of the arrival time window were set as follows: $\underline{k}^*_{s_1} = 4$, $\underline{k}^*_{s_2} = 5$, $\overline{k}^*_{s_1} = 7$, and $\overline{k}^*_{s_2} = 8$. We assume that an accident happened on Link 2, and the following two scenarios are considered:

- **Scenario 1**: The outflow capacities of Link 2 are 30 veh/interval for the first three intervals and 5 veh/interval for the fourth interval, and 0 veh/interval for the rest of time horizon.

- **Scenario 2**: The outflow capacities of Link 1 are 30 veh/interval for the first two intervals and 5 veh/interval for the third interval, and 0 veh/interval for the rest of time horizon.

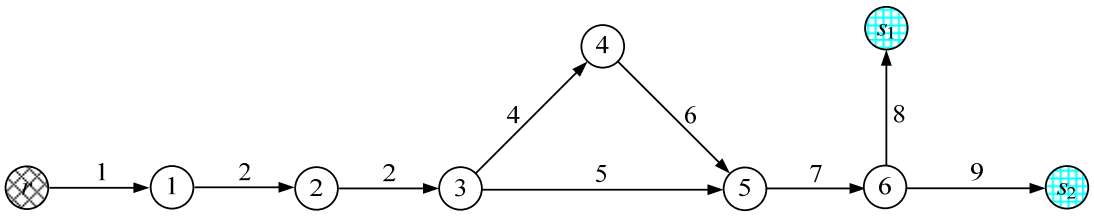

Fig. 4. The test network for Example 5.

Table 7. The setting of link parameter values for the nine-node test network in Example 5.

Link	1	2	3	4	5	6	7	8	9
Length (m)	150	150	150	150	450	150	150	150	150
Number of lanes	10	6	6	3	2	3	6	100	100
Maximum link occupancy (veh)	∞	60	60	30	30	30	60	∞	∞
Flow capacity (veh/interval)	30	30	30	15	10	15	30	30	30

We solved the proposed DSO-SRDTC models for both scenarios and obtained the TSTCs in Table 8. One can observe from the table that the optimal TSTCs for the DSO-SRDTC problems without FIFO constraints are equal to 91 HKD for both scenarios. This result is consistent with Theorem 1 that the link-based, intersection-movement-based, and path-based DSO-SRDTC problems are equivalent in terms of obtaining the same optimal TSTC. One can also observe from Table 8 that the path-based DSO-SRDTC problems give the highest optimal TSTCs, and the link-based DSO-SRDTC problems give the lowest optimal TSTCs. This is consistent with Theorem 9. In addition, the results presented in Table 8 also show that the optimal TSTCs for the DSO-SRDTC problems with FIFO constraints are not less than those for the DSO-SRDTC problems without FIFO constraints. This result is consistent with Theorem 10.

Table 8. TSTCs obtained from different DSO-SRDTC models in Example 5.

Scenario	Formulation	R-DSO	NVH-DSO	FIFO-DSO	NVH-FIFO-DSO
Scenario 1	Link-based	91	91	91	91
	Intersection-movement-based	91	91	92.2	92.2
	Path-based	91	91	92.2	92.2
Scenario 2	Link-based	91	91	91	91
	Intersection-movement-based	91	91	91	92.2
	Path-based	91	91	92.2	92.2

The TSTCs under different values of ϕ for Scenario 1 are shown in Fig. 1. One can observe that the link-based, intersection-movement-based, and path-based NVH-DSO-SRDTC models yield an identical optimal TSTC of 91 HKD when $\phi \le 0.066$, which confirms that LP problems (70), (72), and (73) can obtain an NVH-DSO solution vector when the coefficient of the penalty term is positive and sufficiently small.

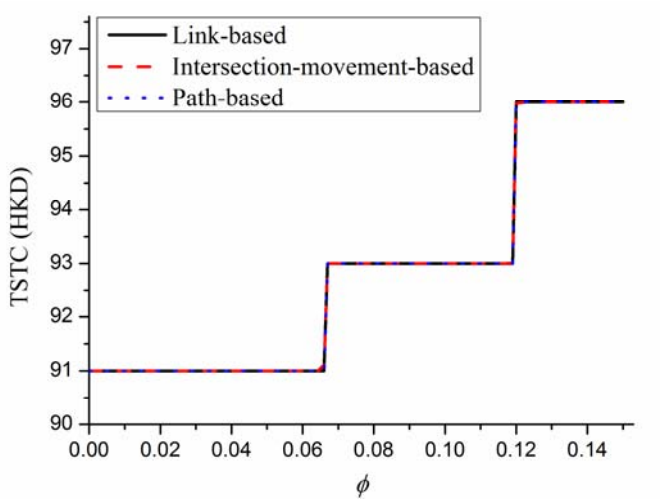

Fig. 5. The TSTCs under different values of ϕ for Scenario 1 in Example 5.

Example 6. Illustration of the existence of cyclic DSO flows in link-based and intersection-movement-based DSO-SRDTC problems in a cyclic network under time-varying capacities.

In this example, a cyclic network shown in Fig. 6 is adopted to illustrate that cyclic flows may not be completely eliminated in optimal solutions to NVH-DSO-SRDTC problems. The network has four nodes, four links, and one OD pair (*r*, *s*). Both the free-flow travel time and backward shock-wave travel time on all links are one interval. The total traffic demand is 30 vehicles. The outflow capacities of Link 1 are 10 veh/interval for the first four intervals, 0 veh/interval for intervals 5-9, and 1 veh/interval for the rest of time horizon. The flow capacity for Link 2 is 10 veh/interval. The inflow capacity of Link 4 is 5 veh/interval. In this example, we construct two scenarios with different flow capacities of Link 3. The flow capacities for Link 3 are 10 veh/interval and 0 veh/interval in Scenarios 3 and 4, respectively. The parameters of the arrival time window were set as follows: $\underline{k}_s^* = \overline{k}_s^* = 4$.

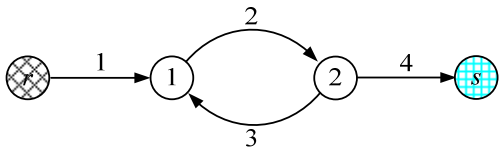

Fig. 6. A cyclic network for Example 6.

We solved the proposed link-based and intersection-movement-based NVH-DSO-SRDTC models in Scenario 3, and find that the TSTCs to both models are the same and equal 41.5 HKD. The optimal cumulative outflows disaggregated by intersection movement and destination are shown in Table 9. One can observe that the flows under the third and fourth columns in Scenario 3 are positive during some intervals. This means that cyclic flows exist in the optimal solutions. The reasons for the existence of cyclic flows in the optimal solutions are as follows: (1) Because the outflow capacity of Link 1 decreases to 0 veh/interval for

intervals 5-9, it is better for all the vehicles to exit Link 1 during the first four intervals; otherwise, some vehicles would exit Link 1 after the ninth interval and experience a large cost of schedule delay late compared with the scheduled delay induced by waiting on other links. (2) Because the inflow capacity of Link 4 is quite low (i.e., 5 veh/interval), some vehicles need to be diverted to Link 3, which is used for storage, in order to avoid spillback from Link 2 to Link 1 and keeping these vehicles on Link 1 until interval 10. In Scenario 4, because the flow capacity for Link 3 is 0 veh/interval, this link cannot be used, and cyclic flows are infeasible in this scenario. We solved the DSO-SRDTC problems to obtain an optimal solution in Scenario 4. We find that the TSTC increases to 46.5 HKD. One can also observe from Table 9 that the cumulative outflows under the first column in Scenario 4 are strictly increasing from interval 9 to interval 14, and five vehicles exit Link 1 after the ninth intervals instead of during the first four intervals due to the queue spillback from Link 2 to Link 1. These five vehicles experience a large cost of schedule delay late, leading to a higher TSTC in Scenario 4 than that in Scenario 3. The implication of this example is that when the downstream capacity is quite low, it is necessary to divert traffic to other links for storage (even if this diversion may cause cyclic flows) in order to avoid queue spillback and travelers facing a large schedule delay cost due to a long closure of an upstream link. Note that complete path-based DSO-SRDTC formulations may not be available for cyclic (time-dependent) networks because it is difficult to enumerate all cyclic paths in a cyclic network. This implies that path-based DSO-SRDTC models may not be able to be used for cyclic networks with time-varying link capacities.

Table 9. The optimal cumulative outflows disaggregated by intersection movement and destination of the DSO-SRDTC problems in the cyclic network.

Time Interval	Scenario 3				Scenario 4			
	$V_{12}^s(k)$	$V_{24}^s(k)$	$V_{23}^s(k)$	$V_{32}^s(k)$	$V_{12}^s(k)$	$V_{24}^s(k)$	$V_{23}^s(k)$	$V_{32}^s(k)$
0	0	0	0	0	0	0	0	0
1	0	0	0	0	0	0	0	0
2	10	0	0	0	5	0	0	0
3	20	5	5	0	15	5	0	0
4	30	10	10	0	25	10	0	0
5	30	15	15	10	25	15	0	0
6	30	20	20	15	25	20	0	0
7	30	25	20	20	25	25	0	0
8	30	30	20	20	25	25	0	0
9	30	30	20	20	25	25	0	0
10	30	30	20	20	26	25	0	0
11	30	30	20	20	27	26	0	0
12	30	30	20	20	28	27	0	0
13	30	30	20	20	29	28	0	0
14	30	30	20	20	30	29	0	0
15	30	30	20	20	30	30	0	0

In the existing literature on SO-DTA (e.g., Merchant and Nemhauser, 1978a,b; Zhu and Ukkusuri, 2013; Ma et al., 2014, 2017; Zheng et al., 2015), most SO-DTA studies only consider time-invariant outflow capacities, so that no cyclic flow should exist in a SO-DTA solution. In this example, the outflow capacities of link 1 are purposely designed to be reduced after the first three intervals. The cyclic network structure is treated as a storage of early-entered flow under such a specific setting on the time-varying outflow capacities. Due to such a specific setting, the flow needs to enter the network at their earliest time; otherwise, they are significantly delayed due to the reduction of the outflow capacity. This means as long as the network can provide enough storage to accommodate the early-entered flow, DSO can be achieved. Note that the results presented in this example do not mean that the storage has to be in a cyclic structure. In practice, one or several long links can also serve as the suitable storage.

Example 7. Comparing the efficiency of solving the proposed models in the modified Nguyen and Dupuis (1984) network.

In this example, we adopt a modified Nguyen and Dupuis network (see Fig. 7) to illustrate the efficiency of solving the proposed models. The network has 17 nodes, 23 links, 4 OD pairs, and 28 paths. The traffic demands are 80 vehicles for all OD pairs. The numbers of lanes are 1 for Links 8-2, 12-8, and 13-3, 2 for Links 7-8 and 9-13, and 3 for other 14 links. The outflow capacities of links going into nodes 2, 3, 5, 6, 9, 10, and 11 are 3.0 veh/interval/lane. The maximum link occupancies and flow capacities of links r_1-1, r_2-4, 2-s_1, and 3-s_2 are infinite. The length of each link is provided in Table 10. There was an incident on Links 1-12 and 4-9. The outflow capacities of Links 1-12 and 4-9 are 15 veh/interval for the first 13 intervals and 0 veh/interval for the rest of time horizon. The parameters of the arrival time window were set as follows: $\underline{k}_{s_1}^* = 18$, $\overline{k}_{s_1}^* = 24$, $\underline{k}_{s_2}^* = 16$, and $\overline{k}_{s_2}^* = 21$. The modeling horizon is set to be 70 intervals.

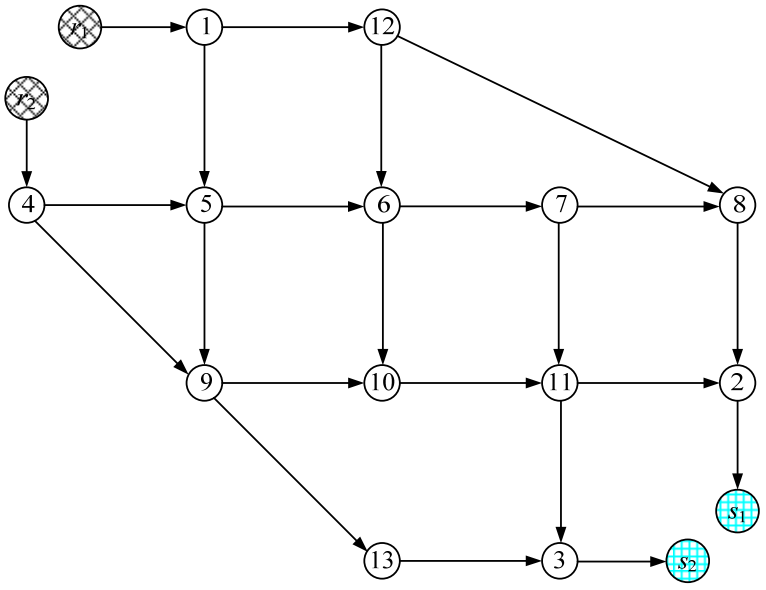

Fig. 7. The modified Nguyen and Dupuis (1984) network for Example 7.

Table 10. The length of each link in the modified Nguyen and Dupius network for Scenario 1 in Example 7.

Link length (m)	150	450	600	600	750
Link	r_1-1	1-12	1-5	4-5	12-8
	r_2-4	7-8	4-9	5-6	
	2-s_1	7-11	5-9	6-7	
	3-s_2	9-13	6-10	9-10	
		8-2	11-2	11-3	
		10-11	12-6	13-3	

In Table 11, we compare the sizes of the link-based, intersection-movement-based, and path-based R-DSO-SRDTC problems without FIFO constraints. We can observe that the link-based and intersection-movement-based formulations have considerably fewer variables and constraints than the path-based formulation. In this example, all DSO-SRDTC models without FIFO constraints give the same TSTCs (967.5 HKD) and all DSO-SRDTC models with FIFO constraints also give the same TSTCs (968.4 HKD). The CPU times required to solve the proposed models are provided in Table 12. We can observe that the link-based and intersection-movement-based formulations can be solved more efficiently than the path-based formulation.

Table 11. The sizes of the R-DSO-SRDTC problem in Example 7.

Formulation	Number of variables	Number of constraints
Link-based	3312	8183
Intersection-movement-based	5040	11089
Path-based	41400	62273

Table 12. The CPU times for solving the proposed models in Example 7.

Formulation	R-DSO	NVH-DSO	FIFO-DSO	NVH-FIFO-DSO
Link-based	0.24	0.26	275.26	276.74
Intersection-movement-based	0.42	0.45	493.16	393.21
Path-based	1.88	1.60	1565.74	1984.23

5. Conclusions

In this paper, the LTM was adopted to formulate link-based, intersection-movement-based, and path-based DSO-SRDTC problems in terms of cumulative flows. Similar to the well-known cell-based DSO-SRDTC models, each of the link-based, intersection-movement-based, and path-based DSO-SRDTC models without FIFO constraints can lead to an LP formulation. However, the DSO-SRDTC problems with FIFO constraints were formulated as non-convex nonlinear programming problems due to non-convex constraint sets yielded by the FIFO requirement. We proved that the three formulations of DSO-SRDTC problems are equivalent in terms of obtaining the same TSTC if FIFO constraints are not considered. However, they can obtain different optimal TSTCs if FIFO constraints are considered. We found that existing link-based NVH constraints cannot

completely eliminate weak VH solutions, and propose both intersection-movement-based and path-based NVH constraints, which can completely eliminate weak VH solutions. Because of the property of the formulations, the DSO-SRDTC problems without FIFO constraints were directly solved by commercial software, and the DSO-SRDTC problems with FIFO constraints were solved by branch-and-bound algorithms.

Examples were given to show the properties and performance of the proposed model. We illustrated that link-based NVH constraints cannot completely eliminate VH phenomena, and the FIFO conditions for link-based, intersection-movement-based, and path-based DSO-SRDTC problems are not equivalent. Our results confirmed that the three formulations of the DSO-SRDTC problems are equivalent in terms of obtaining the same optimal TSTC if FIFO constraints are not considered. However, they can obtain different TSTCs if FIFO constraints are considered. We also found that cyclic flows can help to reduce the TSTC in cyclic networks under time-varying capacities. Because it is difficult to enumerate cyclic paths in a cyclic time-dependent network, we conclude that complete path-based formulations for DSO-SRDTC problem may not be able to be available for these networks. The results also showed that link-based and intersection-movement-based models can be solved more efficiently than path-based models.

Acknowledgments

This work is jointly supported by the National Natural Science Foundation of China (71271075, 71431003, 71522001), a grant from the Research Grants Council of the Hong Kong Special Administrative Region, China (HKU 17201915), and the Fundamental Research Funds for the Central Universities (JZ2016HGPB0736). The authors are grateful to the reviewers for their constructive comments.

Appendix A: Proof of Propositions and Theorems

A.1. Proof of Proposition 1

Proof. According to Eqs. (19)-(21), we have

$$\sum_{b\in\Gamma(a)} U_{ab}^{s}(k) = U_{a}^{s}(k), \forall s \in S, a \in A \setminus A_S, k \in K, \tag{A1}$$

$$\sum_{b\in\Gamma^{-1}(a)} V_{ba}^{s}(k) = U_{a}^{s}(k), \forall s \in S, a \in A_S, k \in K, \text{ and} \tag{A2}$$

$$\sum_{b\in\Gamma(a)} V_{ab}^{s}(k) = V_{a}^{s}(k), \forall s \in S, a \in A \setminus A_S, k \in K. \tag{A3}$$

Substituting Eqs. (A1)-(A3) into constraints (23)-(25) after changing the index notation or argument when necessary, we have constraints (9), (11), and (12). Taking summation of all $b \in \Gamma(a)$ for both sides of constraints (26), (28)-(31), and substituting Eqs. (A1)-(A3) into the resultant constraints, we can obtain constraints (10), (14)-(17).

Taking summation of all $a \in A(i)$ for both sides of constraint (27) and by definition, we have

$$\sum_{a\in A(i)}\sum_{b\in\Gamma^{-1}(a)} V_{ba}^{s}(k) = \sum_{b\in A(i)}\sum_{a\in\Gamma^{-1}(b)} V_{ab}^{s}(k) = \sum_{a\in A(i)}\sum_{b\in\Gamma(a)} U_{ab}^{s}(k), \forall i \in N\setminus\{R,S\}, s\in S, k\in K \text{ .(A4)}$$

By definition, we have $B(i)=\Gamma^{-1}(a)$ for all $a\in A(i), i\in N$, and $A(i)=\Gamma(a)$ for all $a\in B(i), i\in N$. Using these two equations, the middle term of Eq. (A4) can be written as

$$\sum_{b\in A(i)}\sum_{a\in\Gamma^{-1}(b)} V_{ab}^{s}(k) = \sum_{b\in A(i)}\sum_{a\in B(i)} V_{ab}^{s}(k) = \sum_{a\in B(i)}\sum_{b\in A(i)} V_{ab}^{s}(k) = \sum_{a\in B(i)}\sum_{b\in\Gamma(a)} V_{ab}^{s}(k) \text{ .} \quad \text{(A5)}$$

The middle term of Eq. (A4), which is identical to the last term of Eq. (A5), equals the last term of Eq. (A4), and hence we have

$$\sum_{a\in B(i)}\sum_{b\in\Gamma(a)} V_{ab}^{s}(k) = \sum_{a\in A(i)}\sum_{b\in\Gamma(a)} U_{ab}^{s}(k), \forall s\in S, i\in N\setminus\{R,S\}, k\in K \text{ .} \quad \text{(A6)}$$

Substituting Eqs. (A1) and (A3) into Eq. (A6), we have constraints (13). In summary, $\mathbf{x}$ satisfies constraints (9)-(17), and hence $\mathbf{x}=\boldsymbol{\varphi}_1(\mathbf{y})\in\Omega$. This completes the proof. □

A.2. Proof of Proposition 2

Proof. The following notations will be used in this proof:

$Y_a^s(k,l)$	cumulative number of vehicles entering link *a* by the end of interval *k*, exiting the link by interval *l*, and heading to destination *s*.
$u_a^s(k)$	inflow into link *a* during interval *k* and heading to destination *s*.
$u_{ab}^s(k)$	inflow into link *a* during interval *k* and through link $b\in A(h_a)$ to destination *s*.
$v_a^s(k)$	outflow from link *a* during interval *k* heading to destination *s*.
$v_{ab}^s(k)$	outflow from link *a* during interval *k* and through link $b\in A(h_a)$ to destination *s*.
$y_a^s(k,l)$	number of vehicles entering link *a* during interval *k*, exiting the link during interval *l*, and heading to destination *s*.
$y_{ab}^s(k,l)$	number of vehicles entering link *a* during interval *k*, exiting the link during interval *l*, and through link $b\in A(h_a)$ to destination *s*.

For a given link-based solution vector $\mathbf{x}\in\Omega$, by definition, we can obtain link inflows and outflows as follows:

$$u_a^s(k) = U_a^s(k) - U_a^s(k-1), \forall s\in S, a\in A, k\in K \quad \text{and} \quad \text{(A7)}$$

$$v_a^s(k) = V_a^s(k) - V_a^s(k-1), \forall s\in S, a\in A\setminus A_S, k\in K \text{ .} \quad \text{(A8)}$$

The inflow of a given link during a given interval may not exit the link during the same time interval, and hence can be decomposed by several sub-packets that leave the link during different intervals. According to Long et al. (2016), the cumulative flow $Y_a^s(k,l)$ can be formulated as follows:

$$Y_a^s(k,l) = \begin{cases} 0, & \text{if } V_a^s(l) \le U_a^s(k-1), \\ V_a^s(l) - U_a^s(k-1), & \text{if } U_a^s(k-1) < V_a^s(l) < U_a^s(k), \\ U_a^s(k) - U_a^s(k-1), & \text{if } V_a^s(l) \ge U_a^s(k). \end{cases} \forall s\in S, a\in A\setminus A_S, k\in K, l\in K \text{ .} \quad \text{(A9)}$$

By definition, we have

$$y_a^s(k,l) = Y_a^s(k,l) - Y_a^s(k,l-1), \forall s \in S, a \in A \setminus A_S, k \in K, l \in K. \tag{A10}$$

According to conditions (10), we have

$$V_a^s(k + \overline{\tau}_a - 1) \le U_a^s(k-1), \forall s \in S, a \in A \setminus A_S, k \in K. \tag{A11}$$

Substituting inequality (A11) into Eq. (A9), we have

$$Y_a^s(k,l) = 0, \forall s \in S, a \in A \setminus A_S, k \in K, l \le k + \overline{\tau}_a - 1. \tag{A12}$$

Substituting Eq. (A12) into Eq. (A10), we have

$$y_a^s(k,l) = 0, \forall s \in S, a \in A \setminus A_S, k \in K, l \in \{1, 2, \cdots, k - \overline{\tau}_a - 1\}. \tag{A13}$$

Equivalently, we have

$$y_a^s(l,k) = 0, \forall s \in S, a \in A \setminus A_S, k \in K, l \in \{k - \overline{\tau}_a + 1, k - \overline{\tau}_a + 2, \cdots, \underline{K}\}. \tag{A14}$$

Hence, we have

$$u_a^s(k) = \sum_{l=1}^{K} y_a^s(k,l) = \sum_{l=k+\overline{\tau}_a}^{K} y_a^s(k,l), \forall s \in S, a \in A \setminus A_S, k \in K, \tag{A15}$$

$$v_a^s(k) = \sum_{l=1}^{K} y_a^s(l,k) = \sum_{l=1}^{k-\overline{\tau}_a} y_a^s(l,k), \forall s \in S, a \in A \setminus A_S, k \in K, \tag{A16}$$

$$U_a^s(k) = \sum_{h=1}^{k} u_a^s(h) = \sum_{h=1}^{k} \sum_{l=k+\overline{\tau}_a}^{K} y_a^s(h,l), \forall s \in S, a \in A \setminus A_S, k \in K, \text{ and} \tag{A17}$$

$$V_a^s(k) = \sum_{h=1}^{k} v_a^s(h) = \sum_{h=1}^{k} \sum_{l=1}^{k-\overline{\tau}_a} y_a^s(l,h), \forall s \in S, a \in A \setminus A_S, k \in K. \tag{A18}$$

For all $i \in N \setminus \{S\}$, $s \in S$, $a \in B(i)$, $b \in A(i)$, and $k \in K$, the link outflows disaggregated by intersection movement (i.e., $v_{ab}^s(k)$) can be retrieved from the link inflows and outflows disaggregated by destination (i.e., $u_a^s(k)$ and $v_a^s(k)$) according to the following LP problem:

$$\begin{aligned} &\max \psi = \sum_{a \in B(i)} \sum_{b \in A(i)} v_{ab}^s(k) \\ &s.t. \begin{cases} \sum_{b \in A(i)} v_{ab}^s(k) = v_a^s(k), \forall a \in B(i), \\ \sum_{a \in B(i)} v_{ab}^s(k) = u_b^s(k), \forall b \in A(i), \\ v_{ab}^s(k) \ge 0, \forall a \in B(i), b \in A(i), \end{cases} \end{aligned} \tag{A19}$$

where the link inflow $u_b^s(k)$ and outflow $v_a^s(k)$ are inputs, and they can be obtained by Eqs. (A7) and (A8), respectively.

According to Eqs. (13), (A7), and (A8), we have

$$\sum_{a\in B(i)} v_a^s(k) = \sum_{a\in B(i)} V_a^s(k) - \sum_{a\in B(i)} V_a^s(k-1) = \sum_{a\in A(i)} U_a^s(k) - \sum_{a\in A(i)} U_a^s(k-1) = \sum_{a\in A(i)} u_a^s(k). \quad \text{(A20)}$$

Eq. (A20) implies that LP problem (A19) is a balanced transportation problem, and hence at least one solution can be guaranteed (Dantzig and Thapa, 2006). We can adopt an optimal solution to LP problem (A19) as the link outflows disaggregated by intersection movement and destination (i.e., $v_{ab}^s(k)$). Then, for all $a \in A \setminus A_S$, $s \in S$, and $k \in K$, link inflows disaggregated by intersection movement and destination (i.e., $u_{ab}^s(k)$) can be retrieved from link outflows disaggregated by intersection movement and destination (i.e., $v_{ab}^s(k)$) and decomposed link inflows disaggregated by destination (i.e., $y_a^s(l,k)$) according to the following LP problem:

$$\begin{aligned} &\min \psi' = \sum_{b\in\Gamma(a)} \sum_{l=1}^{k-\bar{\tau}_a} y_{ab}^s(l,k) \\ &s.t. \begin{cases} \sum_{l=1}^{k-\bar{\tau}_a} y_{ab}^s(l,k) = v_{ab}^s(k), \forall b \in \Gamma(a), \\ \sum_{b\in\Gamma(a)} y_{ab}^s(l,k) = y_a^s(l,k), \forall l \in \{1,2,\cdots,k-\bar{\tau}_a\}, \\ y_{ab}^s(l,k) \geq 0, \forall b \in \Gamma(a), l \in \{1,2,\cdots,k-\bar{\tau}_a\}, \end{cases} \end{aligned} \quad \text{(A21)}$$

where the decomposed link inflow disaggregated by destination (i.e., $y_a^s(l,k)$) and the link outflows disaggregated by intersection movement and destination (i.e., $v_{ab}^s(k)$) are inputs, and they can be obtained by Eq. (A10) and LP problem (A19), respectively.

According to Eq. (A15) and the first constraints of LP problem (A19), we have

$$\sum_{l=1}^{k-\bar{\tau}_a} y_a^s(l,k) = v_a^s(k) = \sum_{b\in A(i)} v_{ab}^s(k). \quad \text{(A22)}$$

Similarly, Eq. (A22) implies that LP problem (A21) is a balanced transportation problem, and hence at least one solution can be guaranteed (Dantzig and Thapa, 2006). We can adopt an optimal solution to LP problem (A21) as decomposed link inflows disaggregated by intersection movement and destination (i.e., $y_{ab}^s(l,k)$). Then, we can construct an intersection-movement-based solution vector $\mathbf{y}$ as follows:

$$U_{ab}^s(k) = \sum_{h=1}^{k} \sum_{l=k+\bar{\tau}_a}^{K} y_{ab}^s(h,l), \forall s \in S, a \in A \setminus A_S, b \in \Gamma(a), k \in K \quad \text{and} \quad \text{(A23)}$$

$$V_{ab}^s(k) = \sum_{h=1}^{k} \sum_{l=1}^{k-\bar{\tau}_a} y_{ab}^s(l,h), \forall s \in S, a \in A \setminus A_S, b \in \Gamma(a), k \in K. \quad \text{(A24)}$$

According to Eqs. (A17), (A21), and (A23), we have

$$U_a^s(k) = \sum_{h=1}^{k} \sum_{l=k+\bar{\tau}_a}^{K} y_a^s(h,l) = \sum_{h=1}^{k} \sum_{l=k+\bar{\tau}_a}^{K} \sum_{b\in\Gamma(a)} y_{ab}^s(h,l) = \sum_{b\in\Gamma(a)} U_{ab}^s(k), \forall s \in S, a \in A \setminus A_S, k \in K. \quad \text{(A25)}$$

According to Eqs. (A18), (A21), and (A24), we have

$$V_a^s(k)=\sum_{h=1}^{k}\sum_{l=1}^{k-\bar{\tau}_a} y_a^s(l,h)=\sum_{h=1}^{k}\sum_{l=1}^{k-\bar{\tau}_a}\sum_{b\in\Gamma(a)} y_{ab}^s(l,h)=\sum_{b\in\Gamma(a)} V_{ab}^s(k),\forall s\in S,a\in A\setminus A_S,k\in K \text{ .(A26)}$$

According to Eqs. (A19), (A21), and (A24), we have

$$U_a^s(k)=\sum_{h=1}^{k} u_a^s(h)=\sum_{h=1}^{k}\sum_{b\in\Gamma^{-1}(a)} v_{ba}^s(h)=\sum_{b\in\Gamma^{-1}(a)} V_{ba}(k),\forall s\in S,a\in A_S,k\in K\text{ .} \quad \text{(A27)}$$

Eqs. (A25)-(A27) imply that $\mathbf{x}$ and $\mathbf{y}$ satisfy Eqs. (19)-(21). Substituting (A25)-(A27) into constraints (9)-(11), we have constraints (23)-(25). According to Eqs. (A23) and (A24), constraint (26) is satisfied by $\mathbf{y}$, because

$$V_{ab}^s(k)=\sum_{h=1}^{k}\sum_{l=1}^{h-\bar{\tau}_a} y_{ab}^s(l,h)=\sum_{l=1}^{k-\bar{\tau}_a}\sum_{h=l+\bar{\tau}_a}^{k} y_{ab}^s(l,h)\le\sum_{l=1}^{k-\bar{\tau}_a}\sum_{h=l+\bar{\tau}_a}^{K} y_{ab}^s(l,h)=U_{ab}^s(k-\bar{\tau}_a) \quad \text{(A28)}$$
$$\forall a\in s\in S,A\setminus A_S,b\in\Gamma(a),k\in K.$$

According to Eq. (A19), we have

$$u_a^s(k)=\sum_{b\in\Gamma^{-1}(a)} v_{ba}^s(k)\text{ .} \quad \text{(A29)}$$

Hence, constraint (27) is satisfied by $\mathbf{y}$, because of the following:

$$\sum_{b\in\Gamma(a)} U_{ab}^s(k)=U_a^s(k)=\sum_{h=1}^{k} u_a^s(h)=\sum_{b\in\Gamma^{-1}(a)}\sum_{h=1}^{k} v_{ba}^s(h)=\sum_{b\in\Gamma^{-1}(a)} V_{ba}^s(k),\forall s\in S,a\in A\setminus A_S,k\in K\text{ .} \quad \text{(A30)}$$

Because $y_{ab}^s(h,l)$ is non-negative for all $a\in A\setminus A_S,b\in\Gamma(a),s\in S,h\in K,l\in K$, Eqs. (A23) and (A24) imply that the intersection-movement-based solution vector $\mathbf{y}$ satisfies non-decreasing constraints (28) and (29).

In summary, $\mathbf{x}$ and $\mathbf{y}$ satisfy Eqs. (19)-(21), and $\mathbf{y}$ satisfies constraints (23)-(31), i.e., $\mathbf{y}\in\bar{\Omega}$. This completes the proof. □

A.3. Proof of Proposition 3

Proof. According to Eqs. (35) and (36), we have

$$\sum_{p\in P^s}\varsigma_{abp}U_{ap}^s(k)=U_{ab}^s(k),\forall s\in S,a\in A\setminus A_S,k\in K \quad \text{and} \quad \text{(A31)}$$

$$\sum_{p\in P^s}\varsigma_{abp}V_{ap}^s(k)=V_{ab}^s(k),\forall s\in S,a\in A\setminus A_S,k\in K\text{ .} \quad \text{(A32)}$$

By definition, we have

$$\sum_{p\in P^s}U_{ap}^s(k)=U_a^s(k)=\sum_{b\in\Gamma(a)}U_{ab}^s(k),\forall s\in S,a\in A\setminus A_S,k\in K \quad \text{and} \quad \text{(A33)}$$

$$\sum_{p\in P^s}V_{ap}^s(k)=V_a^s(k)=\sum_{b\in\Gamma(a)}V_{ab}^s(k),\forall s\in S,a\in A\setminus A_S,k\in K\text{ .} \quad \text{(A34)}$$

Substituting Eqs. (A33)-(A34) into constraints (38)-(40) after changing the index notation or argument when necessary, we have constraints (23)-(25). Multiplying the 0-1 indicator ς_{abp} to both sides of constraints (41), (43)-(46), and taking summation over $p\in P^s$ and substituting Eqs. (A31) and (A32) into the resultant

constraints, we can obtain constraints (26), (28)-(31). By definition, constraint (42) can be reformulated as follows:

$$U_{ap}^{s}(k)=\sum_{b\in\Gamma^{-1}(a)}\varsigma_{bap}V_{bp}^{s}(k),\forall s\in S,p\in P^{s},a\in A,k\in K. \tag{A35}$$

Substituting Eq. (A35) into the leftmost hand side of Eq. (A33), we have

$$\sum_{p\in P^{s}}U_{ap}^{s}(k)=\sum_{p\in P^{s}}\sum_{b\in\Gamma^{-1}(a)}\varsigma_{bap}V_{bp}^{s}(k)=\sum_{b\in\Gamma^{-1}(a)}\sum_{p\in P^{s}}\varsigma_{bap}V_{bp}^{s}(k),\forall s\in S,a\in A\setminus A_{R},k\in K. \tag{A36}$$

Substituting Eqs. (A33) and (A32) into the leftmost and rightmost hand side of Eq. (A36), respectively, we have

$$\sum_{b\in\Gamma(a)}U_{ab}^{s}(k)=\sum_{b\in\Gamma^{-1}(a)}V_{ba}^{s}(k),\forall s\in S,a\in A\setminus A_{S},k\in K. \tag{A37}$$

Eq. (A37) implies that $\mathbf{x}$ satisfies constraint (27). In summary, $\mathbf{x}$ satisfies constraints (23)-(31), and hence $\mathbf{y}=\boldsymbol{\varphi}_2(\mathbf{z})\in\bar{\Omega}$. According to Proposition 1, we have $\mathbf{x}=\boldsymbol{\varphi}_1(\boldsymbol{\varphi}_2(\mathbf{z}))\in\Omega$. This completes the proof. □

A.4. Proof of Proposition 4

Proof. This proof also uses the notations defined in the proof of Proposition 2. For a given intersection-movement-based solution vector $\mathbf{y}\in\bar{\Omega}$, by definition, we can obtain intersection-movement-based link inflows and outflows (i.e., $u_{ab}^{s}(k)$ and $v_{ab}^{s}(k)$) as follows:

$$u_{ab}^{s}(k)=U_{ab}^{s}(k)-U_{ab}^{s}(k-1),\forall s\in S,a\in A\setminus A_{S},b\in\Gamma(a),k\in K, \text{ and} \tag{A38}$$

$$v_{ab}^{s}(k)=V_{ab}^{s}(k)-V_{ab}^{s}(k-1),\forall s\in S,a\in A\setminus A_{S},b\in\Gamma(a),k\in K. \tag{A39}$$

The intersection-movement-based link inflow of a given time interval can also be decomposed by several sub-packets that leave the link during different intervals. Similar to the decomposition of link-based inflows, the cumulative number of vehicles entering link *a* during interval *k*, exiting the link by interval *l*, and through link $b\in A(h_a)$ to destination *s*, $Y_{ab}^{s}(k,l)$, can be formulated as follows:

$$Y_{ab}^{s}(k,l)=\begin{cases}0, & \text{if } V_{ab}^{s}(l)\le U_{ab}^{s}(k-1),\\ V_{ab}^{s}(l)-U_{ab}^{s}(k-1), & \text{if } U_{ab}^{s}(k-1)<V_{ab}^{s}(l)<U_{ab}^{s}(k),\\ U_{ab}^{s}(k)-U_{ab}^{s}(k-1), & \text{if } V_{ab}^{s}(l)\ge U_{ab}^{s}(k).\end{cases}\forall s\in S,a\in A\setminus A_{S},b\in\Gamma(a),k\in K,l\in K. \tag{A40}$$

By definition, we have

$$y_{ab}^{s}(k,l)=Y_{ab}^{s}(k,l)-Y_{ab}^{s}(k,l-1),\forall s\in S,a\in A\setminus A_{S},b\in\Gamma(a),k\in K,l\in K. \tag{A41}$$

According to condition (26), we have

$$V_{ab}^{s}(k+\bar{\tau}_a-1)\le U_{ab}^{s}(k-1),\forall s\in S,a\in A\setminus A_{S},k\in K. \tag{A42}$$

Substituting inequality (A42) into Eq. (A40), we have

$$Y_{ab}^{s}(k,l)=0,\forall s\in S,a\in A\setminus A_{S},b\in\Gamma(a),k\in K,l\le k+\bar{\tau}_a-1. \tag{A43}$$

Substituting Eq. (A43) into Eq. (A41), we have

$$y^s_{ab}(k,l)=0, \forall s\in S, a\in A\setminus A_S, b\in\Gamma(a), k\in K, l\le k+\bar{\tau}_a-1. \tag{A44}$$

Equivalently, we have

$$y^s_{ab}(l,k)=0, \forall s\in S, a\in A\setminus A_S, b\in\Gamma(a), k\in K, l\ge k-\bar{\tau}_a+1. \tag{A45}$$

Hence, we have

$$\sum_{l=1}^{K} y^s_{ab}(k,l)=\sum_{l=k+\bar{\tau}_a}^{K} y^s_{ab}(k,l), \forall s\in S, a\in A\setminus A_S, b\in\Gamma(a), k\in K \quad \text{and} \tag{A46}$$

$$\sum_{l=1}^{K} y^s_{ba}(l,k)=\sum_{l=1}^{k-\bar{\tau}_b} y^s_{ba}(l,k), \forall s\in S, a\in A\setminus A_S, b\in\Gamma^{-1}(a), k\in K. \tag{A47}$$

We consider a sequence of links $\{a_{i-d},\cdots,a_{i-1},a_i,a_{i+1}\cdots,a_{i+e}\}$. Let $\overleftarrow{u}^s_{a_{i-d},\cdots,a_{i-1},a_i}(k)$ be the number of vehicles that travel through links $a_{i-d},\cdots,a_{i-1}$, enter link a_i during interval *k*, and head to destination *s*, and $\overleftarrow{\alpha}^s_{a_{i-d},\cdots,a_{i-1},a_i}(k)$ be the proportion of vehicles entering link a_i during interval *k* to destination *s* and travel through links $a_{i-d},\cdots,a_{i-1}$. Let $\vec{u}^s_{a_i,a_{i+1}\cdots,a_{i+e}}(k)$ be the number of vehicles that enter link a_i during interval *k*, and travel through links $a_{i+1}\cdots,a_{i+h}$ to destination *s*, and $\vec{\alpha}^s_{a_i,a_{i+1}\cdots,a_{i+e}}(k)$ be the proportion of vehicles entering link a_i during interval *k* to destination *s* and traveling through links $a_{i+1},\cdots,a_{i+e}$. By definition, we have

$$\overleftarrow{u}^s_{a_{i-d},\cdots,a_{i-1},a_i}(k)=u^s_{a_i}(k)\overleftarrow{\alpha}^s_{a_{i-d},\cdots,a_{i-1},a_i}(k)=\sum_{l=1}^{K} y^s_{a_{i-1}a_i}(l,k)\overleftarrow{\alpha}^s_{a_{i-d},\cdots,a_{i-1}}(l) \quad \text{and} \tag{A48}$$

$$\vec{u}^s_{a_i,a_{i+1}\cdots,a_{i+e}}(k)=u^s_{a_i}(k)\vec{\alpha}^s_{a_i,a_{i+1}\cdots,a_{i+e}}(k)=\sum_{l=1}^{K} y^s_{a_ia_{i+1}}(k,l)\vec{\alpha}^s_{a_{i+1}\cdots,a_{i+e}}(l). \tag{A49}$$

Substituting Eqs. (A47) and (A46) into Eqs. (A48) and (A49), respectively, we have

$$\overleftarrow{u}^s_{a_{i-g},\cdots,a_{i-1},a_i}(k)=\sum_{l=1}^{k-\bar{\tau}_{a_i}} y^s_{a_{i-1}a_i}(l,k)\overleftarrow{\alpha}^s_{a_{i-g},\cdots,a_{i-1}}(l) \quad \text{and} \tag{A50}$$

$$\vec{u}^s_{a_i,a_{i+1}\cdots,a_{i+h}}(k)=\sum_{l=k+\bar{\tau}_{a_i}}^{K} y^s_{a_ia_{i+1}}(k,l)\vec{\alpha}^s_{a_{i+1}\cdots,a_{i+h}}(l), \tag{A51}$$

Without loss of generality, we consider vehicles traveling through path $p=\{a_1,a_2,\cdots,a_i,\cdots,a_m\}$, where $p\in P^s$ and $a_m\in A_S$. By definition, we have

$$u^s_{a_ip}(k)=u^s_{a_i}(k)\alpha^s_{a_ip}(k), \tag{A52}$$

where $\alpha^s_{a_ip}(k)$ is the proportion of vehicles entering link a_i during interval *k* to destination *s* that travel through path *p*, and

$$\alpha^s_{a_ip}(k)=\overleftarrow{\alpha}^s_{a_1a_2\ldots a_i}(k)\vec{\alpha}^s_{a_i\ldots a_m}(k). \tag{A53}$$

By the definition of cumulative flow disaggregated by path, we have

$$U^s_{a_i p}(k) = \sum_{h=1}^{k} u^s_{a_i p}(h) \quad \text{and} \tag{A54}$$

$$V^s_{a_i p}(k) = U^s_{a_{i+1} p}(k) = \sum_{h=1}^{k} u^s_{a_{i+1} p}(h). \tag{A55}$$

Using Eqs. (A50)-(A55), we have

$$\begin{aligned}
V^s_{a_i p}(k) &= U^s_{a_{i+1} p}(k) = \sum_{h=1}^{k} u^s_{a_{i+1}}(h) \bar{\alpha}^s_{a_1 a_2 \ldots a_{i+1}}(h) \vec{\alpha}^s_{a_{i+1} \ldots a_m}(h) \\
&= \sum_{h=1}^{k} \sum_{l=1}^{h-\bar{\tau}_{a_i}} y^s_{a_i a_{i+1}}(l,h) \bar{\alpha}^s_{a_1 a_2 \ldots a_i}(l) \vec{\alpha}^s_{a_{i+1} \ldots a_m}(h) \\
&= \sum_{h=\bar{\tau}_{a_i}+1}^{k} \sum_{l=1}^{h-\bar{\tau}_{a_i}} y^s_{a_i a_{i+1}}(l,h) \bar{\alpha}^s_{a_1 a_2 \ldots a_i}(l) \vec{\alpha}^s_{a_{i+1} \ldots a_m}(h) \\
&= \sum_{l=1}^{k-\bar{\tau}_{a_i}} \sum_{h=l+\bar{\tau}_{a_i}}^{k} y^s_{a_i a_{i+1}}(l,h) \bar{\alpha}^s_{a_1 a_2 \ldots a_i}(l) \vec{\alpha}^s_{a_{i+1} \ldots a_m}(h) \\
&\le \sum_{l=1}^{k-\bar{\tau}_{a_i}} \sum_{h=l+\bar{\tau}_{a_i}}^{K} y^s_{a_i a_{i+1}}(l,h) \bar{\alpha}^s_{a_1 a_2 \ldots a_i}(l) \vec{\alpha}^s_{a_{i+1} \ldots a_m}(h) \\
&= \sum_{l=1}^{k-\bar{\tau}_{a_i}} u^s_{a_i}(l) \bar{\alpha}^s_{a_1 a_2 \ldots a_i}(l) \vec{\alpha}^s_{a_i \ldots a_m}(l) \\
&= U^s_{a_i p}(k - \bar{\tau}_{a_i}).
\end{aligned} \tag{A56}$$

By definition, we have

$$\bar{\alpha}^s_{ab}(k) = \sum_{p \in P^s} \varsigma_{abp} \alpha^s_{bp}(k), \forall s \in S, p \in P^s, a \in A, b \in \Gamma(a), k \in K \quad \text{and} \tag{A57}$$

$$\vec{\alpha}^s_{ab}(k) = \sum_{p \in P^s} \varsigma_{abp} \alpha^s_{ap}(k), \forall s \in S, p \in P^s, a \in A, b \in \Gamma(a), k \in K. \tag{A58}$$

According to Eqs. (A48), (A49), (A52), (A57), and (A58), we have

$$v^s_{ab}(k) = \bar{u}^s_{ab}(k) = \bar{\alpha}^s_{ab}(k) u^s_b(k) = \sum_{p \in P^s} \varsigma_{abp} \alpha^s_{bp}(k) u^s_b(k) = \sum_{p \in P^s} \varsigma_{abp} u^s_{bp}(k), \quad \text{and} \tag{A59}$$
$$\forall s \in S, p \in P^s, a \in A, b \in \Gamma(a), k \in K$$

$$\vec{u}^s_{ab}(k) = \vec{\alpha}^s_{ab}(k) u^s_a(k) = \sum_{p \in P^s} \varsigma_{abp} \alpha^s_{ap}(k) u^s_a(k) = \sum_{p \in P^s} \varsigma_{abp} u^s_{ap}(k), \tag{A60}$$
$$\forall s \in S, p \in P^s, a \in A, b \in \Gamma(a), k \in K,$$

We can construct a path-based solution vector $\mathbf{z}$ as follows:

$$U^s_{ap}(k) = \sum_{j=1}^{k} u^s_{ap}(k) = \sum_{j=1}^{k} u^s_a(k) \alpha^s_{ap}(k), \forall s \in S, p \in P^s, a \in A, k \in K \quad \text{and} \tag{A61}$$

$$V^s_{ap}(k) = \sum_{b \in \Gamma(a)} \varsigma_{abp} U^s_{bp}(k), \forall s \in S, p \in P^s, a \in A \setminus A_S, k \in K. \tag{A62}$$

According to Eqs. (A59)-(A62), we have

$$V_{ab}^{s}(k)=\sum_{j=1}^{k}v_{ab}^{s}(k)=\sum_{j=1}^{k}\sum_{p\in P^{s}}\varsigma_{abp}u_{ap}^{s}(k)=\sum_{p\in P^{s}}\varsigma_{abp}U_{bp}^{s}(k)=\sum_{p\in P^{s}}\varsigma_{abp}V_{ap}^{s}(k),\quad \text{and} \qquad \text{(A63)}$$
$$\forall s\in S,a\in A\setminus A_{S},b\in\Gamma(a),k\in K$$

$$U_{ab}^{s}(k)=\sum_{j=1}^{k}\vec{u}_{ab}^{s}(k)=\sum_{j=1}^{k}\sum_{p\in P^{s}}\varsigma_{abp}u_{ap}^{s}(k)=\sum_{p\in P^{s}}\varsigma_{abp}U_{ap}^{s}(k),\forall s\in S,a\in A\setminus A_{S},b\in\Gamma(a),k\in K. \qquad \text{(A64)}$$

Eqs. (A63) and (A64) imply that $\mathbf{y}$ and $\mathbf{z}$ satisfy Eqs. (35) and (36), and hence $\mathbf{y}=\boldsymbol{\varphi}_2(\mathbf{z})$. Substituting (35)and (36) into (23)-(25), we have constraints (38)-(40). Inequality (A56) implies that constraint (41) is satisfied by $\mathbf{z}$, and Eq. (A62) implies that constraint (42) is satisfied by $\mathbf{z}$. Eqs. (A61) and (A62) imply that the path-based solution vector $\mathbf{z}$ satisfies non-decreasing constraints (43) and (44). In summary, $\mathbf{z}$ satisfies constraints (38)-(44), i.e., $\mathbf{z}\in\tilde{\Omega}$, and $\mathbf{y}=\boldsymbol{\varphi}_2(\mathbf{z})$. This completes the proof. □

A.5. Proof of Proposition 6

Proof. Because Proposition 1 holds for any intersection-movement-based solution vector including a weak intersection-movement-based NVH solution vector $\mathbf{y}$, we have the corresponding link-based vector $\mathbf{x}=\boldsymbol{\varphi}_1(\mathbf{y})\in\Omega$. Substituting Eqs. (A1)-(A3) into the system of inequalities (50), we immediately have the system of inequalities (48). This implies that for all $a\in A\setminus A_S$ and $k\in K$, if one of the inequalities in (50) becomes binding, the corresponding inequality in (48) also becomes binding. Equivalently, if $\mathbf{y}\in\bar{\Omega}$ is a weak intersection-movement-based NVH solution vector, then $\mathbf{x}=\boldsymbol{\varphi}_1(\mathbf{y})$ is a weak link-based NVH solution vector. This completes the proof. □

A.6. Proof of Proposition 7

Proof. Because Proposition 3 holds for any path-based solution vector including a weak path-based NVH solution vector $\mathbf{z}$, we have the corresponding intersection-movement-based solution vector $\mathbf{y}=\boldsymbol{\varphi}_2(\mathbf{z})\in\bar{\Omega}$. To prove that $\mathbf{y}$ is a weak intersection-movement-based NVH solution vector corresponding to $\mathbf{z}$, without loss of generality, we consider an index pair $(a,k)\in\Phi$ for $\mathbf{z}$. Substituting Eqs. (A33)-(A34) into the system of inequalities (52) and changing the dummy index, we can obtain the system of inequalities (50). This implies that, for all $a\in A\setminus A_S$ and $k\in K$, if one of inequalities in (52) becomes binding, the corresponding inequality in (50) also becomes binding. Equivalently, if $\mathbf{z}\in\tilde{\Omega}$ is a weak path-based NVH solution vector, then $\mathbf{y}=\boldsymbol{\varphi}_2(\mathbf{z})$ is a weak intersection-movement-based NVH solution vector. Moreover, according to Proposition 6, the corresponding $\mathbf{x}=\boldsymbol{\varphi}_1(\boldsymbol{\varphi}_2(\mathbf{z}))$ is a weak link-based NVH solution vector. This completes the proof. □

A.7. Proof of Proposition 8

Proof. We first prove that $\mathbf{x}$ satisfies the weak link-based condition defined by Definition 9. Because $\mathbf{x}$ is a strong link-based VH solution vector defined by Definition 6, according to this definition, there exists a pair

of link $\bar{a} \in A \setminus A_S$ and interval $\bar{k} \in K$ in $\mathbf{x}$ such that

$$\begin{cases} \sum_{s\in S} V_{\bar{a}}^{s}(\bar{k}) < \sum_{s\in S} U_{\bar{a}}^{s}(\bar{k}-\bar{\tau}_{\bar{a}}), \\ \sum_{s\in S}\left[V_{\bar{a}}^{s}(\bar{k}) - V_{\bar{a}}^{s}(\bar{k}-1)\right] < C_{\bar{a}}(\bar{k}), \\ \sum_{s\in S} U_{\bar{b}}^{s}(\bar{k}) < \sum_{s\in S} V_{\bar{b}}^{s}(\bar{k}-\bar{t}_{\bar{b}}) + L_{\bar{b}}\rho_{jam}, \forall \bar{b} \in \Gamma(\bar{a}), \text{ and} \\ \sum_{s\in S}\left[U_{\bar{b}}^{s}(\bar{k}) - U_{\bar{b}}^{s}(\bar{k}-1)\right] < Q_{\bar{b}}(\bar{k}), \forall \bar{b} \in \Gamma(\bar{a}). \end{cases} \tag{A65}$$

According to constraint (10), there exists a destination $\bar{s} \in S$ such that $V_{\bar{a}}^{\bar{s}}(\bar{k}) < U_{\bar{a}}^{\bar{s}}(\bar{k}-\bar{\tau}_{\bar{a}})$. This implies that a positive amount of flows is delayed on link $\bar{a}$ during interval $\bar{k}$. Let $\bar{b} \in \Gamma(\bar{a})$ be any link that is used by this amount. Hence, there exists a positive value $\Delta > 0$ such that

$$\begin{cases} V_{\bar{a}}^{\bar{s}}(\bar{k}) + \Delta < U_{\bar{a}}^{\bar{s}}(\bar{k}-\bar{\tau}_{\bar{a}}), \\ \sum_{s\in S}\left[V_{\bar{a}}^{s}(\bar{k}) - V_{\bar{a}}^{s}(\bar{k}-1)\right] + \Delta < C_{\bar{a}}(\bar{k}), \\ \sum_{s\in S} U_{\bar{b}}^{s}(\bar{k}) + \Delta < \sum_{s\in S} V_{\bar{b}}^{s}(\bar{k}-\bar{t}_{\bar{b}}) + L_{\bar{b}}\rho_{jam}, \text{ and} \\ \sum_{s\in S}\left[U_{\bar{b}}^{s}(\bar{k}) - U_{\bar{b}}^{s}(\bar{k}-1)\right] + \Delta < Q_{\bar{b}}(\bar{k}). \end{cases}$$

We can construct a link-based solution vector $\tilde{\mathbf{x}}$ as follows:

$$\begin{cases} \tilde{V}_{\bar{a}}^{\bar{s}}(\bar{k}) = V_{\bar{a}}^{\bar{s}}(\bar{k}) + \Delta, \\ \tilde{U}_{\bar{b}}^{\bar{s}}(\bar{k}) = U_{\bar{b}}^{\bar{s}}(\bar{k}) + \Delta, \\ \tilde{V}_{a}^{s}(k) = V_{a}^{s}(k), \forall (s,a,k) \in \Phi_L \setminus \{(\bar{s},\bar{a},\bar{k})\}, \text{ and} \\ \tilde{U}_{a}^{s}(k) = U_{a}^{s}(k), \forall (s,a,k) \in \bar{\Phi}_L \setminus \{(\bar{s},\bar{b},\bar{k})\}. \end{cases} \tag{A66}$$

It is easy to check that $\tilde{\mathbf{x}} \neq \mathbf{x}$ and $\tilde{\mathbf{x}} \geq \mathbf{x}$, and $\tilde{\mathbf{x}} \in \Omega$. This implies that $\mathbf{x}$ satisfies the weak link-based VH condition defined by Definition 9.

We then prove that $\mathbf{x}'$ satisfies the weak link-based NVH condition defined by Definition 6 by contradiction. Assume that $\mathbf{x}'$ satisfies the strong link-based VH condition defined by Definition 6. According to the first part of this proof, $\mathbf{x}'$ satisfies the weak link-based VH condition defined by Definition 9. According to Definition 9, this contradicts that $\mathbf{x}'$ is a strong link-based NVH solution vector. Therefore, $\mathbf{x}'$ must satisfy the weak link-based NVH solution condition defined by Definition 6. This completes the proof. □

A.8. Proof of Proposition 9

Proof. We first prove that if $\mathbf{y}$ satisfies the condition that, for all $a \in A \setminus A_S$, $b \in \Gamma(a)$, and $k \in K$, at least one of the less-than-or-equal-to inequalities in (54) becomes binding, then $\mathbf{y}$ is a strong intersection-movement-based NVH solution vector by contradiction. We assume that $\mathbf{y}$ is a weak intersection-movement-based VH solution vector. This implies that there exists an index pair

$\{\bar{s},\bar{a},\bar{b},\bar{k}\} \in \Phi_I$ such that some holding vehicles on link $\bar{a}$ through link $\bar{b}$ to destination $\bar{s}$ during interval $\bar{k}$. We can construct a solution vector $\tilde{\mathbf{y}} \in \bar{\Omega}$ such that

$$V^{\bar{s}}_{\bar{a}\bar{b}}(\bar{k}) + \Delta = \tilde{V}^{\bar{s}}_{\bar{a}\bar{b}}(\bar{k}), \tag{A67}$$

$$V^{s}_{ab}(k) = \tilde{V}^{s}_{ab}(k), \forall (s,a,b,k) \in \Phi_I \setminus \{\bar{s},\bar{a},\bar{b},\bar{k}\}, \text{ and} \tag{A68}$$

$$U^{s}_{ab}(k) \le \tilde{U}^{s}_{ab}(k), \forall (s,a,b,k) \in \Phi_I, \tag{A69}$$

where $\Delta > 0$.

Because $\mathbf{y} \in \bar{\Omega}$ and $\tilde{\mathbf{y}} \in \bar{\Omega}$, according to the intersection-movement-based flow conservation constraint (27) and condition (A68), we have

$$\sum_{c\in\Gamma(\bar{a})} U^{\bar{s}}_{\bar{a}c}(\bar{k}-\bar{\tau}_{\bar{a}}) = \sum_{c\in\Gamma^{-1}(\bar{a})} V^{\bar{s}}_{c\bar{a}}(\bar{k}-\bar{\tau}_{\bar{a}}) = \sum_{c\in\Gamma^{-1}(\bar{a})} \tilde{V}^{\bar{s}}_{c\bar{a}}(\bar{k}-\bar{\tau}_{\bar{a}}) = \sum_{c\in\Gamma(\bar{a})} \tilde{U}^{\bar{s}}_{\bar{a}c}(\bar{k}-\bar{\tau}_{\bar{a}}). \tag{A70}$$

According to condition (A69), we have

$$U^{\bar{s}}_{\bar{a}c}(\bar{k}-\bar{\tau}_{\bar{a}}) \le \tilde{U}^{\bar{s}}_{\bar{a}c}(\bar{k}-\bar{\tau}_{\bar{a}}), \forall c \in \Gamma(\bar{a}). \tag{A71}$$

Eq. (A70) and inequality (A71) imply that the following equation must be satisfied:

$$U^{\bar{s}}_{\bar{a}c}(\bar{k}-\bar{\tau}_{\bar{a}}) = \tilde{U}^{\bar{s}}_{\bar{a}c}(\bar{k}-\bar{\tau}_{\bar{a}}), \forall c \in \Gamma(\bar{a}). \tag{A72}$$

Because $\tilde{\mathbf{y}} \in \bar{\Omega}$, constraint (26) implies that $\tilde{V}^{\bar{s}}_{\bar{a}\bar{b}}(\bar{k}) \le \tilde{U}^{\bar{s}}_{\bar{a}\bar{b}}(\bar{k}-\bar{\tau}_a)$ must be satisfied. Therefore, according to condition (A67) and Eq. (A72), we have

$$V^{\bar{s}}_{\bar{a}\bar{b}}(\bar{k}) < \tilde{V}^{\bar{s}}_{\bar{a}\bar{b}}(\bar{k}) \le \tilde{U}^{\bar{s}}_{\bar{a}\bar{b}}(\bar{k}-\bar{\tau}_a) = U^{\bar{s}}_{\bar{a}\bar{b}}(\bar{k}-\bar{\tau}_a). \tag{A73}$$

Because $\mathbf{y} \in \bar{\Omega}$, according to constraint (26), we have

$$V^{s}_{\bar{a}\bar{b}}(\bar{k}) \le U^{s}_{\bar{a}\bar{b}}(\bar{k}-\bar{\tau}_{\bar{a}}), \forall s \in S \setminus \{\bar{s}\}. \tag{A74}$$

Using conditions (A73) and (A74), we have

$$\sum_{s\in S} V^{s}_{\bar{a}\bar{b}}(\bar{k}) < \sum_{s\in S} U^{s}_{\bar{a}\bar{b}}(\bar{k}-\bar{\tau}_{\bar{a}}). \tag{A75}$$

Because $\tilde{\mathbf{y}} \in \bar{\Omega}$, conditions (A67), (A68), and constraints (23) imply that the following inequality is satisfied:

$$\sum_{s\in S}\sum_{c\in\Gamma(a)} \left[V^{s}_{ac}(k) - V^{s}_{ac}(k-1)\right] < \sum_{s\in S}\sum_{c\in\Gamma(a)} \left[\tilde{V}^{s}_{ac}(k) - \tilde{V}^{s}_{ac}(k-1)\right] \le C_a(k). \tag{A76}$$

Because $\mathbf{y} \in \bar{\Omega}$ and $\tilde{\mathbf{y}} \in \bar{\Omega}$, according to the intersection-movement-based flow conservation constraint (27) and conditions (A67) and (A68), we have

$$\sum_{c\in\Gamma(\bar{b})} U^{\bar{s}}_{\bar{b}c}(\bar{k}-1) = \sum_{c\in\Gamma^{-1}(\bar{b})} V^{\bar{s}}_{c\bar{b}}(\bar{k}-1) = \sum_{c\in\Gamma^{-1}(\bar{b})} \tilde{V}^{\bar{s}}_{c\bar{b}}(\bar{k}-1) = \sum_{c\in\Gamma(\bar{b})} \tilde{U}^{\bar{s}}_{\bar{b}c}(\bar{k}-1) \text{ and} \tag{A77}$$

$$\sum_{c\in\Gamma(\bar{b})} U^{\bar{s}}_{\bar{b}c}(\bar{k}) = \sum_{c\in\Gamma^{-1}(\bar{b})} V^{\bar{s}}_{c\bar{b}}(\bar{k}) < \sum_{c\in\Gamma^{-1}(\bar{b})} \tilde{V}^{\bar{s}}_{c\bar{b}}(\bar{k}) = \sum_{c\in\Gamma(\bar{b})} \tilde{U}^{\bar{s}}_{\bar{b}c}(\bar{k}). \tag{A78}$$

Using constraints (23), conditions (A67)-(A69), Eq. (A77), and inequality (A78), we have

$$\sum_{c\in\Gamma(\bar{b})} [U^{\bar{s}}_{\bar{b}c}(\bar{k}) - U^{\bar{s}}_{\bar{b}c}(\bar{k}-1)] < \sum_{c\in\Gamma(\bar{b})} [\tilde{U}^{\bar{s}}_{\bar{b}c}(\bar{k}) - \tilde{U}^{\bar{s}}_{\bar{b}c}(\bar{k}-1)] \le Q_b(k) \text{ and} \tag{A79}$$

$$\sum_{s\in S}\sum_{c\in\Gamma(\bar{b})} U^s_{\bar{b}c}(\bar{k}) < \sum_{s\in S}\sum_{c\in\Gamma(\bar{b})} \tilde{U}^s_{\bar{b}c}(\bar{k}) \le \sum_{s\in S}\sum_{c\in\Gamma(\bar{b})} \tilde{V}^s_{\bar{b}c}(\bar{k}-\bar{\iota}_{\bar{b}}) + L_{\bar{b}}\rho_{jam} = \sum_{s\in S}\sum_{c\in\Gamma(\bar{b})} V^s_{\bar{b}c}(\bar{k}-\bar{\iota}_{\bar{b}}) + L_{\bar{b}}\rho_{jam}. \quad \text{(A80)}$$

Inequalities (A75), (A76), (A79), and (A80) imply that no less-than-or-equal-to inequalities in (54) take equality. This contradicts that at least one of the less-than-or-equal-to inequalities in (54) becomes binding. This implies that $\mathbf{y}$ is a strong intersection-movement-based NVH solution vector.

We then prove that if $\mathbf{y}$ is a strong intersection-movement-based NVH solution vector, then $\mathbf{y}$ satisfies the condition that, for all $a \in A \setminus A_S$, $b \in \Gamma(a)$, and $k \in K$, at least one of the less-than-or-equal-to inequalities in (54) becomes binding by contradiction. We assume that there exists link $\bar{a} \in A \setminus A_S$, link $\bar{b} \in \Gamma(\bar{a})$, and interval $\bar{k} \in K$ in $\mathbf{y}$ such that

$$\begin{cases} \sum_{s\in S}\sum_{b'\in\Gamma(a)} \left[V^s_{\bar{a}b'}(\bar{k}) - V^s_{\bar{a}b'}(\bar{k}-1)\right] < C_{\bar{a}}(\bar{k}), \\ \sum_{s\in S}\sum_{c\in\Gamma(\bar{b})} U^s_{\bar{b}c}(\bar{k}) < \sum_{s\in S}\sum_{c\in\Gamma(\bar{b})} V^s_{\bar{b}c}(\bar{k}-\bar{\iota}_{\bar{b}}) + L_{\bar{b}}\rho_{jam}, \\ \sum_{s\in S}\sum_{c\in\Gamma(\bar{b})} \left[U^s_{\bar{b}c}(\bar{k}) - U^s_{\bar{b}c}(\bar{k}-1)\right] < Q_{\bar{b}}(\bar{k}), \text{ and} \\ \sum_{s\in S} V^s_{\bar{a}\bar{b}}(\bar{k}) < \sum_{s\in S} U^s_{\bar{a}\bar{b}}(\bar{k}-\bar{\tau}_{\bar{a}}). \end{cases} \quad \text{(A81)}$$

Eq. (A81) implies that a positive amount of flows is delayed on link $\bar{a}$ to link $\bar{b}$ during interval $\bar{k}$. Let $\bar{c} \in \Gamma(\bar{b})$ be any link that is used by this amount, and $\bar{s} \in S$ be the destination of this amount. Hence, there exists a positive value $\Delta > 0$ such that

$$\begin{cases} \sum_{s\in S}\sum_{b'\in\Gamma(a)} \left[V^s_{\bar{a}b'}(\bar{k}) - V^s_{\bar{a}b'}(\bar{k}-1)\right] + \Delta < C_{\bar{a}}(\bar{k}), \\ \sum_{s\in S}\sum_{c\in\Gamma(\bar{b})} U^s_{\bar{b}c}(\bar{k}) + \Delta < \sum_{s\in S}\sum_{c\in\Gamma(\bar{b})} V^s_{\bar{b}c}(\bar{k}-\bar{\iota}_{\bar{b}}) + L_{\bar{b}}\rho_{jam}, \\ \sum_{s\in S}\sum_{c\in\Gamma(\bar{b})} \left[U^s_{\bar{b}c}(\bar{k}) - U^s_{\bar{b}c}(\bar{k}-1)\right] + \Delta < Q_{\bar{b}}(\bar{k}), \text{ and} \\ \sum_{s\in S} V^s_{\bar{a}\bar{b}}(\bar{k}) + \Delta < \sum_{s\in S} U^s_{\bar{a}\bar{b}}(\bar{k}-\bar{\tau}_{\bar{a}}). \end{cases} \quad \text{(A82)}$$

We can construct an intersection-movement-based solution vector $\tilde{\mathbf{y}}$ as follows:

$$\begin{cases} \tilde{V}^{\bar{s}}_{\bar{a}\bar{b}}(\bar{k}) = V^{\bar{s}}_{\bar{a}\bar{b}}(\bar{k}) + \Delta, \\ \tilde{U}^{\bar{s}}_{\bar{b}\bar{c}}(\bar{k}) = U^{\bar{s}}_{\bar{b}\bar{c}}(\bar{k}) + \Delta, \\ \tilde{V}^s_{ab}(k) = V^s_{ab}(k), \forall (s,a,k) \in \Phi_I \setminus \{(\bar{s},\bar{a},\bar{b},\bar{k})\}, \text{ and} \\ \tilde{U}^s_{ab}(k) = U^s_{ab}(k), \forall (s,a,k) \in \bar{\Phi}_I \setminus \{(\bar{s},\bar{b},\bar{c},\bar{k})\}. \end{cases} \quad \text{(A83)}$$

It is easy to check that $\tilde{\mathbf{y}} \neq \mathbf{y}$, $\tilde{\mathbf{y}} \geq \mathbf{y}$, and $\tilde{\mathbf{y}} \in \bar{\Omega}$. This implies that $\mathbf{y}$ is a weak intersection-movement-based VH solution vector. This contradicts that $\mathbf{y}$ is a strong intersection-movement-based NVH solution vector. This implies that $\mathbf{y}$ satisfies the condition that, for all $a \in A \setminus A_S$, $b \in \Gamma(a)$, and $k \in K$, at least one of the less-than-or-equal-to inequalities in (54) becomes binding. This completes the proof. □

A.9. Proof of Proposition 11

Proof. Because Proposition 3 holds for any path-based solution vector including a strong path-based NVH solution vector $\mathbf{z}$, we have the corresponding intersection-movement-based solution vector $\mathbf{y} = \boldsymbol{\varphi}_2(\mathbf{z}) \in \overline{\Omega}$. To prove that $\mathbf{y}$ is a strong intersection-movement-based NVH solution vector corresponding to $\mathbf{z}$, without loss of generality, we consider an index pair $(a,k) \in \Phi$ for $\mathbf{z}$. According to Eqs. (A31) and (A32), we have

$$\sum_{s\in S}\sum_{p\in P^s} \varsigma_{abp} U^s_{ap}(k) = \sum_{s\in S} U^s_{ab}(k) \quad \text{and} \tag{A84}$$

$$\sum_{s\in S}\sum_{p\in P^s} \varsigma_{abp} V^s_{ap}(k) = \sum_{s\in S} V^s_{ab}(k)\,. \tag{A85}$$

According to Proposition 10, $\mathbf{z}$ satisfies the condition that, for all $a \in A \setminus A_S$, $b \in \Gamma(a)$, and $k \in K$, at least one of the less-than-or-equal-to inequalities in (56) becomes binding. Substituting Eqs. (A33)-(A34) into the first three inequalities in (56) and changing the dummy index, we can obtain the first three inequalities in (54). Modifying the argument of (A54) from k to $k - \overline{\tau}_a$ and substituting Eq. (A84) and the revised equation of (A85) into the last inequality in (56), we can obtain the last inequality in (54). Therefore, we can conclude that when any less-than-or-equal-to inequalities in (56) becomes binding, the corresponding less-than-or-equal-to inequalities in (54) also becomes binding. According to Proposition 10, for all $a \in A \setminus A_S$, $b \in \Gamma(a)$, and $k \in K$, at least one of less-than-or-equal-to inequalities in (56) becomes binding. Therefore, for all $a \in A \setminus A_S$, $b \in \Gamma(a)$, and $k \in K$, at least one of the corresponding less-than-or-equal-to inequalities in (54) becomes binding. According to Proposition 9, $\mathbf{y} = \boldsymbol{\varphi}_2(\mathbf{z}) \in \overline{\Omega}$ is a strong intersection-movement-based NVH solution vector. This completes the proof. □

A.10. Proof of Proposition 12

Proof. For any $a \in A \setminus A_S$, $b \in \Gamma(a)$, and $k \in K$, if $\omega^1_a(k) = 1$, constraint (55a) implies

$$\sum_{s\in S}\sum_{b\in\Gamma(a)} \left[V^s_{ab}(k) - V^s_{ab}(k-1)\right] \geq C_a(k)\,. \tag{A86}$$

Combining inequality (A86) with constraint (23), we have

$$\sum_{s\in S}\sum_{b\in\Gamma(a)} \left[V^s_{ab}(k) - V^s_{ab}(k-1)\right] = C_a(k)\,. \tag{A87}$$

Similarly, if $\omega^2_b(k) = 1$, we have

$$\sum_{s\in S}\sum_{c\in\Gamma(b)} U^s_{bc}(k) = \sum_{s\in S}\sum_{c\in\Gamma(b)} V^s_{bc}(k - \overline{t}_b) + L_b \rho_{jam}\,. \tag{A88}$$

If $\omega^3_b(k) = 1$, we have

$$\sum_{s\in S}\sum_{c\in\Gamma(b)} \left[U^s_{bc}(k) - U^s_{bc}(k-1)\right] = Q_b(k)\,. \tag{A89}$$

If $\omega_{ab}(k) = 1$, we have

$$\sum_{s\in S} V^s_{ab}(k) = \sum_{s\in S} U^s_{ab}(k - \overline{\tau}_a)\,. \tag{A90}$$

Constraints (55e)-(55g) imply at least one of the four binary variables on the left-hand side of constraint

(55e) equals one. This implies that at least one of Eqs. (A87)-(A90) holds. Equivalently, at least one of the less-than-or-equal-to inequalities in (54) becomes binding. According to Proposition 9, $\mathbf{y}$ is a strong intersection-movement-based NVH solution vector. This completes the proof. □

A.11. Proof of Proposition 14

Proof. Let $\mathbf{x} = \boldsymbol{\varphi}_1(\mathbf{y})$. Substituting Eq. (A2) into Eq. (60), we can obtain $\bar{\eta}(\mathbf{y}) = \eta(\mathbf{x})$. This completes the proof. □

A.12. Proof of Proposition 15

Proof. Let $\mathbf{y} = \boldsymbol{\varphi}_2(\mathbf{z})$, and $\mathbf{x} = \boldsymbol{\varphi}_1(\mathbf{y}) = \boldsymbol{\varphi}_1(\boldsymbol{\varphi}_2(\mathbf{z}))$. Substituting Eq. (A32) into the rightmost hand side of Eq. (A36), we have

$$\sum_{p \in P^s} U_{ap}^s(k) = \sum_{b \in \Gamma^{-1}(a)} V_{ba}^s(k), \forall s \in S, a \in A_S, k \in K. \tag{A91}$$

Substituting Eqs. (A91) into Eq. (61), we can obtain $\tilde{\eta}(\mathbf{z}) = \bar{\eta}(\mathbf{y})$. According to Proposition 14, we have $\bar{\eta}(\mathbf{y}) = \eta(\mathbf{x})$. Hence, we have $\tilde{\eta}(\mathbf{z}) = \bar{\eta}(\mathbf{y}) = \eta(\mathbf{x})$. This completes the proof. □

A.13. Proof of Proposition 16

Proof. Same as the proof of Proposition 8, for any weak link-based VH solution vector $\mathbf{x} \in \Omega$, we can construct a link-based VH solution vector $\tilde{\mathbf{x}} \in \Omega$ according to the system of equations (A66). Substituting the system of equations (A66) into Eqs. (59) and (68), we have

$$\eta(\tilde{\mathbf{x}}) = \eta(\mathbf{x}) - \begin{cases} (\alpha - \beta)\Delta, \text{ if } \bar{b} \in A_S \text{ and } \bar{k} < \underline{k}_s^*, \\ \alpha\Delta, \text{ if } \bar{b} \in A_S \text{ and } \underline{k}_s^* \le \bar{k} < \bar{k}_s^*, \\ (\alpha + \gamma)\Delta, \text{ if } \bar{b} \in A_S \text{ and } \bar{k} \ge \bar{k}_s^*, \\ 0, \text{ otherwise,} \end{cases} \text{ and} \tag{A92}$$

$$\xi(\tilde{\mathbf{x}}) = \xi(\mathbf{x}) + \Delta > \xi(\mathbf{x}). \tag{A93}$$

Because $0 < \beta < \alpha < \gamma$, we have $\eta(\tilde{\mathbf{x}}) \le \eta(\mathbf{x})$.

Let $\mathbf{x}^*$ be an optimal solution to LP problem (68)-(69). Assume that $\mathbf{x}^*$ is a weak link-based VH solution vector. We can construct a link-based VH solution vector $\tilde{\mathbf{x}}^* \in \Omega$ according to the system of equations (A66) by using $\mathbf{x}^*$. According to Eqs. (A92) and (A93), we have $\eta(\tilde{\mathbf{x}}^*) \le \eta(\mathbf{x}^*)$ and $\xi(\tilde{\mathbf{x}}^*) > \xi(\mathbf{x}^*)$. According to constraint (69), we have $\eta(\mathbf{x}^*) = \eta^*$. Because $\tilde{\mathbf{x}}^* \in \Omega$, $\tilde{\mathbf{x}}^*$ is a feasible solution to LP problem (62), and we have $\eta(\tilde{\mathbf{x}}^*) \ge \eta^* = \eta(\mathbf{x}^*)$. Hence, we have $\eta(\tilde{\mathbf{x}}^*) = \eta^* = \eta(\mathbf{x}^*)$. This implies that $\tilde{\mathbf{x}}^*$ is a feasible solution to LP problem (68)-(69). Hence, its objective value $\xi(\tilde{\mathbf{x}}^*)$ cannot be greater than the optimal value $\xi(\mathbf{x}^*)$ (i.e., $\xi(\tilde{\mathbf{x}}^*) \le \xi(\mathbf{x}^*)$). This condition contradicts with $\xi(\tilde{\mathbf{x}}^*) > \xi(\mathbf{x}^*)$ deduced earlier. Therefore, $\mathbf{x}^*$ must be a strong link-based NVH solution vector. This completes the proof.□

A.14. Proof of Proposition 17

Proof. Constraint (69) implies that $\eta(\mathbf{x}^*) = \eta^*$ and $\mathbf{x}^*$ is an optimal solution to LP problem (62). Let $[\tilde{\mathbf{x}}^*, \tilde{\boldsymbol{\theta}}^*]$ be an optimal solution to MILP problem (65). By definition, we have $\tilde{\mathbf{x}}^* \in \Omega$, and hence $\tilde{\mathbf{x}}^*$ is a feasible solution to LP problem (62). This implies $\eta(\tilde{\mathbf{x}}^*) \geq \eta(\mathbf{x}^*) = \eta^*$.

According to Propositions 8 and 16, $\mathbf{x}^* \in \Omega$ satisfies the weak link-based NVH condition defined by Definition 9. By definition, for all $a \in A \setminus A_S$ and $k \in K$, at least one of the less-than-or-equal-to inequalities in (48) becomes binding. Based on the solution vector $\mathbf{x}^*$, we can retrieve the vector $\boldsymbol{\theta}^*$ as follows: (i) if $\sum_{s\in S} V_a^{s*}(k) = \sum_{s\in S} U_a^{s*}(k - \vec{t}_a)$ is satisfied, we set $\theta_a^{i*}(k) = 0, \forall i \in \{0,1,\cdots,m_a\}$; (ii) if $\sum_{s\in S}\left[V_a^{s*}(k) - V_a^{s*}(k-1)\right] = C_a(k)$ is satisfied, we set $\theta_a^{0*}(k) = 1$ and $\theta_a^{i*}(k) = 0, \forall i \in \{1,\cdots,m_a\}$; (iii) for all $j \in J_a$, if $\sum_{s\in S} U_b^{s*}(k) = \sum_{s\in S} V_b^{s*}(k - \bar{t}_b) + L_b \rho_{jam}$ is satisfied, we set $\theta_a^{0*}(k) = 0$ and $\theta_a^{i*}(k) = \sigma_i^j, \forall i \in \{1,\cdots,m_a\}$; and (iv) for all $j \in J_a$, if $\sum_{s\in S}\left[U_b^{s*}(k) - U_b^{s*}(k-1)\right] = Q_b(k)$, we set $\theta_a^{0*}(k) = 1$ and $\theta_a^{i*}(k) = \sigma_i^j, \forall i \in \{1,\cdots,m_a\}$. We can check that $[\mathbf{x}^*, \boldsymbol{\theta}^*]$ satisfies constraint (49) for all $a \in A \setminus A_S, k \in K$. Because $\mathbf{x}^* \in \Omega$, $[\mathbf{x}^*, \boldsymbol{\theta}^*]$ is a feasible solution to MILP problem (65). This implies $\eta(\tilde{\mathbf{x}}^*) \leq \eta(\mathbf{x}^*) = \eta^*$. Combining this condition with $\eta(\tilde{\mathbf{x}}^*) \geq \eta(\mathbf{x}^*) = \eta^*$, we have $\eta(\tilde{\mathbf{x}}^*) = \eta^*$. This implies $[\mathbf{x}^*, \boldsymbol{\theta}^*]$ is an optimal solution to MILP problem (65). This completes the proof.□

A.15. Proof of Theorem 1

Proof. Let $\mathbf{x}^*$, $\mathbf{y}^*$, and $\mathbf{z}^*$ be optimal solutions to the link-based, intersection-movement-based, and path-based R-DSO-SRDTC problems, respectively. By definition, we have $\eta^* = \eta(\mathbf{x}^*)$, $\bar{\eta}^* = \bar{\eta}(\mathbf{y}^*)$, and $\tilde{\eta}^* = \tilde{\eta}(\mathbf{z}^*)$. According to Propositions 1 and 14, we have $\boldsymbol{\varphi}_1(\mathbf{y}^*) \in \Omega$ and $\bar{\eta}(\mathbf{y}^*) = \eta(\boldsymbol{\varphi}_1(\mathbf{y}^*))$. Because $\mathbf{x}^*$ is an optimal solution to the link-based R-DSO-SRDTC problem, we have $\bar{\eta}(\mathbf{y}^*) = \eta(\boldsymbol{\varphi}_1(\mathbf{y}^*)) \geq \eta(\mathbf{x}^*)$. Meanwhile, according to Propositions 3 and 15, we have $\boldsymbol{\varphi}_2(\mathbf{z}^*) \in \bar{\Omega}$ and $\tilde{\eta}(\mathbf{z}^*) = \bar{\eta}(\boldsymbol{\varphi}_2(\mathbf{z}^*))$. Because $\mathbf{y}^*$ is an optimal solution to the intersection-movement-based R-DSO-SRDTC problem, we have $\tilde{\eta}(\mathbf{z}^*) = \bar{\eta}(\boldsymbol{\varphi}_2(\mathbf{z}^*)) \geq \bar{\eta}(\mathbf{y}^*)$. Hence, we have $\eta^* \leq \bar{\eta}^* \leq \tilde{\eta}^*$. Moreover, according to Proposition 5, there exists a vector $\mathbf{z}' \in \tilde{\Omega}$ such that $\mathbf{x}^* = \boldsymbol{\varphi}_1(\boldsymbol{\varphi}_2(\mathbf{z}'))$. According to Proposition 15, we have $\tilde{\eta}(\mathbf{z}') = \eta(\mathbf{x}^*)$. Because $\mathbf{z}^*$ is an optimal solution to the path-based R-DSO-SRDTC problem, we have $\eta^* = \eta(\mathbf{x}^*) = \tilde{\eta}(\mathbf{z}') \geq \tilde{\eta}(\mathbf{z}^*) = \tilde{\eta}^*$. This together with $\eta^* \leq \bar{\eta}^* \leq \tilde{\eta}^*$ implies that $\eta^* = \bar{\eta}^* = \tilde{\eta}^*$ must hold. According to constraint (69), we have $\eta_N^* = \eta^*$. Similarly, we have $\bar{\eta}^* = \bar{\eta}_N^*$ and $\tilde{\eta}^* = \tilde{\eta}_N^*$. Therefore, we have $\eta^* = \bar{\eta}^* = \tilde{\eta}^* = \eta_N^* = \bar{\eta}_N^* = \tilde{\eta}_N^*$. This completes the proof. □

A.16. Proof of Proposition 22

Proof. According to Proposition 1, there is a corresponding link-based solution vector $\mathbf{x} = \boldsymbol{\varphi}_1(\mathbf{y}) \in \Omega$. Taking summation of $b \in \Gamma(a)$ for both sides of Eq. (81) and substituting Eqs. (A1) and (A3) into the resultant equation, we obtain Eq. (80). This implies that $\mathbf{x}$ is a link-based FIFO solution vector. This completes the proof. □

A.17. Proof of Proposition 23

Proof. According to Proposition 3, there is a corresponding intersection movement-based solution vector $\mathbf{y} = \boldsymbol{\varphi}_2(\mathbf{z}) \in \bar{\Omega}$. Multiplying 0-1 indicators ς_{abp} to both sides of Eq. (82), taking summation over $p \in P$, and substituting Eqs. (A31) and (A32) into the resultant equation after changing the argument when necessary, we can obtain Eq. (81). This implies that $\mathbf{y}$ is an intersection-movement-based FIFO solution vector. According to Proposition 22, $\mathbf{x} = \boldsymbol{\varphi}_1(\boldsymbol{\varphi}_2(\mathbf{z}))$ is a link-based FIFO solution vector. This completes the proof. □

A.18. Proof of Theorem 5

Proof. Let $\mathbf{x}^*$, $\mathbf{y}^*$, and $\mathbf{z}^*$ be optimal solutions to the link-based, intersection-movement-based, and path-based FIFO-DSO-SRDTC problems, respectively. By definition, we have $\eta^* = \eta(\mathbf{x}^*)$, $\bar{\eta}^* = \bar{\eta}(\mathbf{y}^*)$, and $\tilde{\eta}^* = \tilde{\eta}(\mathbf{z}^*)$. Because $\mathbf{y}^*$ is an optimal solutions to the intersection-movement-based FIFO-DSO-SRDTC problem, $\mathbf{y}^* \in \bar{\Omega}$ is an intersection-movement-based FIFO solution vector. According to Proposition 22, $\boldsymbol{\varphi}_1(\mathbf{y}^*)$ is a link-based FIFO solution vector, and hence is a feasible solution to the link-based FIFO-DSO-SRDTC problem. According to Proposition 14, we have $\bar{\eta}(\mathbf{y}^*) = \eta(\boldsymbol{\varphi}_1(\mathbf{y}^*))$. Because $\mathbf{x}^*$ is an optimal solution to the link-based FIFO-DSO-SRDTC problem, we have $\bar{\eta}(\mathbf{y}^*) = \eta(\boldsymbol{\varphi}_1(\mathbf{y}^*)) \geq \eta(\mathbf{x}^*)$. Because $\mathbf{z}^*$ is an optimal solutions to the path-based FIFO-DSO-SRDTC problem, $\mathbf{z}^* \in \tilde{\Omega}$ is a path-based FIFO solution vector. According to Proposition 23, $\boldsymbol{\varphi}_2(\mathbf{z}^*)$ is an intersection-movement-based FIFO solution vector, and hence is a feasible solution to the intersection-movement-based FIFO-DSO-SRDTC problem. According to Proposition 15, we have $\tilde{\eta}(\mathbf{z}^*) = \bar{\eta}(\boldsymbol{\varphi}_2(\mathbf{z}^*))$. Because $\mathbf{y}^*$ is an optimal solution to the intersection-movement-based FIFO-DSO-SRDTC problem, we have $\tilde{\eta}(\mathbf{z}^*) = \bar{\eta}(\boldsymbol{\varphi}_2(\mathbf{z}^*)) \geq \bar{\eta}(\mathbf{y}^*)$. Therefore, we have $\eta^* \leq \bar{\eta}^* \leq \tilde{\eta}^*$. This completes the proof. □

A.19. Proof of Theorem 9

Proof. Let $\mathbf{x}^*$, $\mathbf{y}^*$, and $\mathbf{z}^*$ be optimal solutions to the link-based, intersection-movement-based, and path-based NVH-FIFO-DSO-SRDTC problems, respectively. By definition, we have $\eta^* = \eta(\mathbf{x}^*)$, $\bar{\eta}^* = \bar{\eta}(\mathbf{y}^*)$, and $\tilde{\eta}^* = \tilde{\eta}(\mathbf{z}^*)$. According to Propositions 1, 6, and 22, $\boldsymbol{\varphi}_1(\mathbf{y}^*) \in \Omega$ is a link-based NVH-FIFO solution vector, and hence is a feasible solution to the link-based NVH-FIFO-DSO-SRDTC problem. According to Proposition 14, we have $\bar{\eta}(\mathbf{y}^*) = \eta(\boldsymbol{\varphi}_1(\mathbf{y}^*))$. Because $\mathbf{x}^*$ is an optimal solution to the link-based NVH-FIFO-DSO-SRDTC problem, we have $\bar{\eta}(\mathbf{y}^*) = \eta(\boldsymbol{\varphi}_1(\mathbf{y}^*)) \geq \eta(\mathbf{x}^*)$. According to Propositions 3, 7, and 23, we have $\boldsymbol{\varphi}_2(\mathbf{z}^*) \in \bar{\Omega}$ is an intersection-movement-based NVH-FIFO solution vector, and hence is a feasible solution to the intersection-movement-based NVH-FIFO-DSO-SRDTC problem. According to Proposition 15, we have $\tilde{\eta}(\mathbf{z}^*) = \bar{\eta}(\boldsymbol{\varphi}_2(\mathbf{z}^*))$. Because $\mathbf{y}^*$ is an optimal solution to the intersection-movement-based NVH-FIFO-DSO-SRDTC problem, we have $\tilde{\eta}(\mathbf{z}^*) = \bar{\eta}(\boldsymbol{\varphi}_2(\mathbf{z}^*)) \geq \bar{\eta}(\mathbf{y}^*)$. Therefore, we have $\eta^* \leq \bar{\eta}^* \leq \tilde{\eta}^*$. This completes the proof. □

A.20. Proof of Theorem 10

Proof. According to Theorem 1, we have $\eta_1^* = \eta_2^*$. Because the feasible solution set of the FIFO-DSO-SRDTC problem is a subset of that of R-DSO-SRDTC problem, $\eta_1^* \le \eta_3^*$. Similarly, because the feasible solution set of the NVH-FIFO-DSO-SRDTC problem is a subset of that of the FIFO-DSO-SRDTC problem, $\eta_3^* \le \eta_4^*$. This completes the proof. □

References

Astarita, V., 1996. A continuous time link model for dynamic network loading based on travel time function. Lesort J-B, ed. Proc. 13th Internat. Sympos. Theory of Traffic Flow. Elsevier, Oxford, U.K., 79–102.

Ban, X., Liu, H., Ferris, M., Ran, B., 2008. A link-node complementarity model and solution algorithm for dynamic user equilibria with exact flow propagations. Transp. Res. Part B 42(9), 823–842.

Ban, X., Pang, J.S., Liu, H., Ma, R., 2012. Continuous-time point-queue models in dynamic network loading. Transp. Res. Part B 46(3), 360–380.

Carey, M., 1992. Non-convexity of the dynamic traffic assignment problem. Transp. Res. Part B 26(2), 127–133.

Carey, M., Ge, Y.E., 2012. Comparison of methods for path inflow reassignment for dynamic user equilibrium. Netw. Spat. Econ. 12(3), 337-376.

Carey, M., Humphreys, P., McHugh, M., McIvor, R., 2014. Extending travel-time based models for dynamic network loading and assignment, to achieve adherence to first-in-first-out and link capacities. Transp. Res. Part B 65, 90–104.

Carey, M., Srinivasan, A., 1993. Externalities, average and marginal costs, and tolls on congested networks with time-varying flows. Oper. Res. 41(1), 217–231.

Carey, M., Subrahmanian, E., 2000. An approach to modelling time-varying flows on congested networks. Transp. Res. Part B 34(3), 157–183.

Carey, M., Watling, D., 2012. Dynamic traffic assignment approximating the kinematic wave model: System optimum, marginal costs, externalities and tolls. Transp. Res. Part B 46(5), 634–648.

Chiu, Y.C., Zheng, H., Villalobos, J., Gautam, B., 2007. Modeling no-notice mass evacuation using a dynamic traffic flow optimization model. IIE Trans. 39(1), 83–94.

Chow, A., 2009a. Dynamic system optimal traffic assignment – A state-dependent control theoretic approach. Transportmetrica 5(2), 85-106.

Chow, A., 2009b. Properties of system optimal traffic assignment with departure time choice and its solution method. Transp. Res. Part B 43(3), 325-344.

Daganzo, C.F., 1995. Properties of link travel time functions under dynamic loads. Transp. Res. Part B 29(2), 95–98.

Dantzig, G.B., Thapa, M.N., 2006. Linear programming 2: theory and extensions. Springer Science & Business Media.

Doan, K., Ukkusuri, S.V., 2012. On the holding-back problem in the cell transmission based dynamic traffic assignment models. Transp. Res. Part B 46(9), 1218-1238.

Friesz, T.L., Bernstein, D., Smith, T.E., Tobin, R.L., Wie, B., 1993. A variational inequality formulation of the dynamic networks user equilibrium problem. Oper. Res. 41(1), 179–191.

Ghali, M., Smith, M., 1995. A model for the dynamic system optimum traffic assignment problem. Transp. Res. Part B 29(3), 155–171.

Han, K., Friesz, T.L., Yao, T., 2013. Existence of simultaneous route and departure choice dynamic user equilibrium. Transp. Res. Part B 53, 17-30.

Han, K, Gayah, V, Piccoli, B, Friesz, TL, Yao, T, 2014. On the continuum approximation of the on-and-off signal control on dynamic traffic networks. Transp. Res. Part B, 61, 73-97.

Han, K, Liu, H, Gayah, VV, Friesz, TL, Yao, T., 2016. A robust optimization approach for dynamic traffic signal control with emission considerations. Transp. Res. Part C, 70, 3-26.

Han, K., Szeto, W.Y., Friesz, T.L., 2015. Formulation, existence, and computation of boundedly rational dynamic user equilibrium with fixed or endogenous user tolerance. Transp. Res. Part B 79, 16-49.

Huang, H.J., Lam, W.H.K., 2002. Modeling and solving the dynamic user equilibrium route and departure time choice problem in network with queues. Transp. Res. Part B 36(3), 253–273.

Jiang, Y., Szeto, W.Y., Long, J.C., Han, K., 2016. Multi-class dynamic traffic assignment with physical queues: Intersection-movement-based formulation and paradox. Transportmetrica A 12(10), 878-908.

Lin, WH., Wang, C., 2004. An enhanced 0–1 mixed-integer LP formulation for traffic signal control. IEEE Trans.Intell. Transp. Syst. 5(4), 238–245.

Liu, Y., Lai, X., Chang, G.L., 2006. Cell-based network optimization model for staged evacuation planning under emergencies. Transp. Res. Record 1964, 127–135.

Liu, Y., Nie, Y., Hall, J., 2015. A semi-analytical approach for solving the bottleneck model with general user heterogeneity. Transp. Res. Part B 71, 56–70.

Lo, H.K., Szeto, W.Y., 2002. A cell-based variational inequality formulation of the dynamic user optimal assignment problem. Transp. Res. Part B 36(5), 421–443.

Lo, H.K., 2001. A cell-based traffic control formulation: strategies and benefits of dynamic timing plans. Transp. Sci. 35(2), 149-164.

Long, J.C., Chen, J.X., Szeto, W.Y., Shi, Q., 2016. Link-based system optimum dynamic traffic assignment problems with environmental objectives. Transp. Res. Part D, DOI: 10.1016/j.trd.2016.06.003.

Long, J.C., Gao, Z.Y., Szeto, W.Y., 2011. Discretised link travel time models based on cumulative flows: formulation and properties. Transp. Res. Part B 45 (1), 232–254.

Long, J.C., Huang, H.J., Gao, Z.Y., Szeto, W.Y., 2013. An intersection-movement-based dynamic user optimal route choice problem. Oper. Res. 61(5), 1134–1147.

Long, J.C., Szeto, W.Y., 2017. Link-based system optimum dynamic traffic assignment problems in general networks. Oper. Res. (revised and resubmitted for publication).

Long, J.C., Szeto, W.Y., Huang, H.J., Gao, Z.Y., 2015. An intersection-movement-based stochastic dynamic user optimal route choice model for assessing network performance. Transp. Res. Part B 74, 182-217.

Ma, R., Ban, X.J., Pang, J.S., 2014. Continuous-time dynamic system optimum for single-destination traffic networks with queue spillbacks. Transp. Res. Part B 68:98–122.

Ma, R., Ban, X. J., Szeto, W.Y., 2017. Emission modeling and pricing on single-destination dynamic traffic networks. Transp. Res. Part B 100, 255-283.

Merchant, D.K., Nemhauser, G.L., 1978a. A model and an algorithm for the dynamic traffic assignment. Transp. Sci. 12(3), 183–199.

Merchant, D.K., Nemhauser, G.L., 1978b. Optimality conditions for a dynamic traffic assignment model. Transp. Sci. 12(3), 200–207.

Newell, G.F., 1993. A simplified theory on kinematic wave in highway traffic, part I: general theory; part II: queuing at freeway bottlenecks; part III: multi-destination flows. Transp. Res. Part B 27(4), 281–314.

Ngoduy, D., Hoang, N.H., Vu, H.L., Watling, D., 2016. Optimal queue placement in dynamic system optimum solutions for single origin-destination traffic networks. Transp. Res. Part B 110 92, 148-169.

Nguyen, S., Dupuis, C., 1984. An efficient method for computing traffic equilibria in networks with asymmetric transportation costs. Transp. Sci. 18(2), 185–202.

Nie, Y., 2011. A cell-based Merchant-Nemhauser model for the system optimum dynamic traffic assignment problem. Transp. Res. Part B 45(2), 329–342.

Osorio, C., Flötteröd, G., Bierlaire, M., 2011. Dynamic network loading: a stochastic differentiable model that derives link state distributions. Transp. Res. Part B 45 (9), 1410–1423.

Pavlis, Y., Recker, W., 2009. A mathematical logic approach for the transformation of the linear conditional piecewise functions of dispersion-and-store and cell transmission traffic flow models into linear mixed-integer form. Transp. Sci. 43(1), 98–116.

Peeta, S., Mahmassani, H., 1995. System optimal and user equilibrium time-dependent traffic assignment in congested networks. Ann. Oper. Res. 60(1), 80–113.

Qian, Z.S., Shen, W., Zhang, H.M., 2012. System-optimal dynamic traffic assignment with and without queue spillback: its path-based formulation and solution via approximate path marginal cost. Transp. Res. Part B 46(7), 874–893.

Shen, W., Nie, Y., Zhang, H.M., 2007. On path marginal cost analysis and its relation to dynamic system-optimal traffic assignment. Allsop RE, Bell MGH, Heydecker BG, ed. Proc. 17th Internat.

Sympos. Transportation Traffic Theory. Elsevier, New York, 327–360.

Szeto, W.Y., Lo, H.K., 2004. A cell-based simultaneous route and departure time choice model with elastic demand. Transp. Res. Part B 38(7), 593–612.

Szeto, W.Y., Lo, H.K., 2006. Dynamic traffic assignment: properties and extensions. Transportmetrica 2(1), 31–52.

Vickrey, W.S., 1969. Congestion theory and transport investment. Am. Econ. Rev. 59 (2), 251–260.

Waller, S.T., Mouskos, K.C., Kamaryiannis, D., Ziliaskopoulos, A.K., 2006. A linear model for the continuous network design problem. Comput. Aided Civil. Infrastructure Engrg. 21(5), 334-345

Waller, S.T., Ziliaskopoulos, A.K. 2001. Stochastic dynamic network design problem. Transp. Res. Rec. 1771, 106-113.

Wardrop, J.G., 1952. Some theoretical aspects of road traffic research. Proc. Inst. Civil Engineers Part II, 1(2), 325–378.

Wie, B.W., Tobin, R.L., Carey, M., 2002. The existence, uniqueness and computation of an arc-based dynamic network user equilibrium formulation. Transp. Res. Part B 36(10), 897–918.

Wu, J.H., Florian, M., Xu, Y.W., Rubio-Ardanaz, J.M., 1998. A projection algorithm for the dynamic network equilibrium problem. Proc. 1998 Internat. Conf. Traffic and Transportation Stud. (American Society of Civil Engineers, Reston, VA), 379–390.

Yang, H., Meng, Q., 1998. Departure time, route choice and congestion toll in a queuing network with elastic demand. Transp. Res. Part B 32(4), 247-260.

Yperman, I., 2007. The link transmission model for dynamic network loading. Ph.D. dissertation, Katholieke Universiteit Leuven, Leuven, Belgium.

Yu, H., Ma, R., Zhang, H.M., 2018. Optimal traffic signal control under dynamic user equilibrium and link constraints in a general network. Transp. Res. Part B 110, 302-325.

Zheng, H., Chiu, Y.C., 2011. A network flow algorithm for the cell-based single-destination system optimal dynamic traffic assignment problem. Transp. Sci. 45(1), 121–137.

Zheng, H., Chiu, Y.C., Mirchandani, P.B., 2015. On the system optimum dynamic traffic assignment and earliest arrival flow problems. Transp. Sci. 49(1), 13-27.

Zhu, F., Ukkusuri, S.V., 2013. A cell based dynamic system optimum model with non-holding back flows. Transp. Res. Part C 36, 367–380.

Zhu, F., Ukkusuri, S.V., 2017. Efficient and fair system states in dynamic transportation networks. Transp. Res. Part B 104, 272-289.

Ziliaskopoulos, A.K., 2000. A linear programming model for the single destination system optimum dynamic traffic assignment problem. Transp. Sci. 34(1), 37-49.